

DTIC FILE COPY . . .

2



US Army Corps  
of Engineers

AD-A227 457



TECHNICAL REPORT HL-90-12

# NEW MADRID PUMPING STATION GRAVITY FLOW CONDUIT AND CONFLUENCE NEW MADRID FLOODWAY, MISSOURI

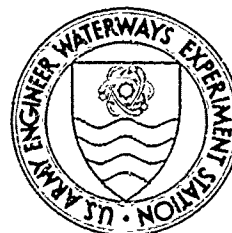
## Hydraulic Model Investigation

by

J. R. Leech

Hydraulics Laboratory

DEPARTMENT OF THE ARMY  
Waterways Experiment Station, Corps of Engineers  
3909 Halls Ferry Road, Vicksburg, Mississippi 39180-6199



September 1990  
Final Report

DTIC  
ELECTE  
OCT 02 1990

S

6

E

D

Approved For Public Release; Distribution Unlimited

Prepared for US Army Engineer District, Memphis  
Memphis, Tennessee 38103-1894



90 10 01 024

Destroy this report when no longer needed. Do not return  
it to the originator.

The findings in this report are not to be construed as an official  
Department of the Army position unless so designated  
by other authorized documents.

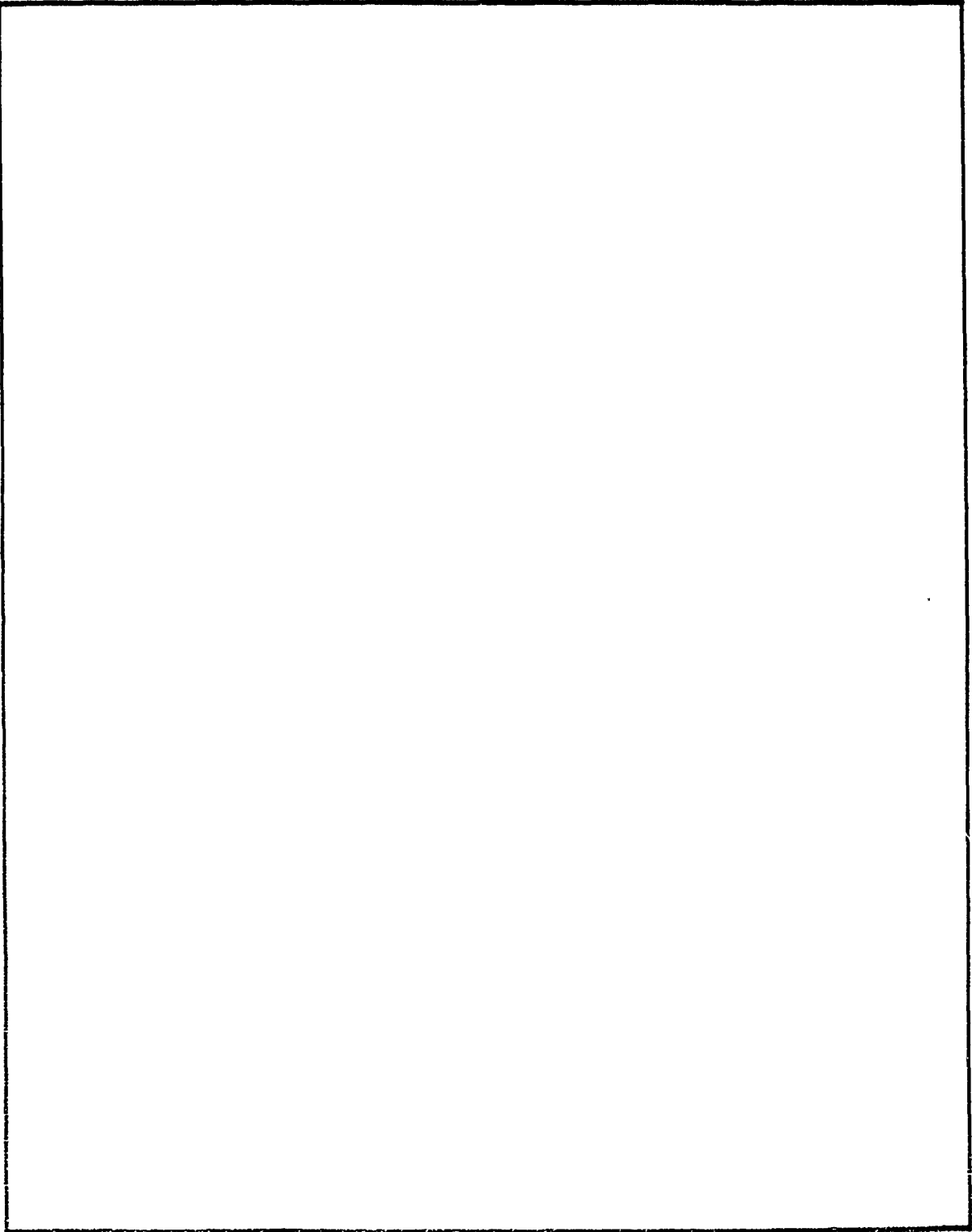
The contents of this report are not to be used for  
advertising, publication, or promotional purposes.  
Citation of trade names does not constitute an  
official endorsement or approval of the use of  
such commercial products.

Unclassified

SECURITY CLASSIFICATION OF THIS PAGE

REPORT DOCUMENTATION PAGE				Form Approved OMB No. 0704-0188	
1a. REPORT SECURITY CLASSIFICATION Unclassified			1b. RESTRICTIVE MARKINGS		
2a. SECURITY CLASSIFICATION AUTHORITY			3. DISTRIBUTION/AVAILABILITY OF REPORT Approved for public release; distribution unlimited.		
2b. DECLASSIFICATION/DOWNGRADING SCHEDULE					
4. PERFORMING ORGANIZATION REPORT NUMBER(S) Technical Report HL-90-12			5. MONITORING ORGANIZATION REPORT NUMBER(S)		
6a. NAME OF PERFORMING ORGANIZATION USAEWES Hydraulics Laboratory		6b. OFFICE SYMBOL (If applicable) CEWES-HS-S	7a. NAME OF MONITORING ORGANIZATION		
6c. ADDRESS (City, State, and ZIP Code) 3909 Halls Ferry Road Vicksburg, MS 39180-6199			7b. ADDRESS (City, State, and ZIP Code)		
8a. NAME OF FUNDING/SPONSORING ORGANIZATION USAED, Memphis		8b. OFFICE SYMBOL (If applicable)	9. PROCUREMENT INSTRUMENT IDENTIFICATION NUMBER		
8c. ADDRESS (City, State, and ZIP Code) B-202, 167 North Main Memphis, TN 38103-1894			10. SOURCE OF FUNDING NUMBERS		
			PROGRAM ELEMENT NO.	PROJECT NO.	TASK NO.
					WORK UNIT ACCESSION NO.
11. TITLE (Include Security Classification) New Madrid Pumping Station, Gravity Flow Conduit and Confluence, New Madrid Floodway, Missouri; Hydraulic Model Investigation					
12. PERSONAL AUTHOR(S) Leech, J. R.					
13a. TYPE OF REPORT Final report		13b. TIME COVERED FROM _____ TO _____		14. DATE OF REPORT (Year, Month, Day) September 1990	
15. PAGE COUNT 112					
16. SUPPLEMENTARY NOTATION Available from National Technical Information Service, 5285 Port Royal Road, Springfield, VA 22161.					
17. COSATI CODES			18. SUBJECT TERMS (Continue on reverse if necessary and identify by block number)		
FIELD	GROUP	SUB-GROUP			
			Confluence Riprap Formed suction inlet Saxophone outlet Geometry Vortex		
19. ABSTRACT (Continue on reverse if necessary and identify by block number)					
<p>Site-specific hydraulic model studies of hydraulic structures and channels on the New Madrid Floodway, Missouri, were conducted to give three-dimensional analyses of the open channels, to provide design information, and to minimize prototype cost. The proposed pumping station on the New Madrid Floodway consisted of a draft tube type sump design, referred to as a formed suction inlet (FSI). The FSI has an advantage over conventional rectangular sumps by having a constantly decreasing cross-sectional area, which causes the flow to accelerate, eliminating vortices caused by geometry. A satisfactory FSI was developed by adding a cone section to the throat, which improved the dimensionless velocity contours. The riprap protection was found to be stable except for the area adjacent to the opening of the gravity flow intake. A recommended plan to correct the instability was developed. The original drop structure in the model located at the confluence of the two channels was replaced by a riprap-lined channel, which provided satisfactory performance for all conditions tested.</p>					
20. DISTRIBUTION/AVAILABILITY OF ABSTRACT <input checked="" type="checkbox"/> UNCLASSIFIED/UNLIMITED <input type="checkbox"/> SAME AS RPT. <input type="checkbox"/> DTIC USERS			21. ABSTRACT SECURITY CLASSIFICATION Unclassified		
22a. NAME OF RESPONSIBLE INDIVIDUAL			22b. TELEPHONE (Include Area Code)		22c. OFFICE SYMBOL

SECURITY CLASSIFICATION OF THIS PAGE



SECURITY CLASSIFICATION OF THIS PAGE

# PREFACE

The model investigation reported herein was authorized by the Headquarters, US Army Corps of Engineers, on 31 August 1987 at the request of the US Army Engineer District, Memphis (LMM).

The study was conducted during the period September 1987 to December 1988 in the Hydraulics Laboratory (HL) of the US Army Engineer Waterways Experiment Station (WES), under the direction of Messrs. F. A. Herrmann, Jr., Chief, HL, and R. A. Sager, Assistant Chief, HL; and under the general supervision of Messrs. G. A. Pickering, Chief, Hydraulic Structures Division (HSD), HL, and N. R. Oswalt, Chief, Spillways and Channels Branch (SCB), HSD. The project engineer for the model study was Mr. J. R. Leech, SCB. This report was prepared by Mr. Leech with assistance from Mr. J. R. Rucker, SCB, and edited by Mrs. M. C. Gay, Information Technology Laboratory, WES.

During the course of the investigation, Messrs. J. McCormick, L. Eckenrod, L. Holman, US Army Engineer Division, Lower Mississippi Valley; and Messrs. J. Harman, D. Baretta, H. Stricker, and S. Barry, LMM, visited WES to discuss the program and results of model tests, observe the model in operation, and correlate these results with design studies.

Commander and Director of WES during preparation of this report was COL Larry B. Fulton, EN. Technical Director was Dr. Robert W. Whalin.

Section For	
1. General	<input checked="" type="checkbox"/>
2. Technical	<input checked="" type="checkbox"/>
3. Financial	<input type="checkbox"/>
4. Classification	
By _____	
Distribution/	
Availability Codes	
Dist	Avail and/or Special
A-1	



## CONTENTS

	<u>Page</u>
PREFACE.....	1
CONVERSION FACTORS, NON-SI TO SI (METRIC) UNITS OF MEASUREMENT.....	3
PART I: INTRODUCTION.....	5
The Prototype.....	5
Purpose and Scope of Model Study.....	5
PART II: MODEL.....	7
Description.....	7
Scale Relation.....	7
PART III: TESTS AND RESULTS.....	13
The Approach Channel.....	13
Formed Suction Inlet.....	13
Gravity Flow Outlet Channel.....	18
Confluence.....	18
Saxophone Discharge Outlet.....	18
PART IV: CONCLUSIONS AND RECOMMENDATIONS.....	20
PHOTOS 1-15	
PLATES 1-72	

CONVERSION FACTORS, NON-SI TO SI (METRIC)  
UNITS OF MEASUREMENT

Non-SI units of measurement used in this report can be converted to SI  
(metric) units as follows:

<u>Multiply</u>	<u>By</u>	<u>To Obtain</u>
acres	4,046.873	square metres
cubic feet	0.02831685	cubic metres
degrees (angle)	0.01745329	radians
feet	0.3048	metres
inches	2.54	centimetres
miles (US statute)	1.609347	kilometres
square miles	2.589998	square kilometres

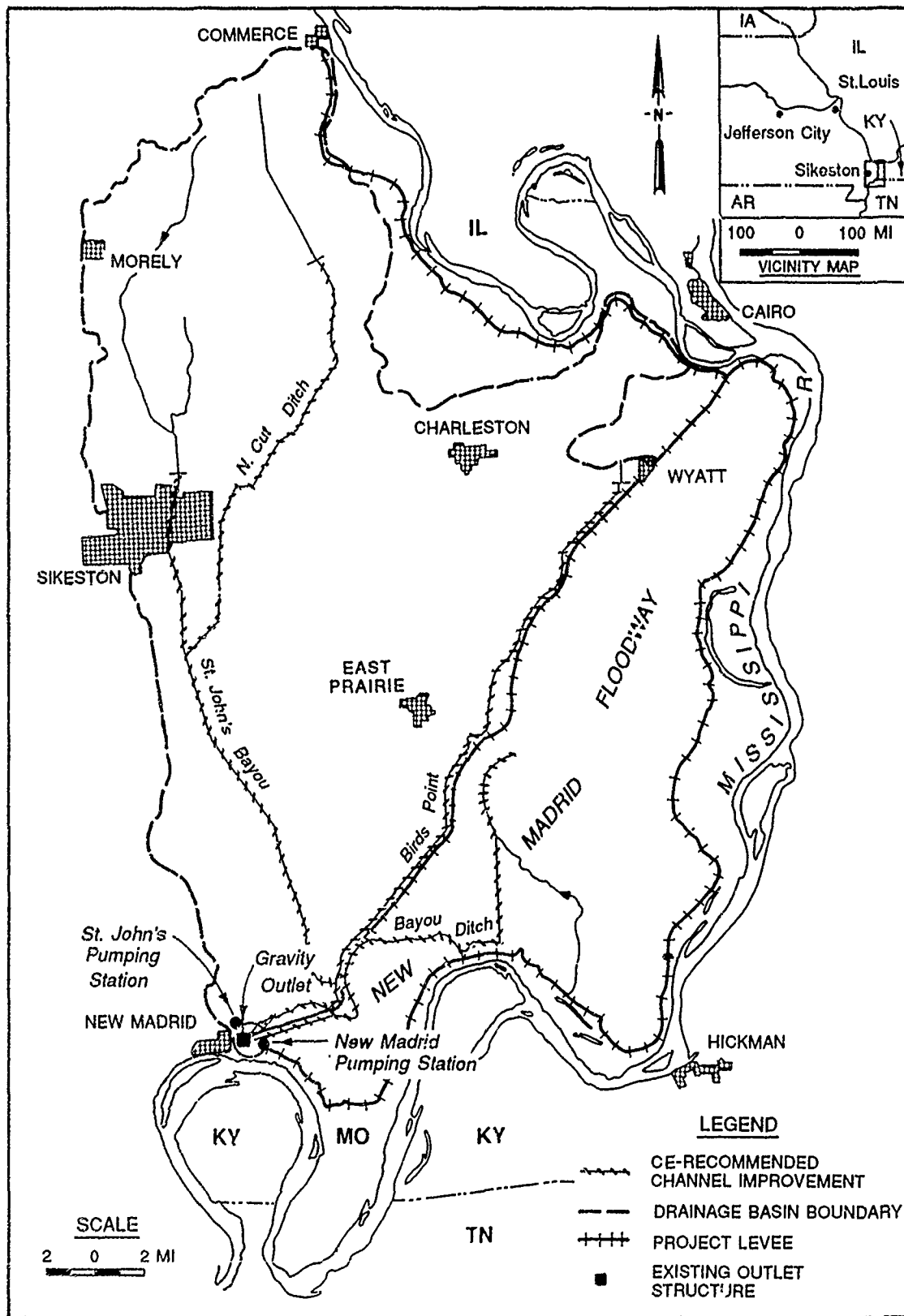


Figure 1. Vicinity and location map



NEW MADRID PUMPING STATION, GRAVITY FLOW CONDUIT  
AND CONFLUENCE, NEW MADRID FLOODWAY, MISSOURI

Hydraulic Model Investigation

PART I: INTRODUCTION

The Prototype

1. The New Madrid pumping station, gravity flow conduits, and channel improvements are an integral part of the recommended plan of improvement for the St. Johns Bayou and New Madrid Floodway drainage basins. The New Madrid basin drains 183 square miles\* of floodway. The project (Figure 1) is located about 20 miles due south of Sikeston, MO. The floodway area is currently subject to both Mississippi River backwater and headwater flooding. Construction of the authorized levee closure and gravity flow conduit outlet would alleviate the Mississippi River backwater flooding; however, backwater flooding in the floodway would remain a problem due to impoundment of interior runoff during high Mississippi River stages. The 100-year headwater flood event along the channels in the project area of New Madrid Floodway would inundate approximately 28,500 acres. The recommended plan of improvement includes channel clearing and improvement of 137 miles of rural channels; improvement of 6.7 miles of urban channels in Sikeston, MO; construction of a 1 000-cfs pumping station at the outlet of St. Johns Bayou Main Ditch; and construction of a 1,500-cfs pumping station at the outlet of the East Bayou Ditch (Figure 2).

Purpose and Scope of Model Study

2. The primary purpose of the hydraulic model study was to develop a formed suction inlet (FSI) for the proposed New Madrid pumping station, evaluate the approach conditions to the pumping station and the gravity flow

---

\* A table of factors for converting non-SI to SI (metric) units of measurement is presented on page 3.

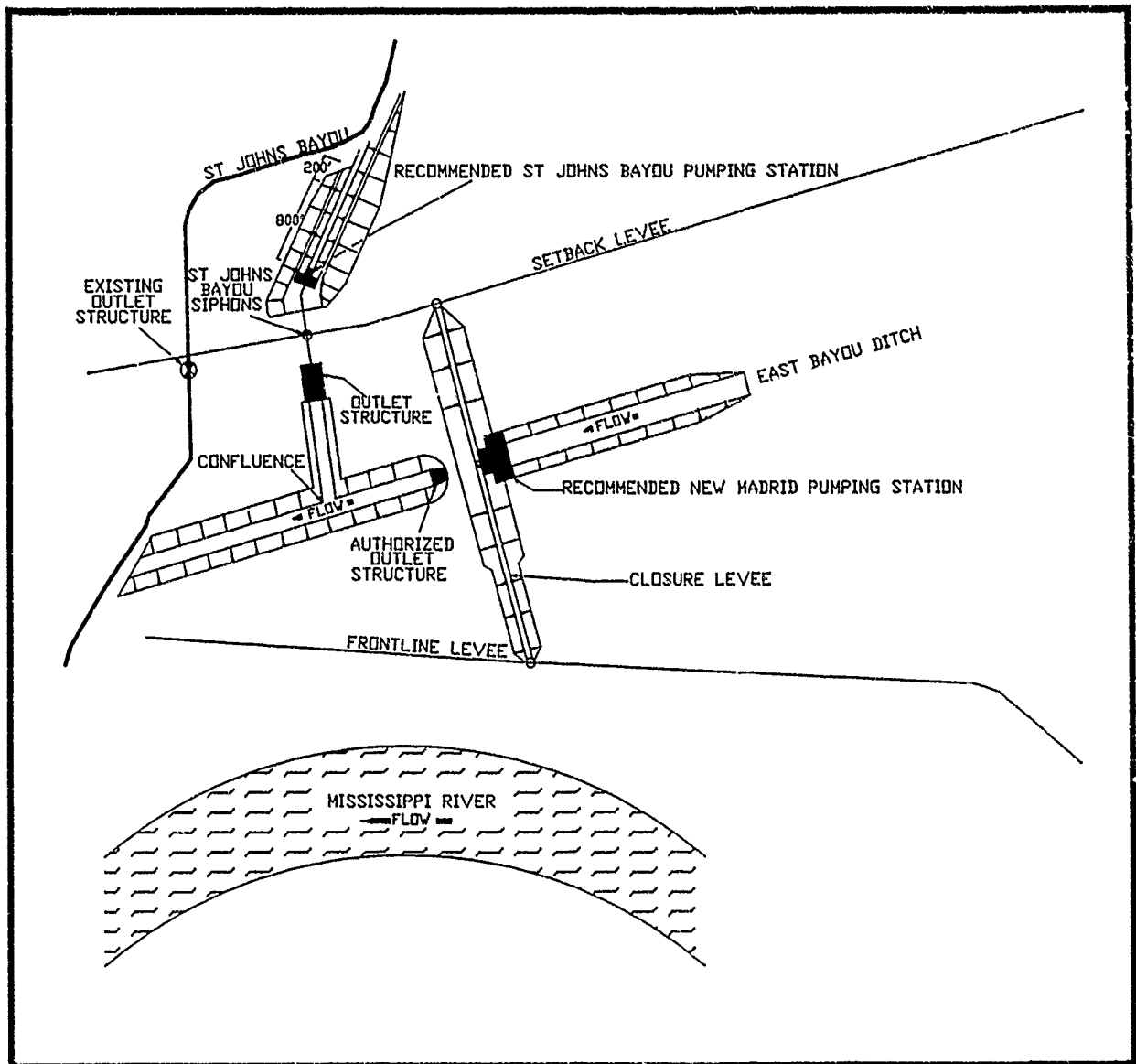


Figure 2. Location of proposed pumping stations

conduit, and ensure that the gravity flow conduit could pass the required discharge of 5,000 cfs. Downstream of the pumping station, efforts focused on the stilling action of the stilling basin, riprap stability in the exit channel and in the confluence of the St. Johns saxophone outlet channel, the performance of the drop structure at the confluence, and the performance of the St. Johns siphon saxophone discharge outlet. The determination of the exact dimensions of the FSI and its performance proved to be a significant part of the overall study effort.

## PART II: MODEL

### Description

3. A 1:15-scale model was constructed to reproduce the approach (Figure 3) and exit channel to the New Madrid pumping station, the four gravity flow intakes (Figure 4) and the transition conduit (Figure 5), three pump bays equipped with FSI's (Figure 4), stilling basin for the gravity flow conduit (Figure 6), riprap protection of the New Madrid and St. Johns Bayou pumping station exit channels, the confluence of these two channels (Figure 7), and saxophone discharge outlets for the three St. Johns Bayou siphons (Figure 8). The siphons were not reproduced in the model. The model reproduced a design pumped flow rate of 500 cfs per pump, gravity flow discharge of 5,000 cfs, and saxophone outlet discharge of 333 cfs per outlet.

4. The model flume was constructed of plastic-coated plywood. Riprap was simulated in the model using limestone rock. The FSI's, gravity flow conduit, and the saxophone discharge outlets were constructed of Plexiglas. Flow in the model was provided by pumps and measured using a flowmeter installed in the supply line to the model, and the factory calibration was verified volumetrically. Velocities in the model were measured with a Nixon probe (paddle wheel type) velocity meter, which was calibrated in a calibration flume before and after the study. Water surfaces were measured using point gages mounted on rails and zeroed on the invert of the model channel. Pressures in the pump column were measured with pressure transducers and recorded with a personal computer.

### Scale Relation

5. The accepted equations of hydraulic similitude, based upon the Froudian criteria, were used to express mathematical relations between the dimensions and hydraulic quantities of the model and prototype. General relations expressed in terms of the model scale or length ratio  $L_r$  are presented in the following tabulation. Model measurements of discharge and water-surface elevations can be transferred quantitatively to prototype equivalents by means of these scale relations.

<u>Dimension*</u>	<u>Ratio</u>	<u>Scale Relation</u> <u>Model:Prototype</u>
Length	$L_r = L_r$	1:15
Area	$A_r = L_r^2$	1:225
Time	$T_r = L_r^{1/2}$	1:3.873
Velocity	$V_r = L_r^{1/2}$	1:3.873
Discharge	$Q_r = L_r^{5/2}$	1:871.4

---

\* Dimensions are in terms of length.

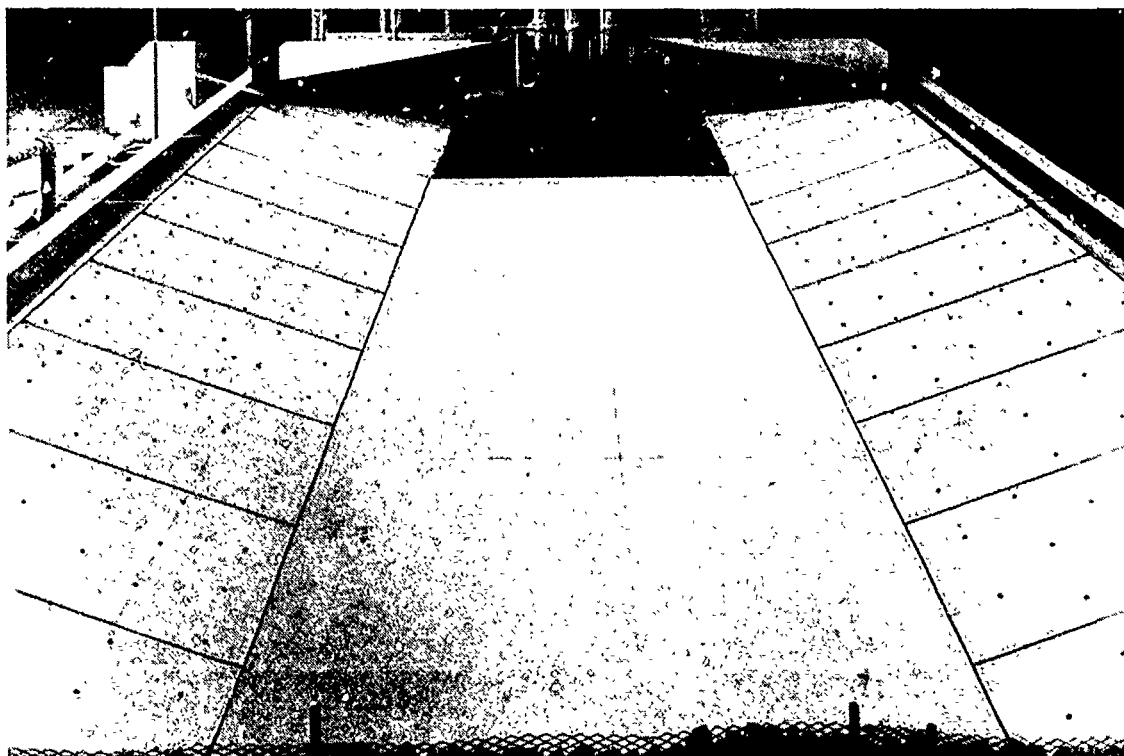


Figure 3. Approach channel

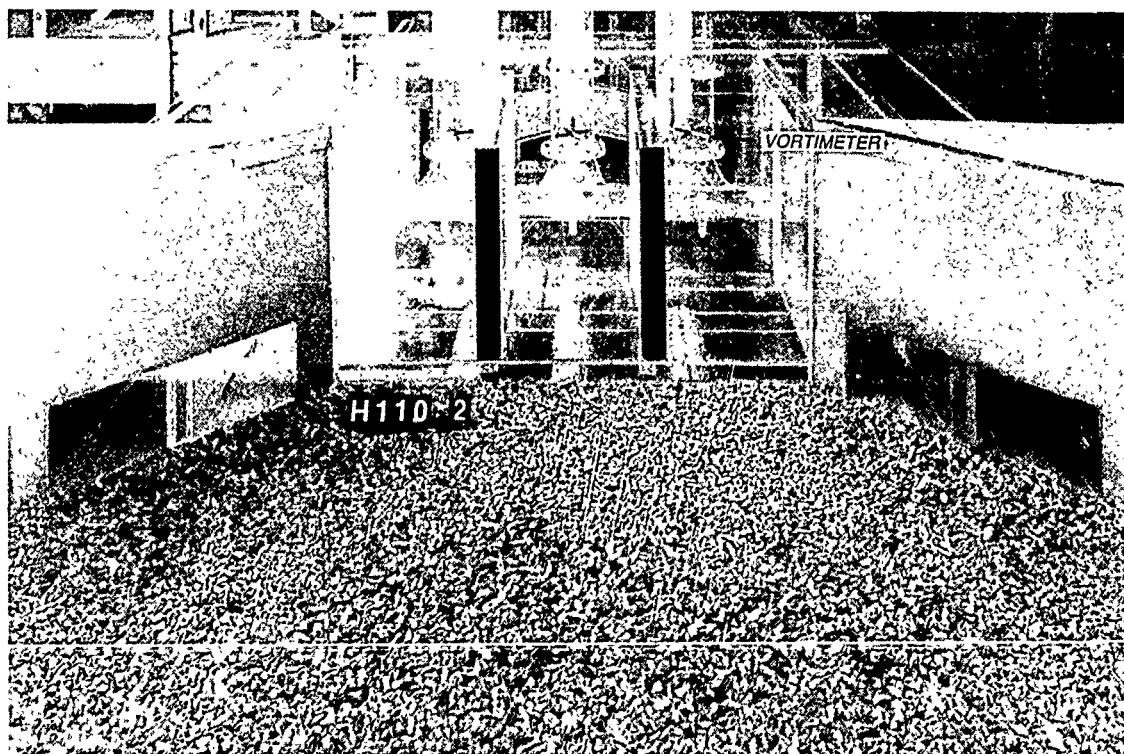
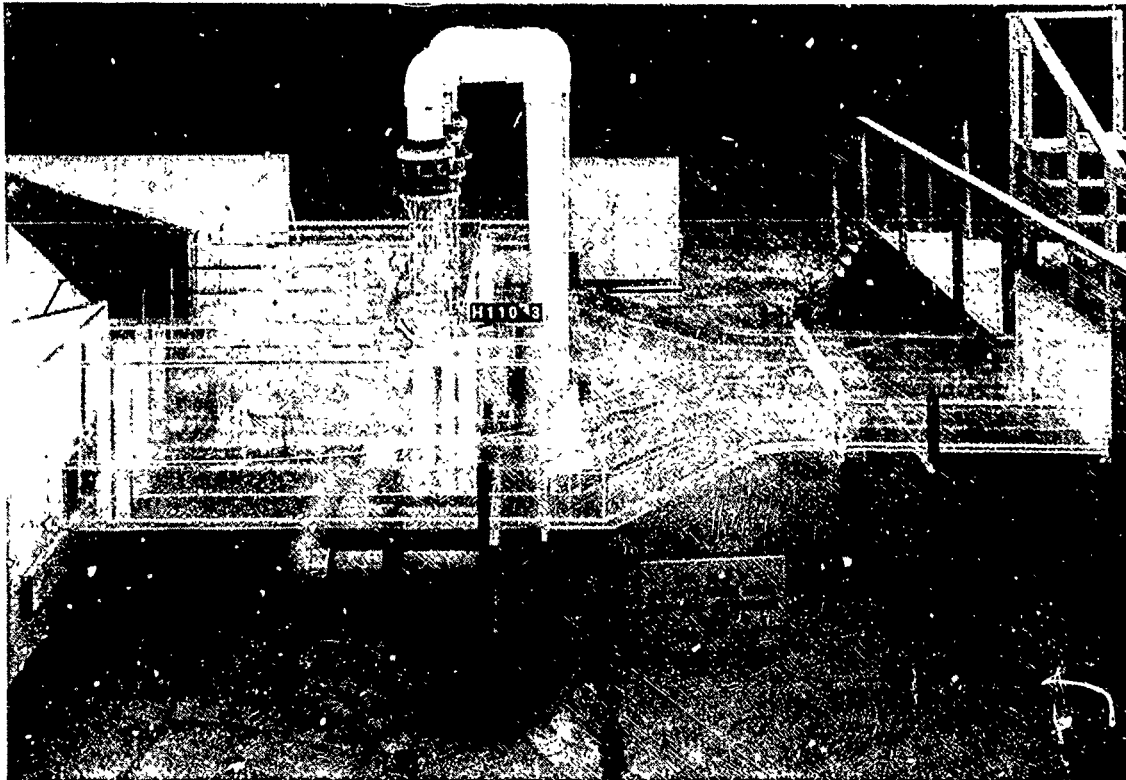
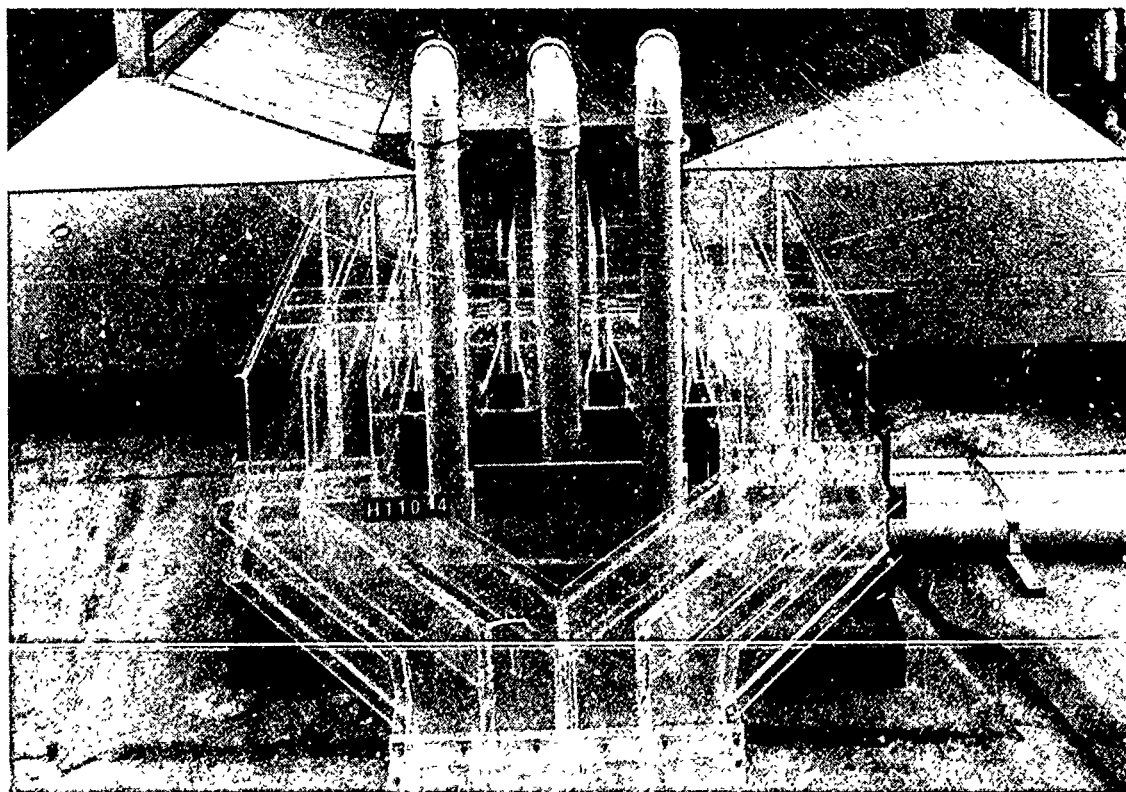


Figure 4. Gravity flow intakes and pump bays



a. Profile



b. Looking upstream

Figure 5. Gravity flow transition conduit

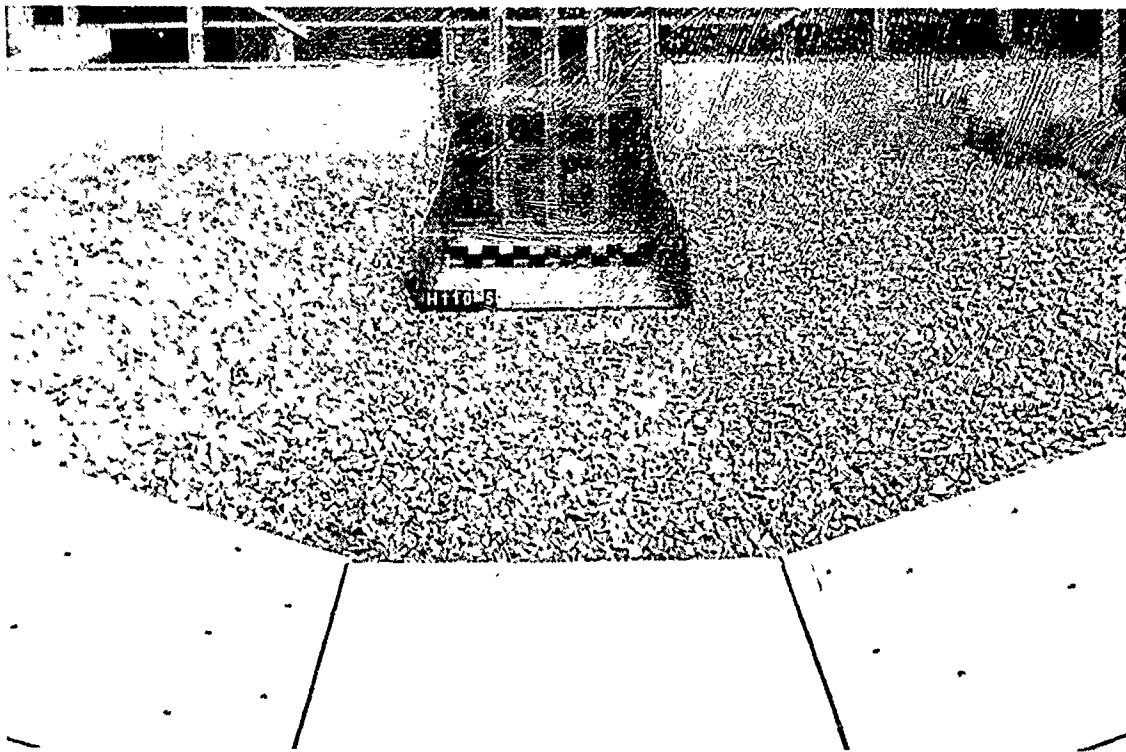


Figure 6. Stilling basin

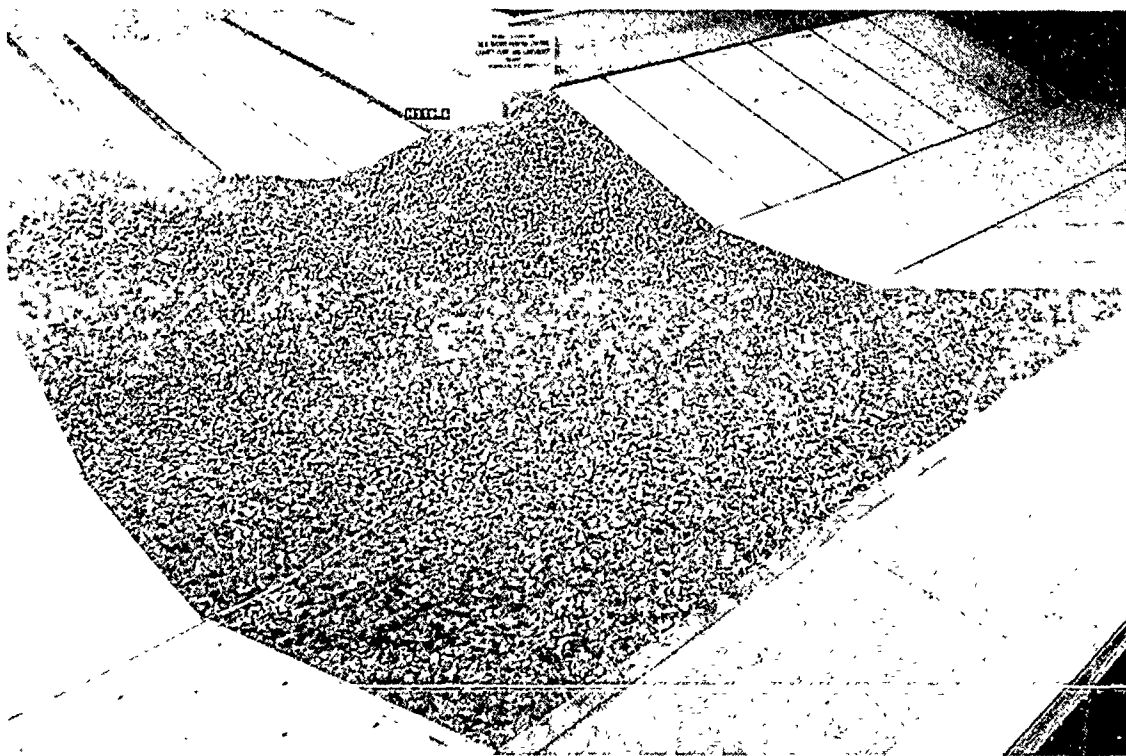


Figure 7. Confluence of New Madrid and St. Johns Bayou channels, looking upstream

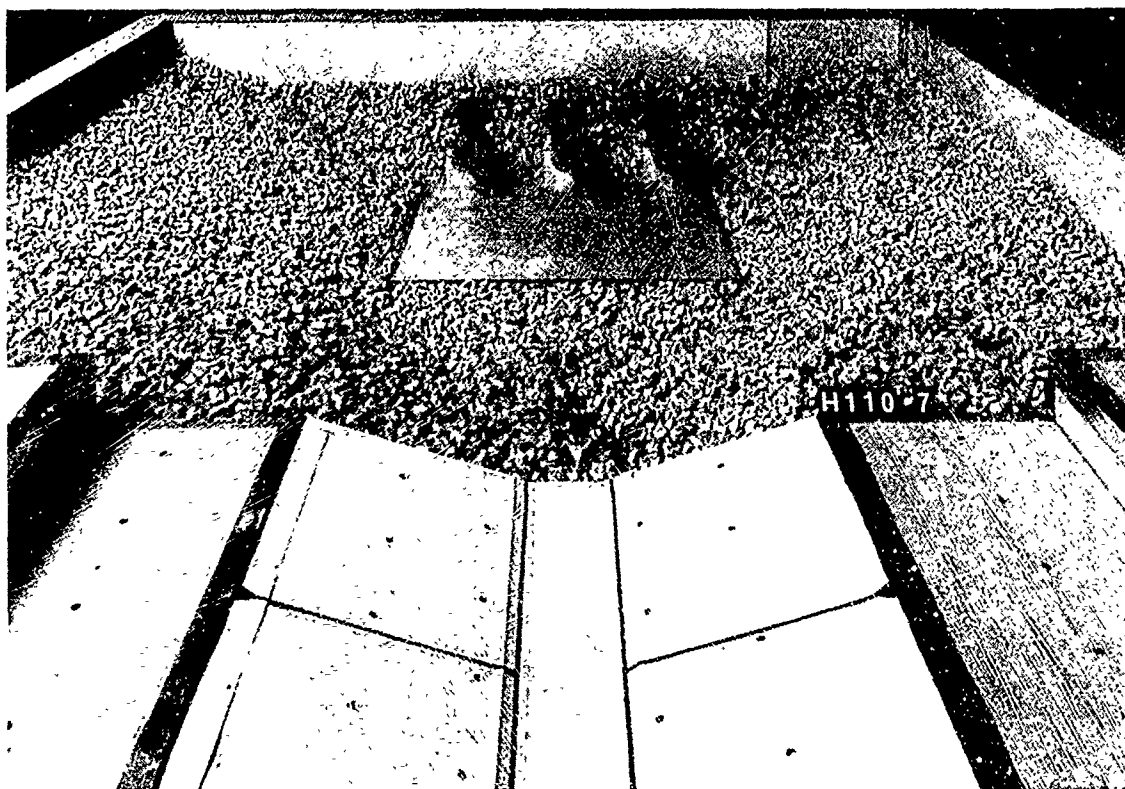


Figure 8. Saxophone discharge outlets for St. Johns Bayou siphons



### PART III: TESTS AND RESULTS

#### The Approach Channel

6. The approach channel (Figure 3) was evaluated by observing different flow conditions and measuring velocities. The channel was protected by an 18-in.-thick riprap blanket. Figure 4 shows the riprap blanket at the same elevation as the invert of the gravity flow conduit. Model velocities are presented in Plates 1-3 for the surface, middepth, and bottom with gravity flow conduits operating with a design discharge of 5,000 cfs, pool el 276,\* and tailwater el 270.3. Velocity measurement locations are as follows: surface, 2 ft below the pool elevation; middepth, halfway between the pool elevation and the channel invert; and bottom, 3 ft above the channel invert. Plate 3 shows the bottom velocities increasing as the flow accelerates and concentrates toward the conduit opening. The average velocity in the conduit was 12.5 fps. The increased velocity caused riprap to be washed into the gravity flow conduit. A scour slab (Plate 4) was extended upstream, reducing the velocities in the vicinity of the riprap interface and creating a stable situation. The scour slab was replaced by a 36-in.-thick riprap blanket, which provided for a stable condition. The surface pattern for this flow condition, presented in Photo 1, shows the flow concentrating at the conduit opening.

7. The surface, middepth, and bottom approach velocities with three pumps operating at maximum discharge of 500 cfs per pump and minimum water-surface elevation in the sump of 275 ft are presented in Plates 5-7, respectively. The velocities were obtained for the same surface, middepth, and bottom locations as described in the preceding paragraph. All velocities for this condition were less than 1 fps and did not affect the stability of the riprap.

#### Formed Suction Inlet

8. The FSI is a draft tube type sump design (Plate 8) having a

---

\* All elevations (el) cited herein are in feet referred to the National Geodetic Vertical Datum (NGVD).

constantly decreasing cross-sectional area, which causes the flow to accelerate, eliminating vortices caused by geometry. Design A (Plate 8) was constructed without the cone section above the FSI. Velocities measured in the approach to the three FSI's are presented in Plates 9-11 for the surface, mid-depth, and bottom with design discharge and minimum sump elevation. The increase in velocities in the approach to the sump indicates flow acceleration over the entire cross section.

9. According to Larsen and Padmanabhan,\*

Swirl is a general term for any flow condition (due to vortexing or a pipe bend) where there is a tangential velocity component in addition to a usually predominating axial flow component. *Prerotation* is a specific term to denote a cross-sectional average swirl in the suction line of a pump, or, in case of a vertical wet-pit pump, upstream of the impeller.

The prerotation angle  $\theta$  is a measure of the strength of the tangential velocity component  $u_t$ , relative to that of the axial velocity component  $u$  in the flow approaching the pump impeller; i.e.,  $\theta = \tan^{-1} (u_t/u)$ . Adverse effects on the pump are decreased capacity and head when the rotation is in the direction of pump rotation and increased capacity and head when the rotation is opposite the pump rotation (antirotation). The increased capacity is associated with an increase in power requirement and may cause motor overheating.

Prerotation will influence pump performance since the flow approaching the impeller already has a rotational flow field which may oppose or add to the impeller rotation, depending on direction. The design of the pump vanes (i.e., shape and angle) assumes no prerotation, and the existence of prerotation implies flow separation along one side of the impeller vanes....Prerotation could be quantified in a model by an average cross-sectional swirl angle, determined by detailed velocity measurements or by readings on a swirl meter. Since swirl decays along a pipe as a result of wall friction, internal fluid shear, and turbulence, the swirl meter in a model suction pipe should be located near the impeller.

10. Model tests were conducted to determine the swirl angle in each FSI. Each FSI was fitted with a vortimeter (Figure 4), which is a four-bladed device with zero pitch located at the eye of the prototype pump impeller.

---

\* Johannes Larsen and Mahadevan Padmanabhan. 1986. "Intake Modeling," Section 10.2, Pump Handbook, Igor J. Karassik et al., eds., 2nd ed, McGraw-Hill, New York.

Vortimeter readings were obtained by counting the revolutions of the vortimeter in a 3-min period. The blade tip speed  $V_\theta$  was then computed and divided by the average velocity  $V_a$  to obtain the swirl angle  $\theta$  :

$$V_\theta = \frac{\pi d n}{60} \quad (1)$$

where

$d$  = diameter of the vortimeter, ft

$n$  = revolutions per minute of the vortimeter

The average velocity is computed by

$$V_a = \frac{Q}{A} \quad (2)$$

where

$Q$  = pump discharge, cfs

$A$  = cross-sectional area of suction column,  $\text{ft}^2$

The swirl angle  $\theta$  is computed from the following formula:

$$\tan \theta = \frac{V_\theta}{V_a} \quad (3)$$

The swirl angle has the advantage of having the same value in the model and the prototype and is considered unacceptable for values greater than 3 deg. Plates 12 and 13 present the swirl angle for each pump with different combinations of pumps operating at design discharge and sump levels as indicated. All swirl angles for this condition were within the standard. Plates 14 and 15 show the swirl angle for each pump with different combinations of pumps operating at 130 percent of the design discharge and sump levels as indicated. Test results showed the swirl angles for design A (Plate 8) were acceptable in all cases and no visible vortices existed.

11. To further evaluate the FSI, a matrix of impact tubes and static pressure ports (Plate 16) was installed in pump column 2 at the elevation of the eye of the impeller. A 1-ft model section of pump column was replaced by the section with the impact tubes and static pressure ports shown in Figure 9 to evaluate the velocity distribution at the eye of the impeller. The impact tubes measure the dynamic head while the static ports measure the static head, thus giving a point pressure for each tube, which is converted to a velocity. Contour plots were made of a dimensionless velocity  $R_v$  determined by

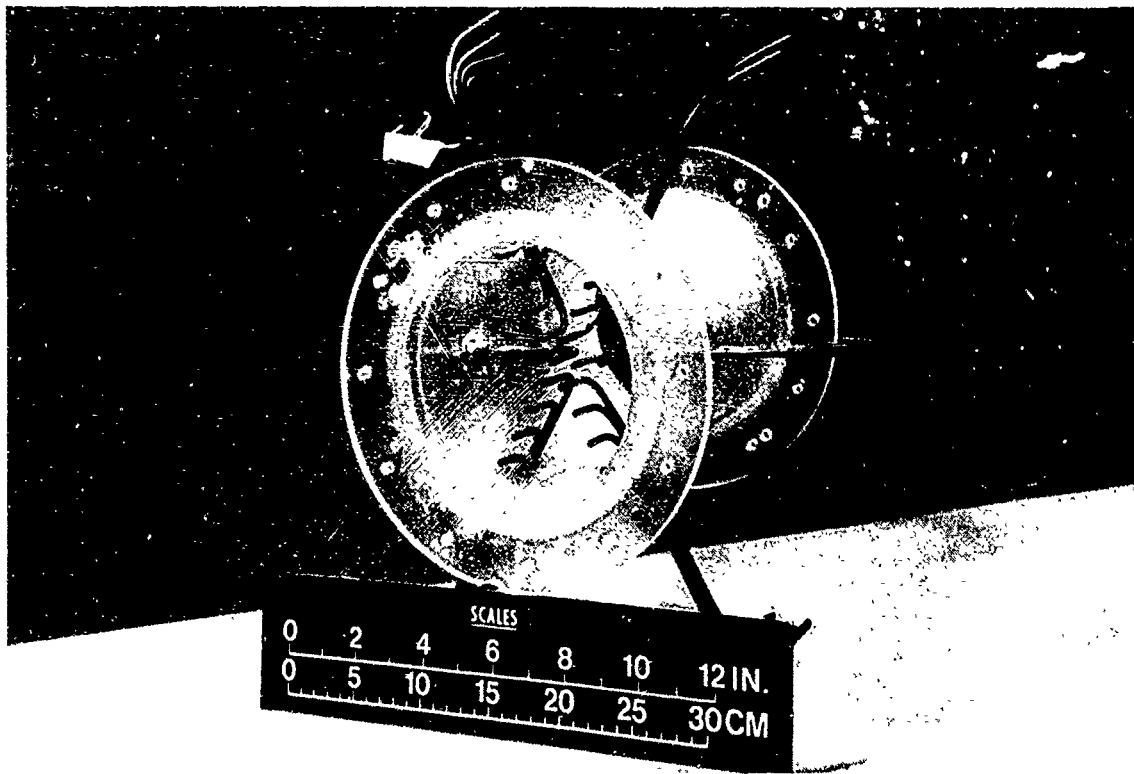


Figure 9. Replacement section of model pump column with impact tubes and static pressure ports

dividing the average measured axial velocity  $V_M$  by the computed cross-sectional average axial velocity  $V_C$ . Ideally, this ratio would have a value of 1. The standard to evaluate a given sump design is that a ratio of  $\pm 10$  percent of the ideal value indicates a fairly uniform velocity distribution.

12. Design A (Plate 8) was developed based on an 8-ft-diam prototype pump column with the eye of the impeller set at el 275. Other critical dimensions were based on ratios of the column diameter as used to develop the Yazoo Pumping Station.\* To give more flexibility to contracting pump manufacturers, the typical cone section of design A (Plate 8) was omitted. The reasoning was if uniform velocity could be obtained without a cone section below the pump impeller, a larger variation of pump sizes could be installed in the sump. Manufacturers would provide the cone section based on the size of the proposed pump.

---

\* Bobby P. Fletcher. "Yazoo Backwater Pumping Station Sump, West-Central Mississippi; Hydraulic Model Investigation" (in preparation), US Army Engineer Waterways Experiment Station, Vicksburg, MS.

13. Results of model tests to determine the velocity distribution at the eye of the impeller were obtained using the impact tube configuration shown in Figure 9. The results are presented in Plates 17-35. The contour plots indicate that flow separation from the roof curve as the flow made the transition from horizontal to vertical still persisted at the eye of the impeller, therefore forcing more flow to the back side of the pump column and causing a zone of low pressure at the front (upstream) side of the column. The lower velocities fell outside the 10 percent standard for all test conditions.

14. Design A was tested with the splitter wall removed (design A-1), as shown in Plate 36, and the results are presented in Plates 37-41. Removal of the splitter wall caused the flow to separate even more severely from the roof curve. The splitter wall caused the flow to separate laterally, creating a low-pressure zone downstream of the wall and reducing the velocities around the roof curve. The additional turbulence caused by the splitter allowed the flow to hold closer to the roof curve.

15. Design B (Plate 42) was equipped with a cone section below the eye of the impeller originating at the point of tangency of the roof curve and the pump column and extending upward at a 7-deg angle, reducing the diameter of the pump column at the eye of the impeller to 7.35 ft. The 7-deg cone angle was selected as the minimum angle of convergence based on the design of a draft tube where the angle can vary between 7 and 11 deg. Results of model tests to measure the swirl angle are presented in Plates 43-46. All conditions tested were within the 3-deg standard. Tests were conducted using the impact tubes (Plate 47) to evaluate the velocity distribution, and the results are shown in Plates 48-64. For all conditions tested, the velocity distribution fell within the 10 percent standard, indicating that the cone section is necessary to prevent separation of the flow at the roof curve.

16. The results of these tests show the value of measuring the velocity distribution with the impact tubes to detect zones of low pressure that were undetected by the vortimeter. In this case, flow separated from the boundary without inducing significant amounts of swirl, setting up a zone of low pressure approximately equal on either side of a center-line axis along the direction of flow. The vortimeter blade, when entering this zone, was subject to equal pressure on either side and remained almost stationary.

17. Photos 2-6 present the surface patterns for various combinations of

pumps operating at minimum sump. Small eddies formed in the pump bays due to the restriction of the piers. Vortices were not observed for any of the tested conditions.

#### Gravity Flow Outlet Channel

18. Results of tests to evaluate the energy dissipation of the stilling basin (Plate 65) and riprap protection of the exit channel indicated sufficient energy dissipation in the basin by maintaining the hydraulic jump within the stilling basin and adequate riprap protection for the channel bottom. Minimum design tailwater elevation was 270.3 and the absolute minimum tailwater elevation obtained in the model was 267.4. The riprap remained stable for all conditions tested. Velocities measured in the model exit channel (Plates 66-68) ranged from 10.1 to 13.9 fps over the end sill. The computed average velocity over the end sill for maximum discharge and absolute minimum tailwater in the model was 11.9 fps. Surface patterns (Photos 7-9) show a uniform flow distribution downstream past the confluence of the two channels. The gravity flow conduits would not likely be operated in conjunction with the pumping station.

#### Confluence

19. The proposed drop structure located at the confluence of the New Madrid and St. Johns Bayou outlet channels was replaced during model construction with a sloping riprap-lined channel, as shown in Figure 7. Photos 10 and 11 show the surface patterns at the confluence for siphon discharges only with the minimum tailwater during pumping and the average tailwater during pumping, respectively, and represent the worst case for flow impacting on the opposite bank. The 36-in.-thick riprap blanket remained stable for all test conditions.

#### Saxophone Discharge Outlet

20. The proposed St. Johns Bayou pumping station will provide for siphonic recovery over the setback levee shown in Figure 2. Each of the three siphons will be equipped with a saxophone outlet (Plate 69). Plate 69

presents data obtained for the width  $w$  and height  $h$  of the water plume for a tailwater elevation of 277.0 (minimum river during pumping) and the discharges  $Q$  specified. The plume and surface patterns are presented in Photos 12-15 for tailwater elevations of 279.0 and 290.0. Plates 70-72 show velocities measured to evaluate the saxophone discharge outlet channel. The riprap remained stable for all conditions tested.

#### PART IV: CONCLUSIONS AND RECOMMENDATIONS

21. Tests conducted to evaluate the approach channel indicated the 18-in.-thick riprap blanket was unstable in the vicinity of the gravity flow conduit openings due to local increased velocities. The recommended approach channel consists of adding a scour slab as shown in Plate 4 or the equivalent area of the slab replaced with 36-in.-thick riprap blanket.

22. Although the swirl angle with the original design FSI was acceptable, the velocity distribution at the eye of the impeller was not. A satisfactory design, design B, was developed by adding a cone section with a 7-deg angle, reducing the diameter at the top of the cone to 7.35 ft (Plate 42). Test results concluded that the design B FSI performed satisfactorily by having swirl angles less than 3 deg and dimensionless velocity contours within the 10 percent standard deviation criterion. Design B is the recommended FSI design.

23. The original gravity flow conduit passed the design flow (5,000 cfs) satisfactorily for all tests conducted. The model stilling basin maintained the jump even with tailwaters less than the design. The lowest tailwater elevation obtained in the model was 267.4 and channel control was then established. The 36-in.-thick riprap blanket provided adequate channel protection in the outlet channel. The riprap-lined sloping channel at the confluence remained stable for all tests. The riprap-lined sloping channel is recommended in place of the originally proposed drop structure.

24. The original saxophone discharge outlet performed satisfactorily and riprap protection in the outlet channel remained stable during all test conditions. The original saxophone outlet is recommended.





Photo 1. Surface flow pattern for design discharge 5,000 cfs, pool el 275, tailwater el 270.3

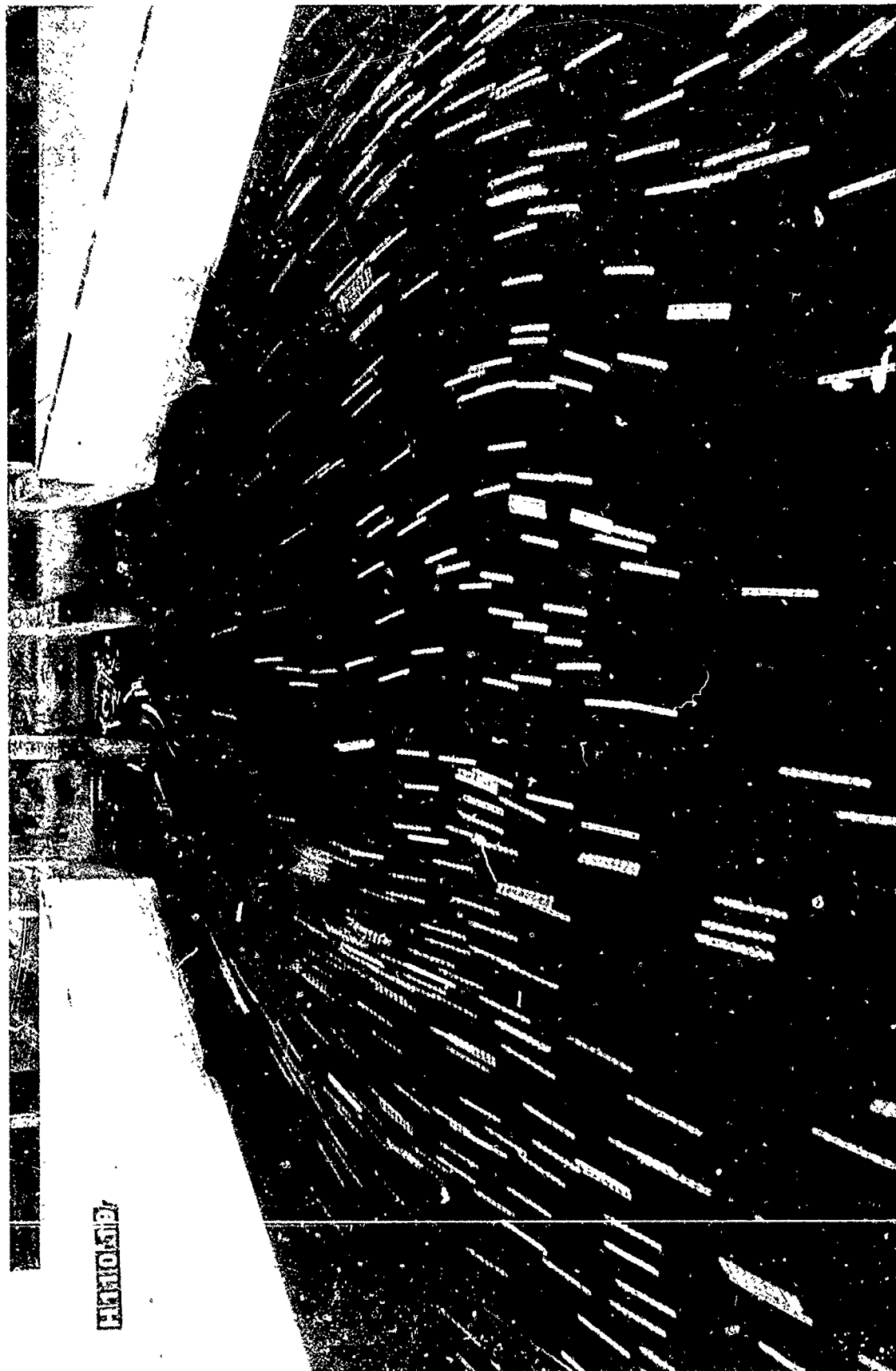


Photo 2. Surface flow pattern, three pumps operating, discharge per pump 500 cfs, pool el 275.0

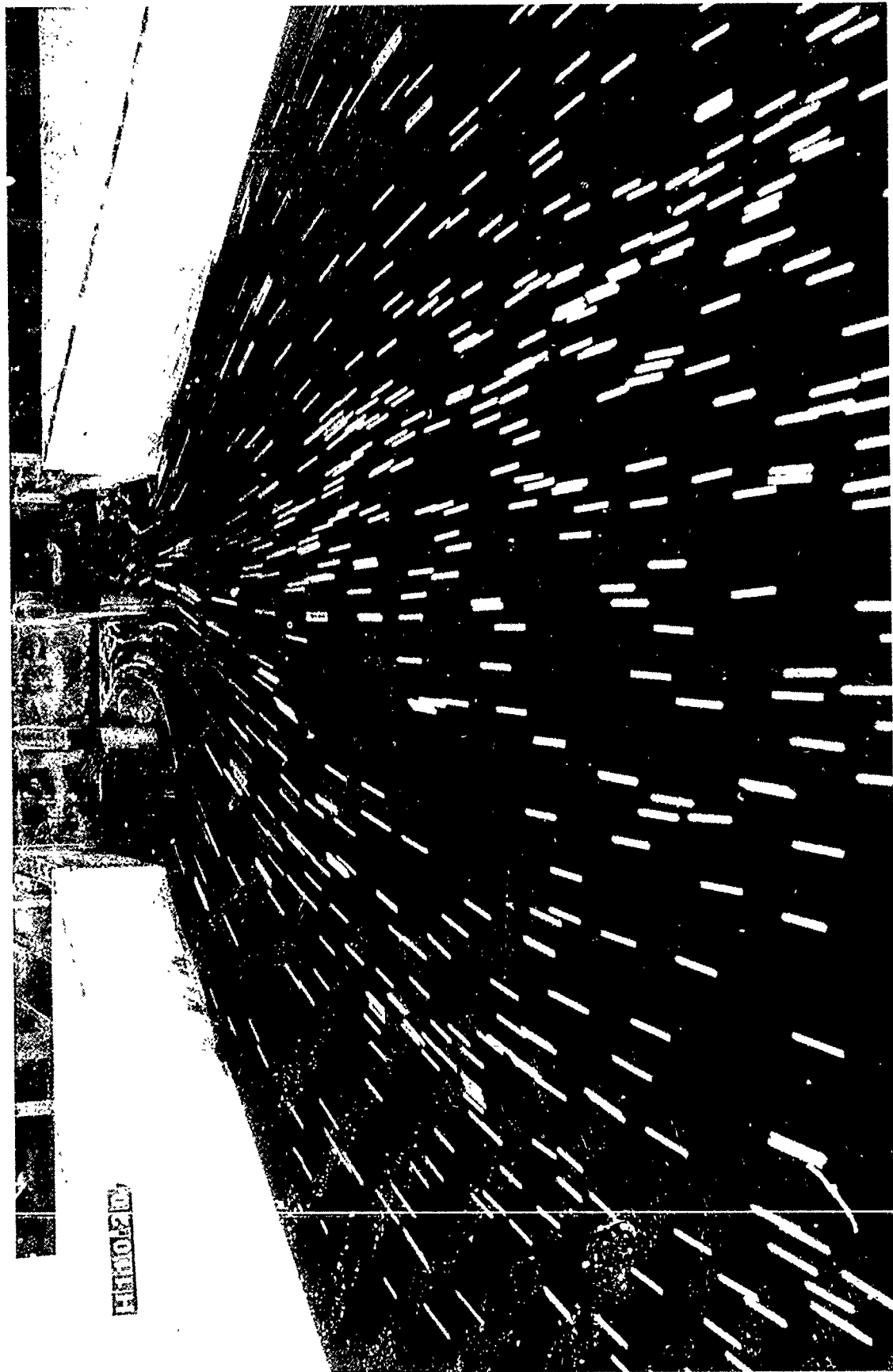


Photo 3. Surface flow pattern, two pumps operating, discharge per pump 500 cfs, pool el 275.0

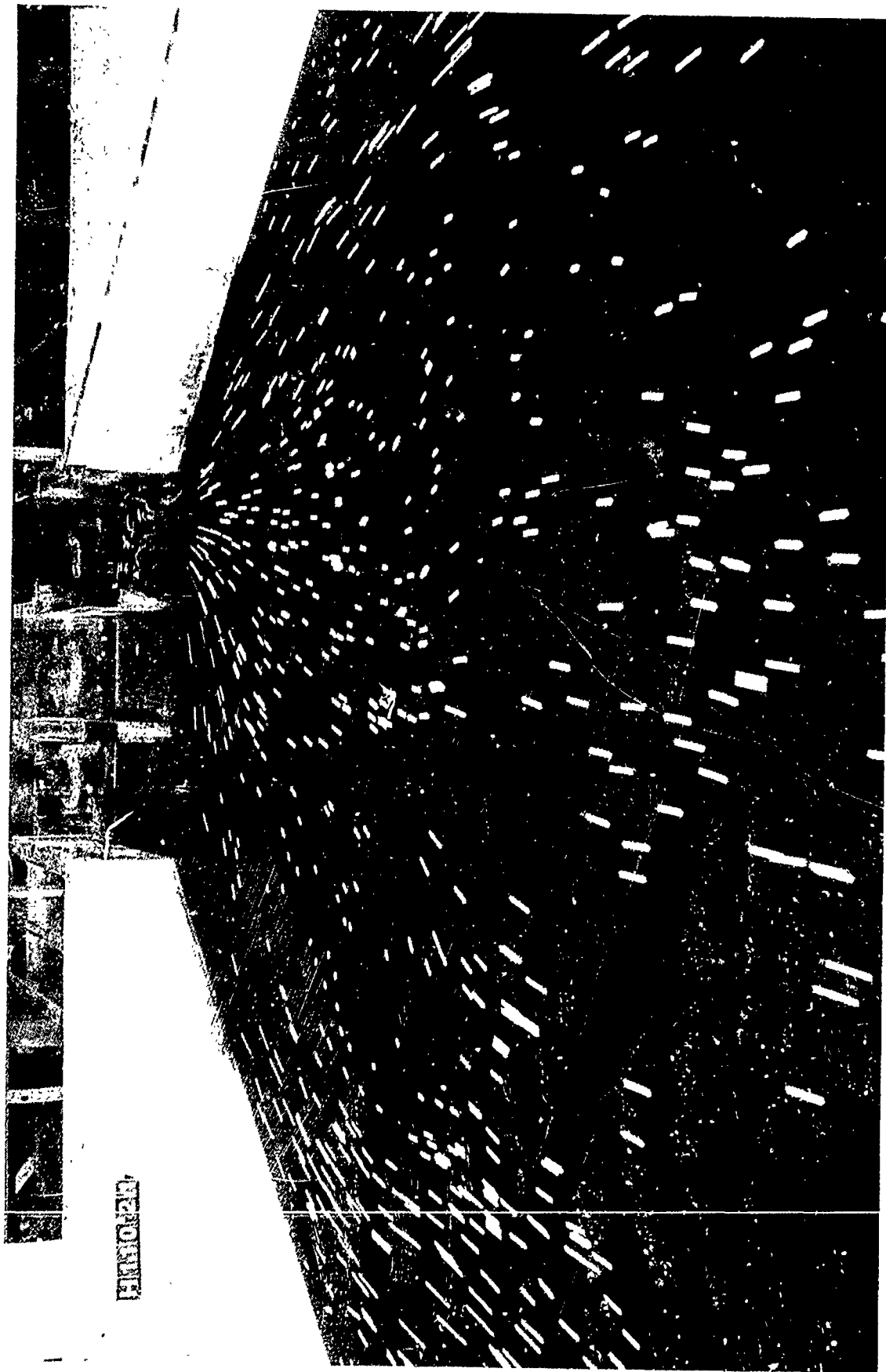


Photo 4. Surface flow pattern, one pump operating, discharge per pump 500 cfs, pool el 275.0

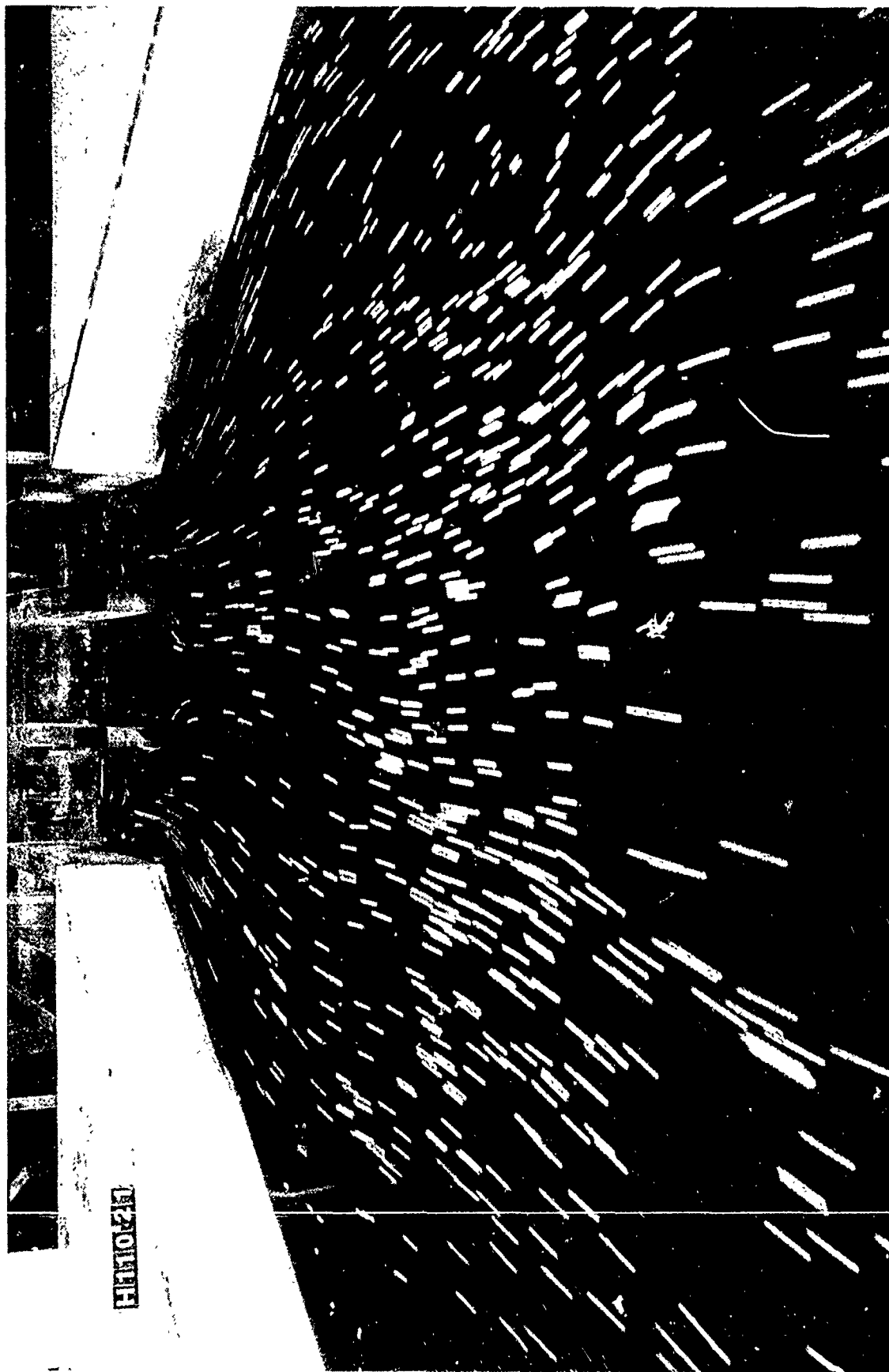


Photo 5. Surface pattern, pumps 1 and 3 operating, discharge per pump 500 cfs, pool el 275.0

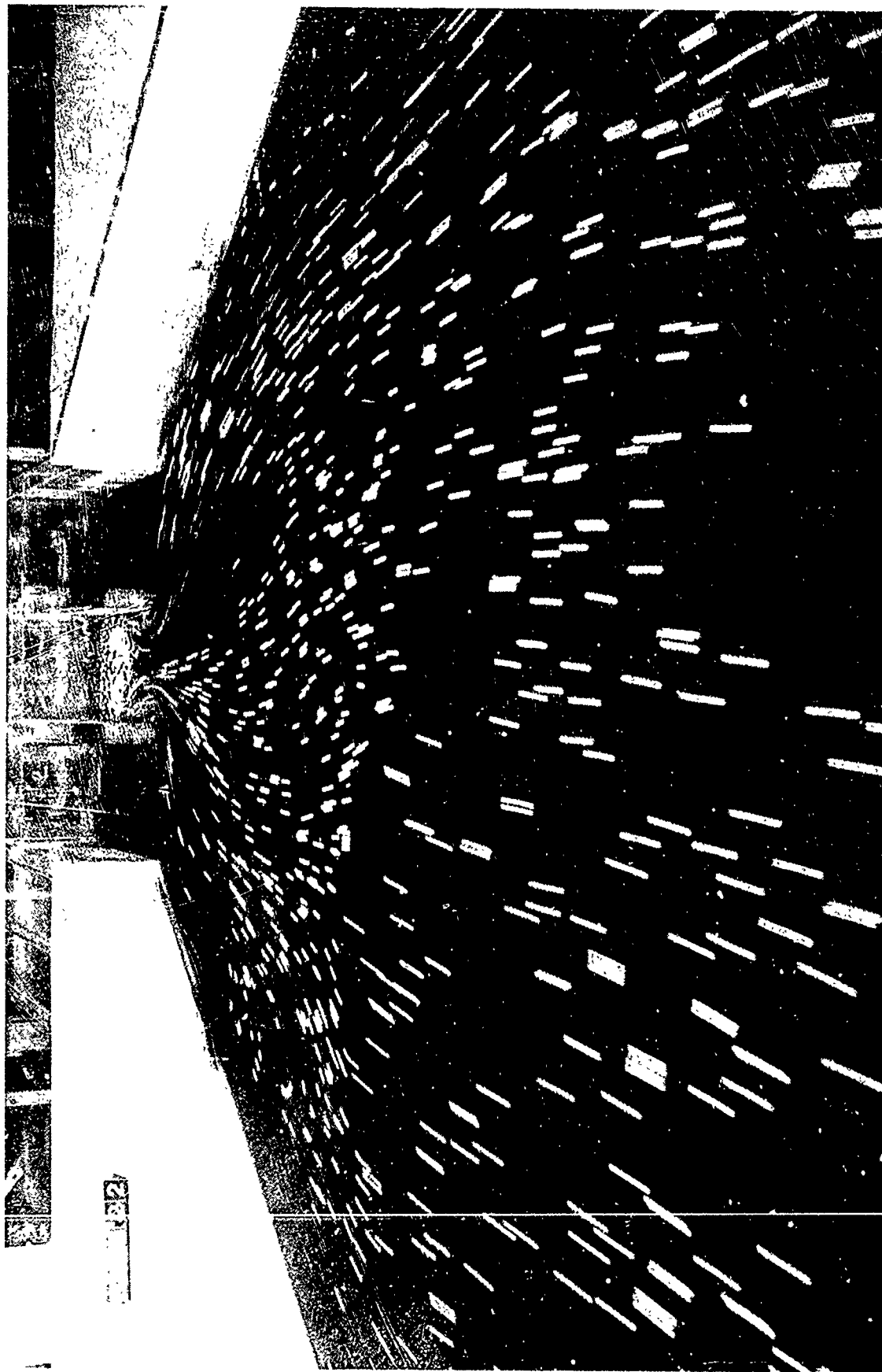


Photo 6. Surface pattern, pump 2 operating, discharge per pump 500 cfs, pool el 275.0

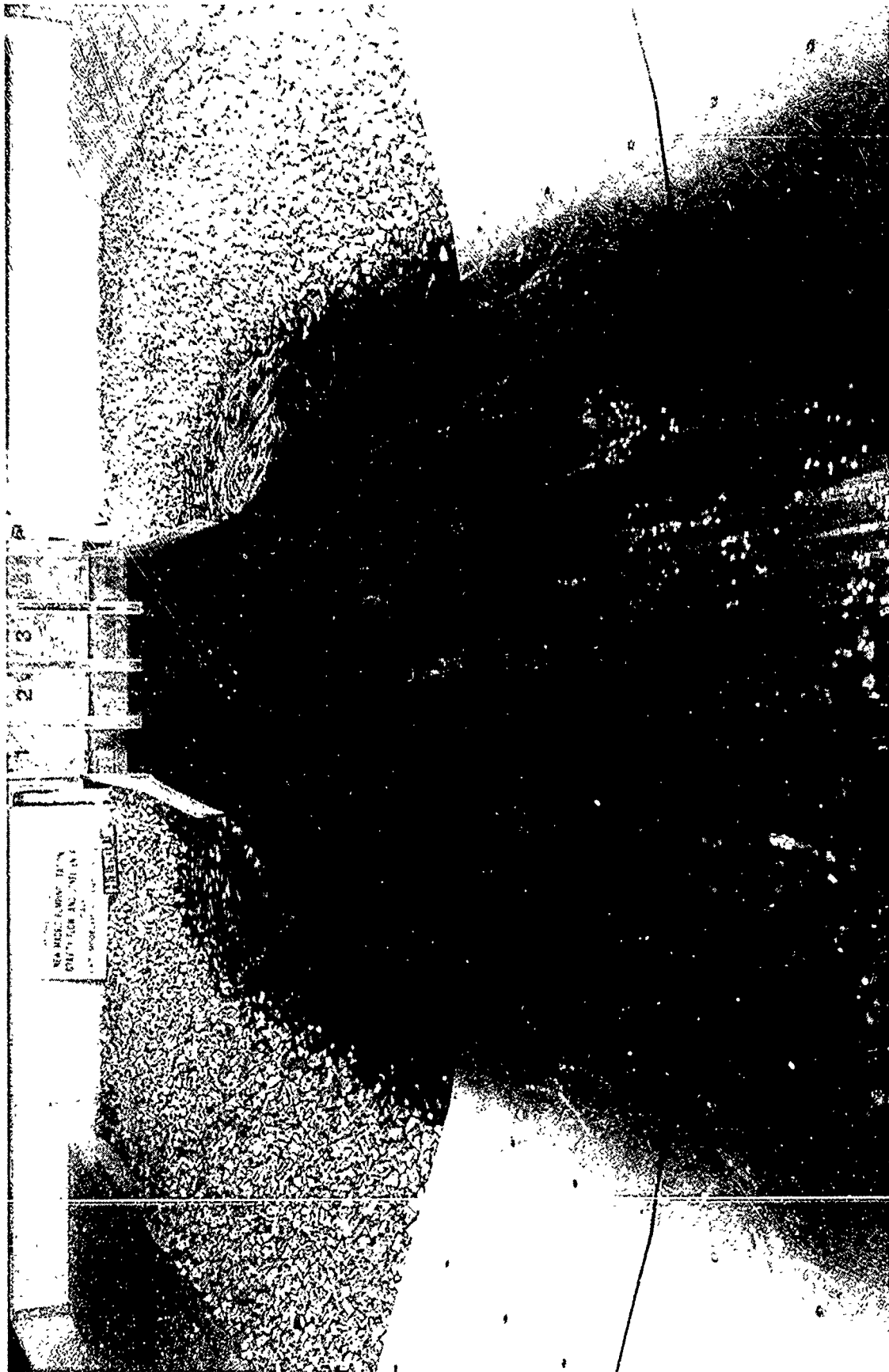


Photo 7. Surface flow pattern, gravity flow stilling basin, discharge 5,000 cfs, tailwater el 270.3

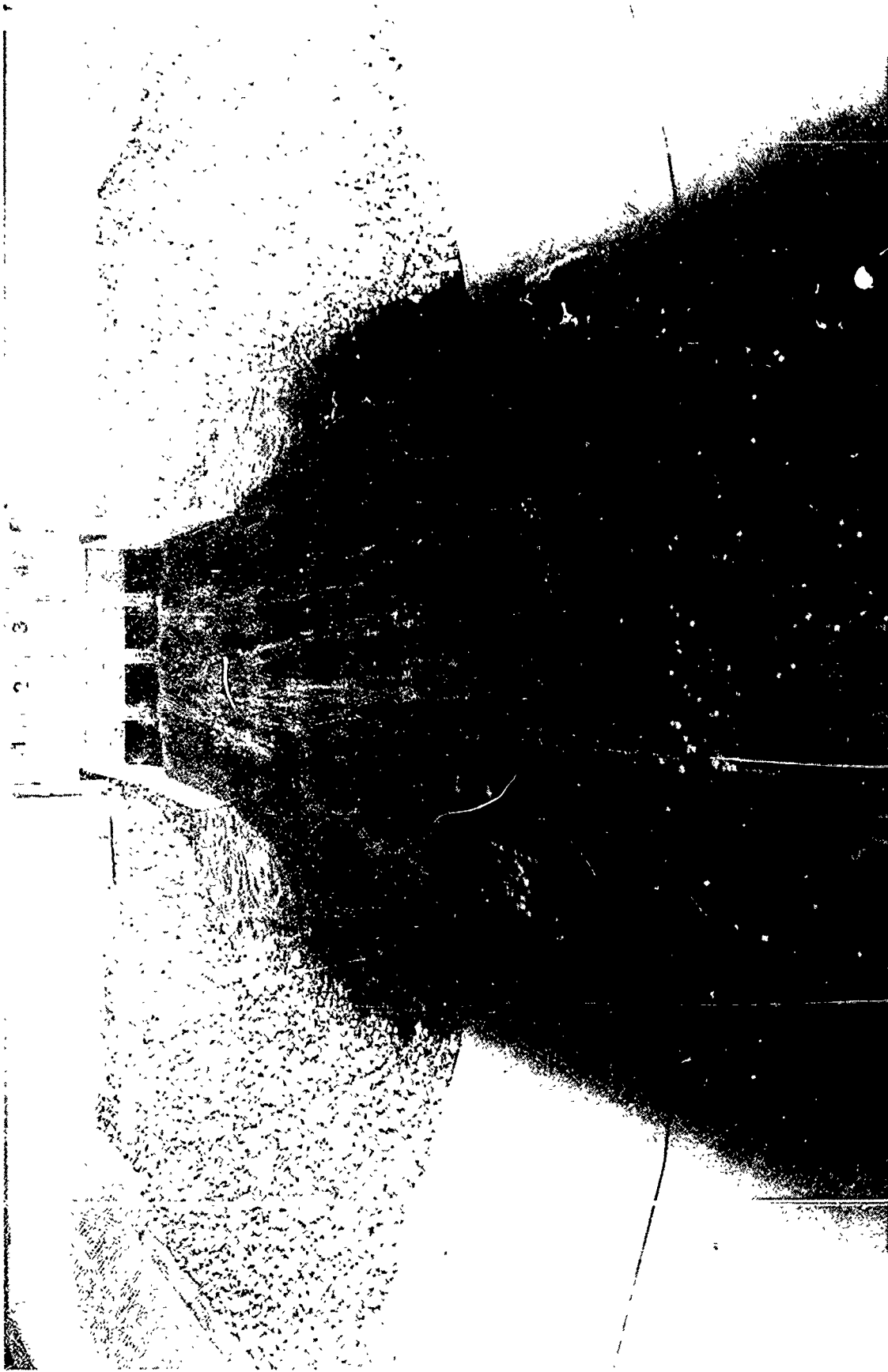


Photo 8. Surface flow pattern, gravity flow stilling basin, discharge 5,000 cfs, tailwater el 267.4





Photo 9. Surface flow pattern, confluence of channels, discharge 5,000 cfs, tailwater: el 270.3



Photo 10. Surface flow pattern at the confluence of the channels,  
siphon discharges only, discharge 1,000 cfs, tailwater el 279.0

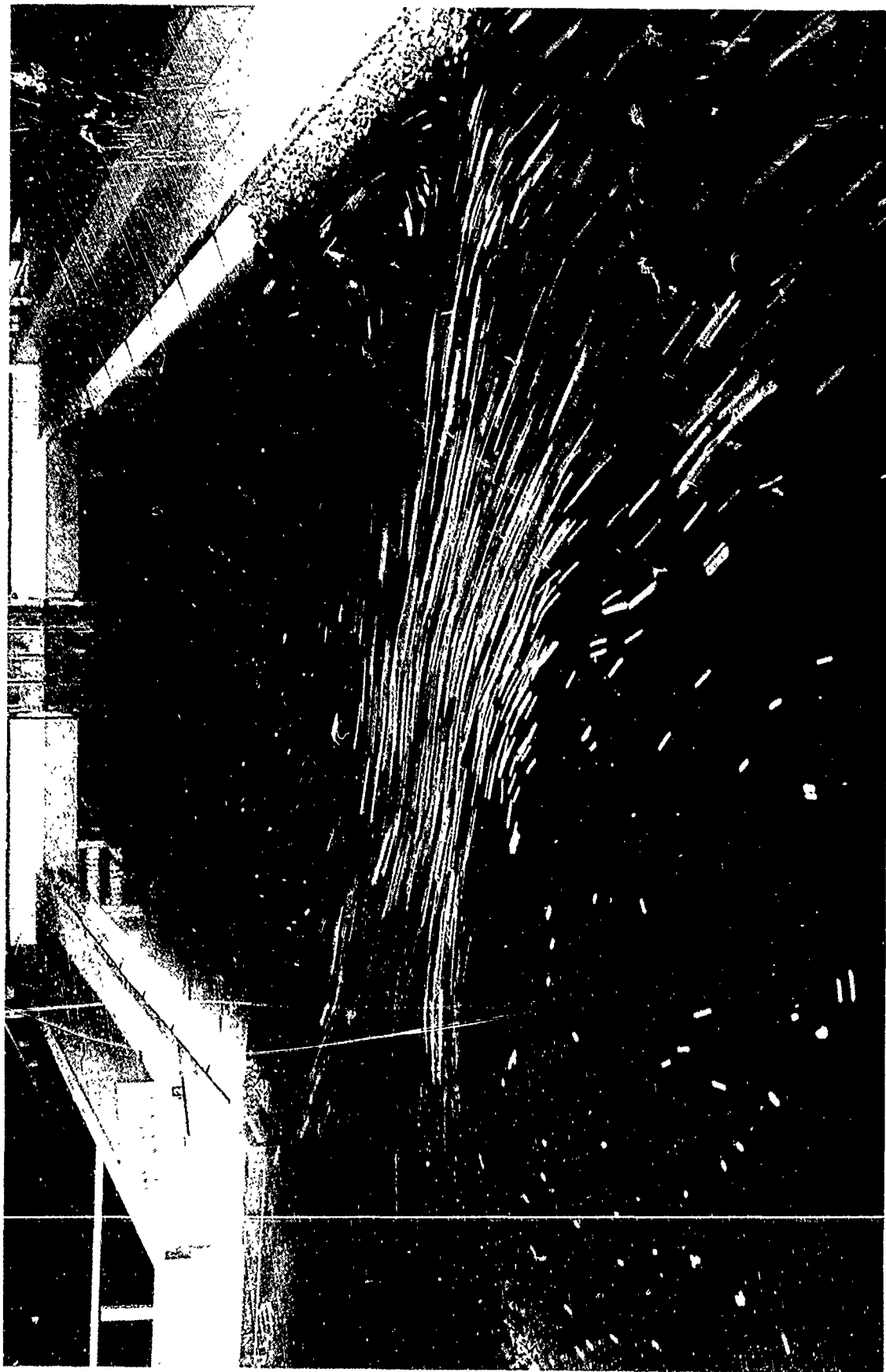


Photo 11. Surface flow pattern at the confluence of the channels,  
siphon discharges only, discharge 1,000 cfs, tailwater el 290.0

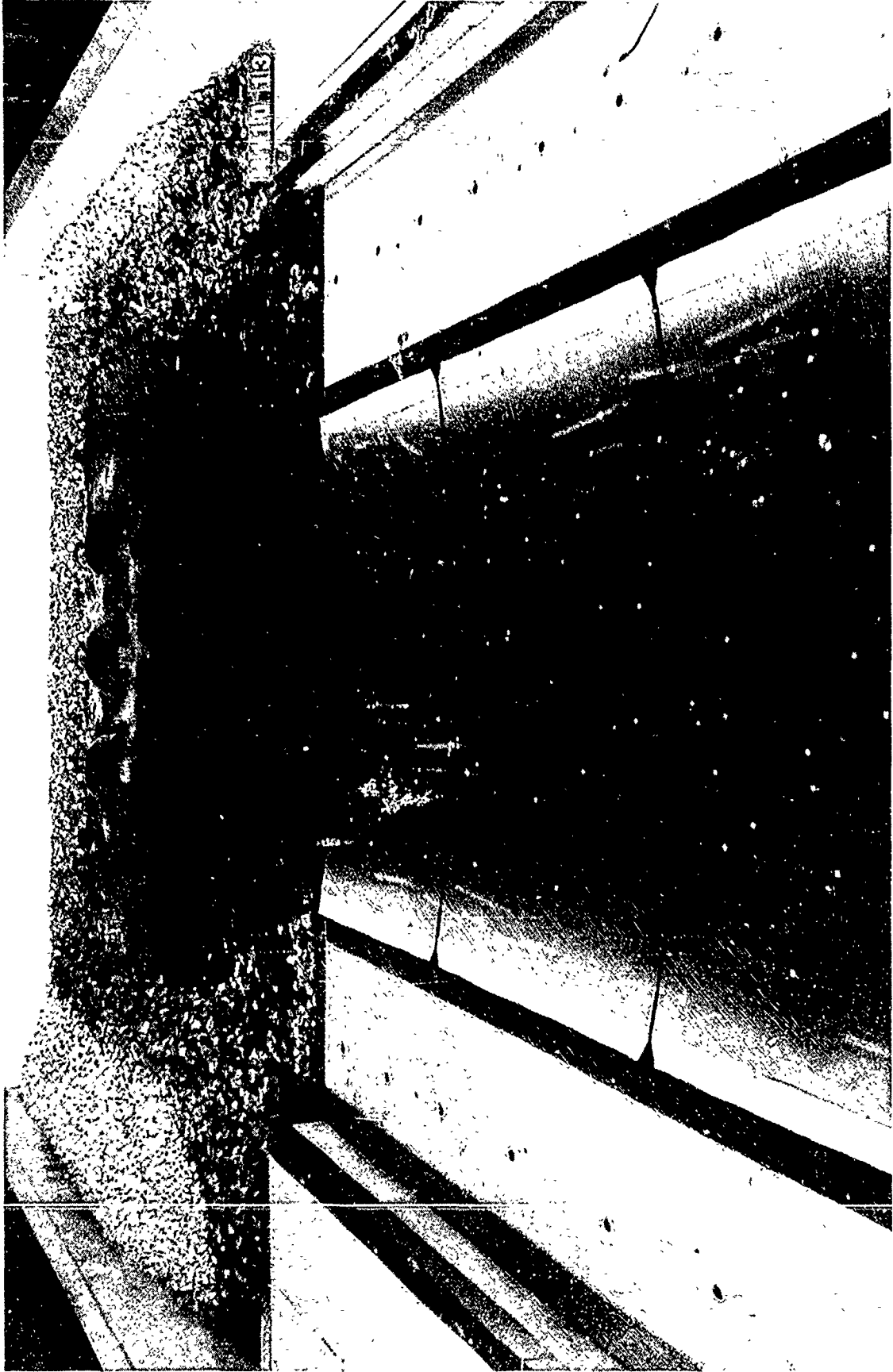


Photo 12. Plume and surface patterns, saxophone outlet operating, discharge per pump 333 cfs, tailwater el 279.0



Photo 13. Plume and surface patterns, confluence with saxophone outlet, discharge per pump 333 cfs, tailwater el 279.0



Photo 14. Plume and surface patterns, saxophone outlet operating, discharge per pump 333 cfs, tailwater el 290.0

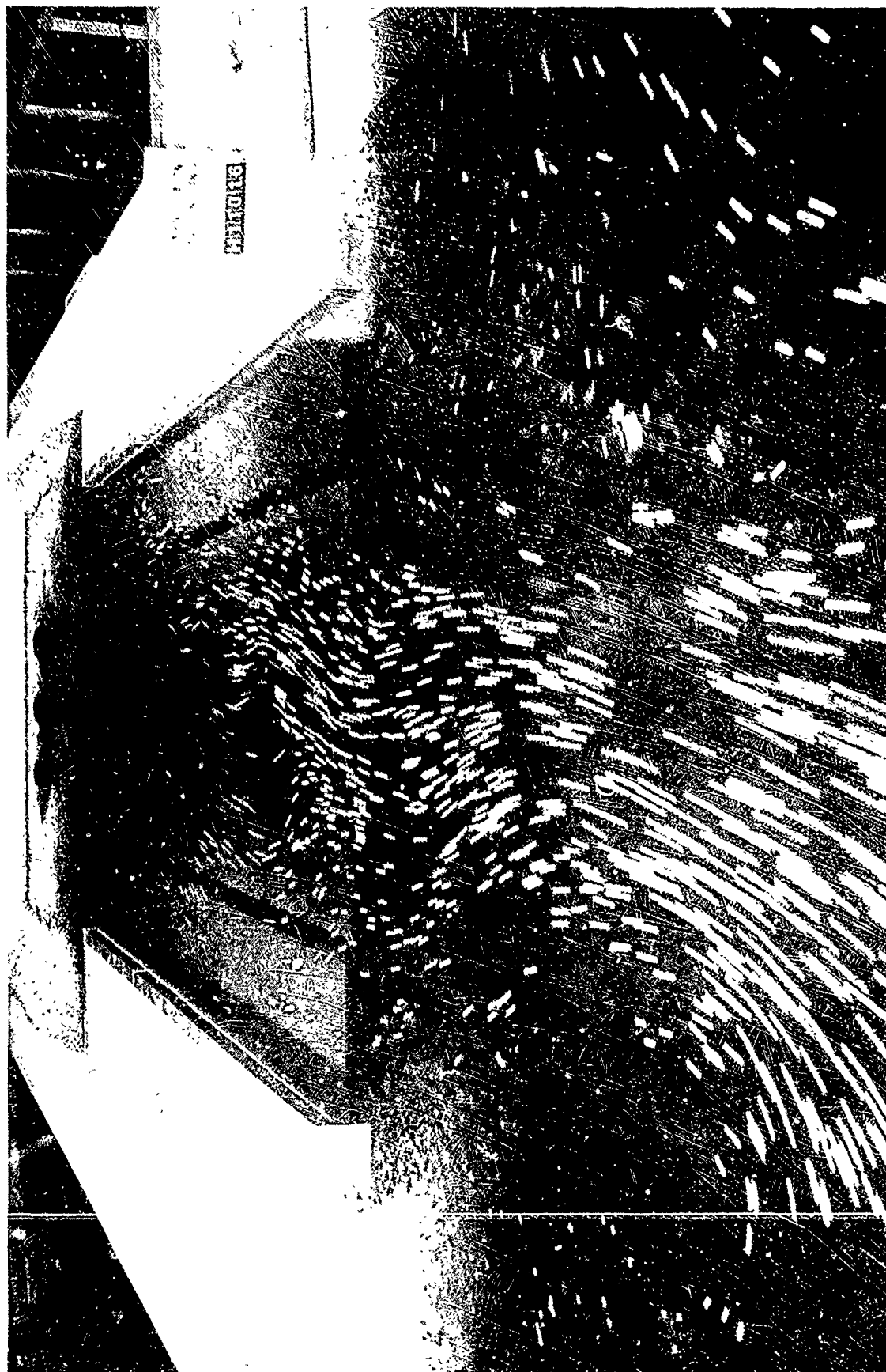
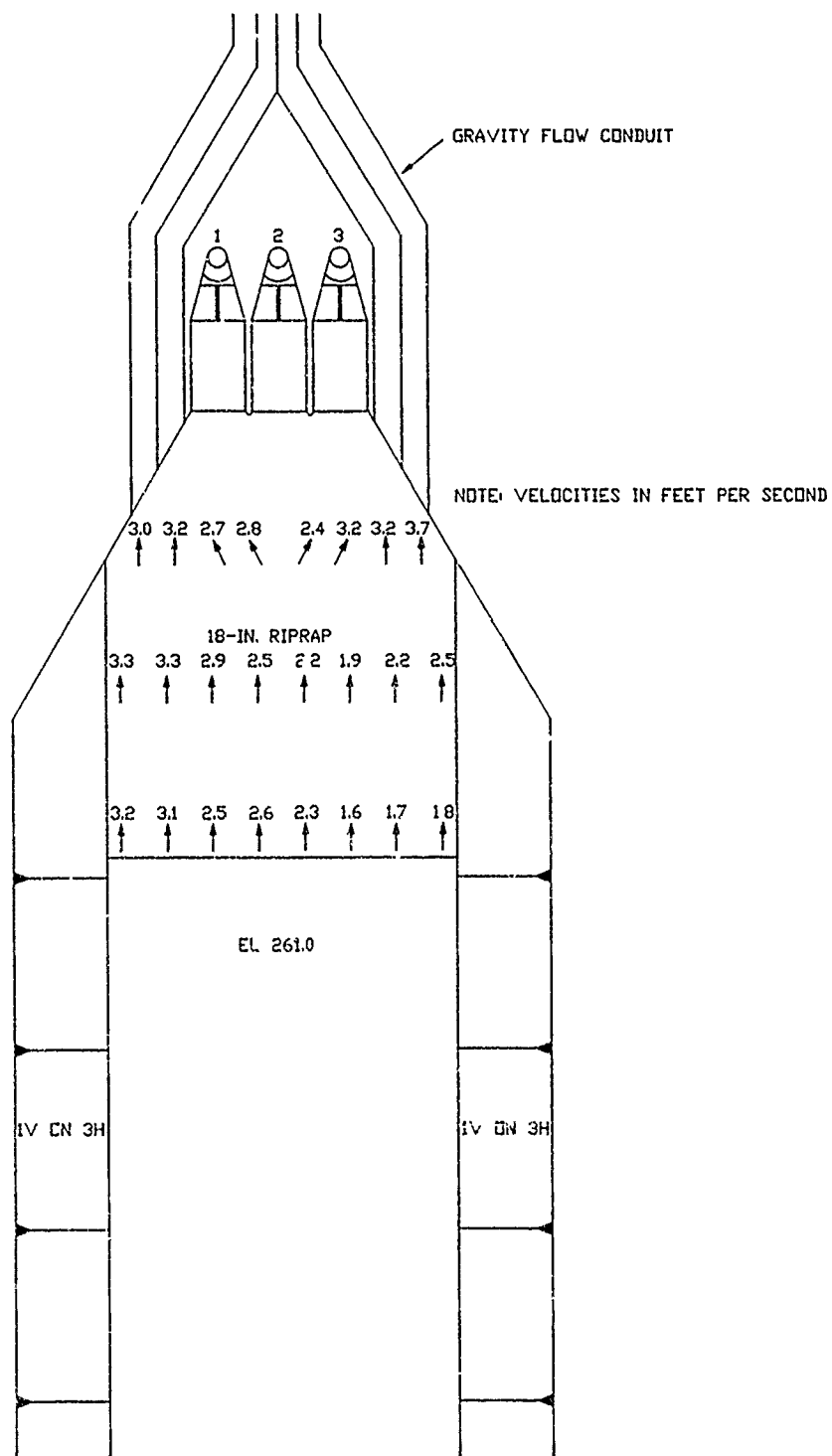
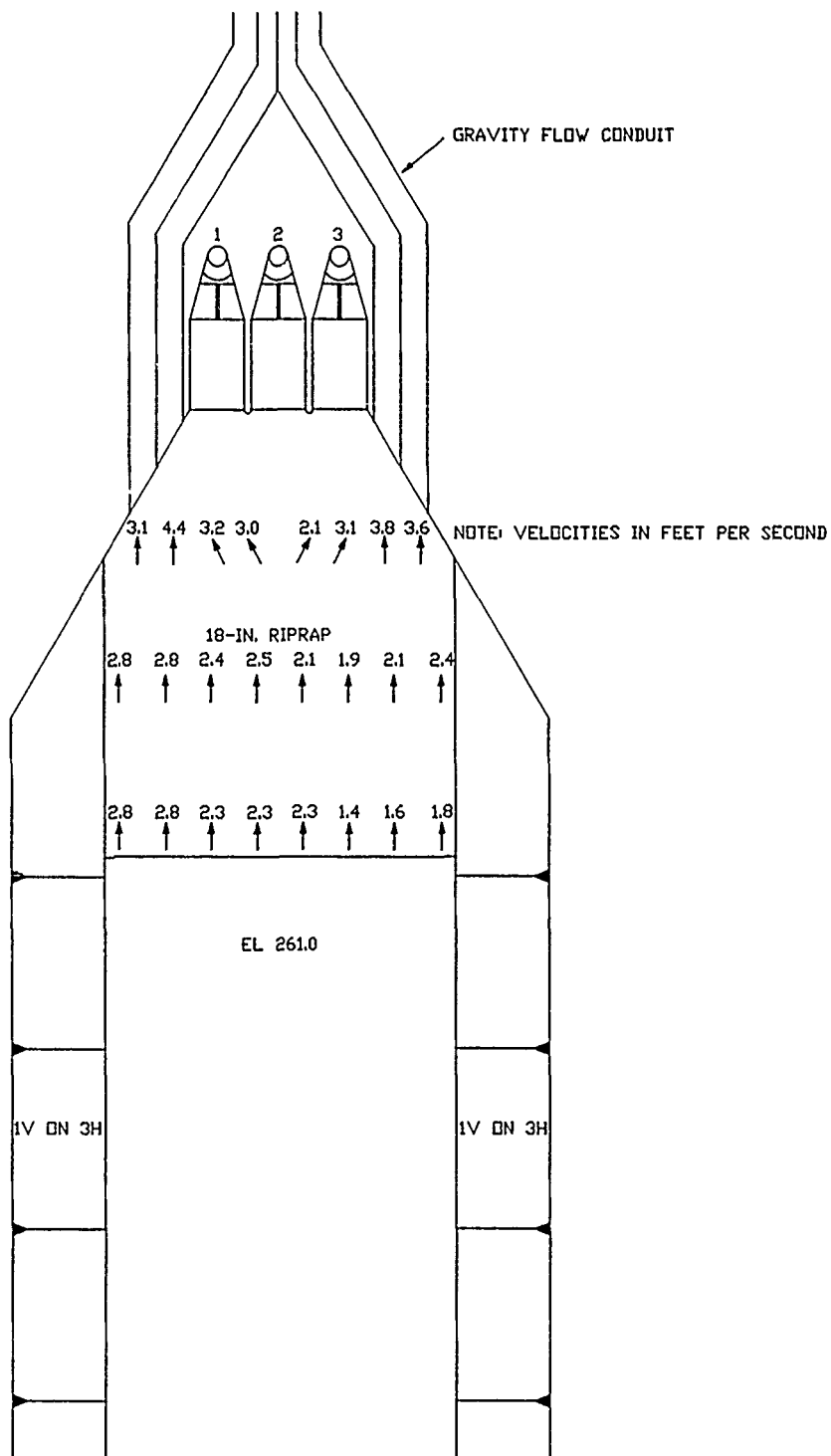


Photo 15. Plume and surface patterns, confluence with saxophone outlet,  
discharge per pump 333 cfs, tailwater el 290.0

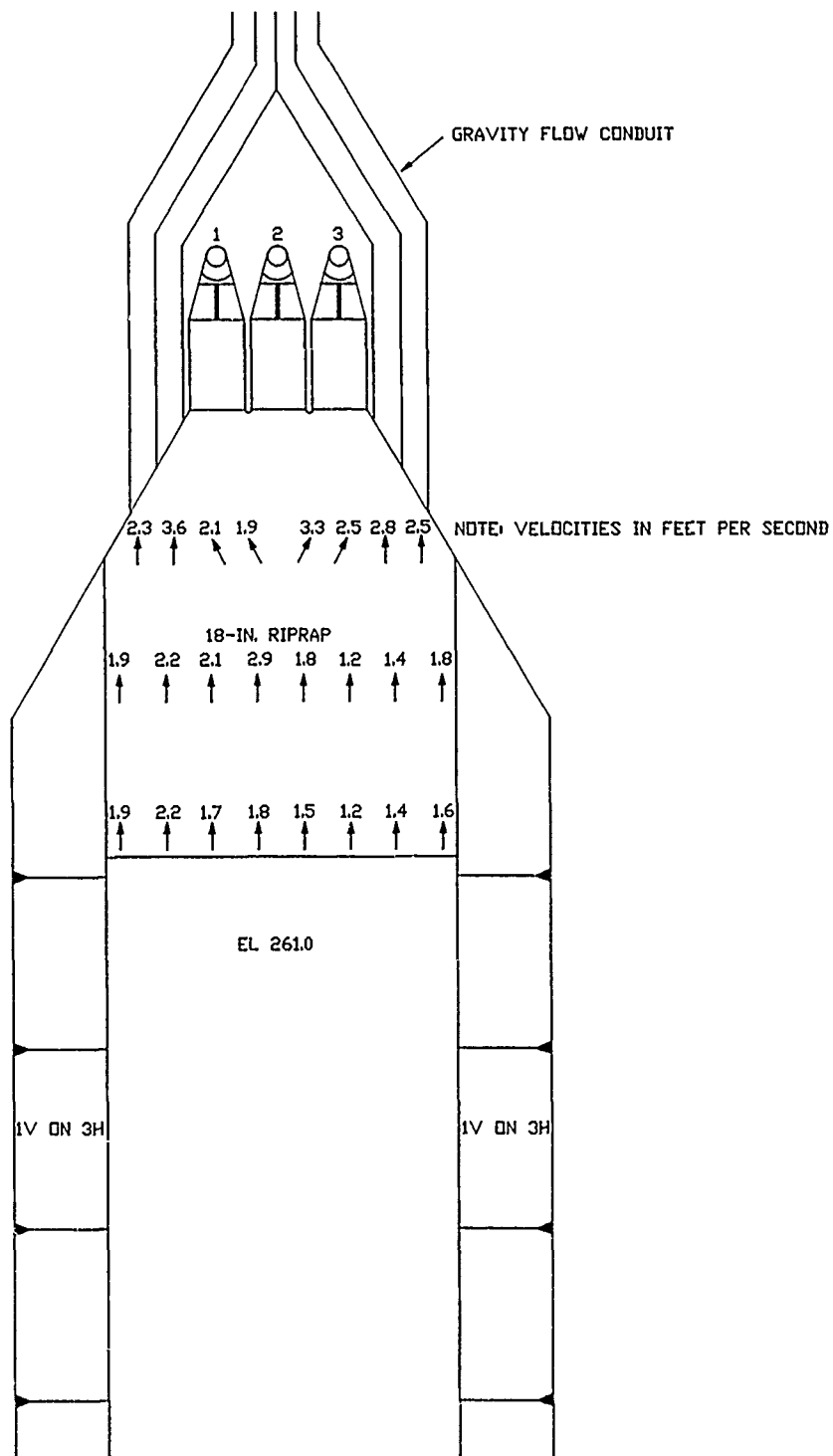


SURFACE VELOCITY IN CHANNEL WITH GRAVITY FLOW  
 5,000-CFS GRAVITY FLOW  
 TAILWATER EL 270.3

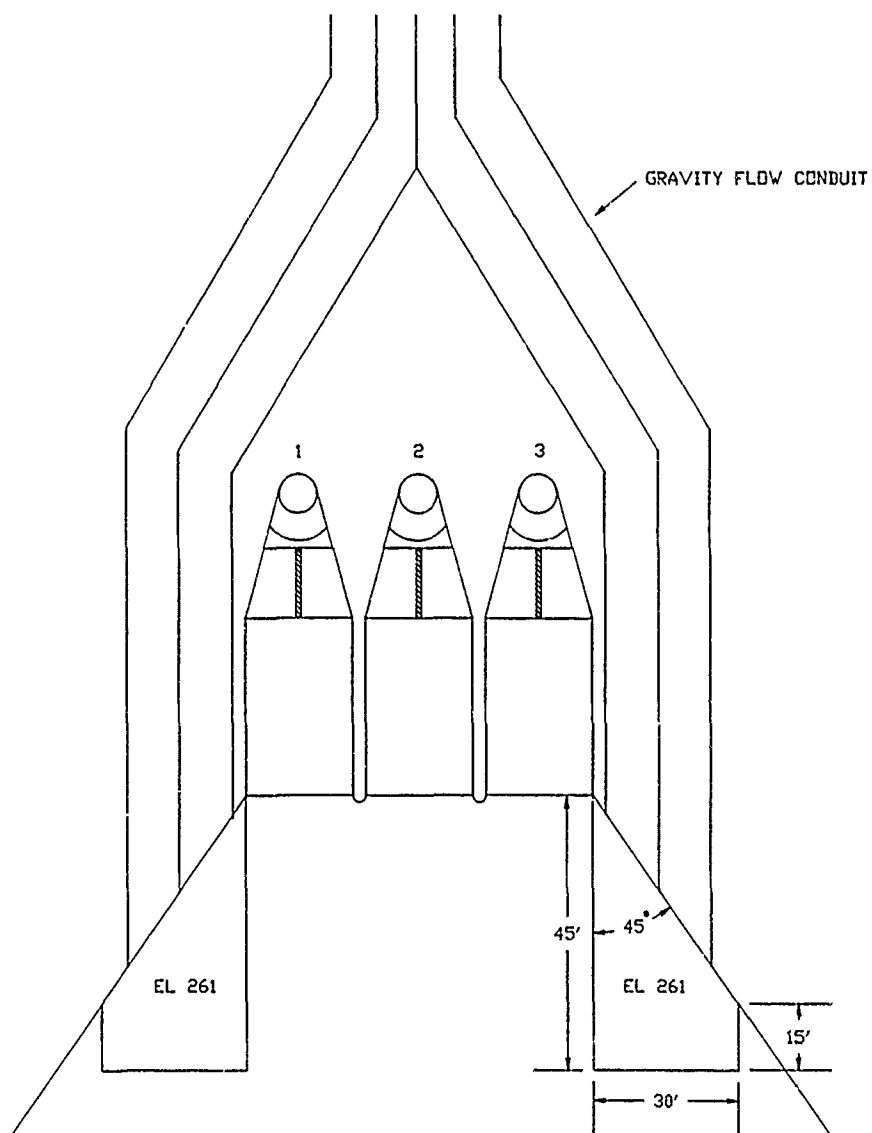




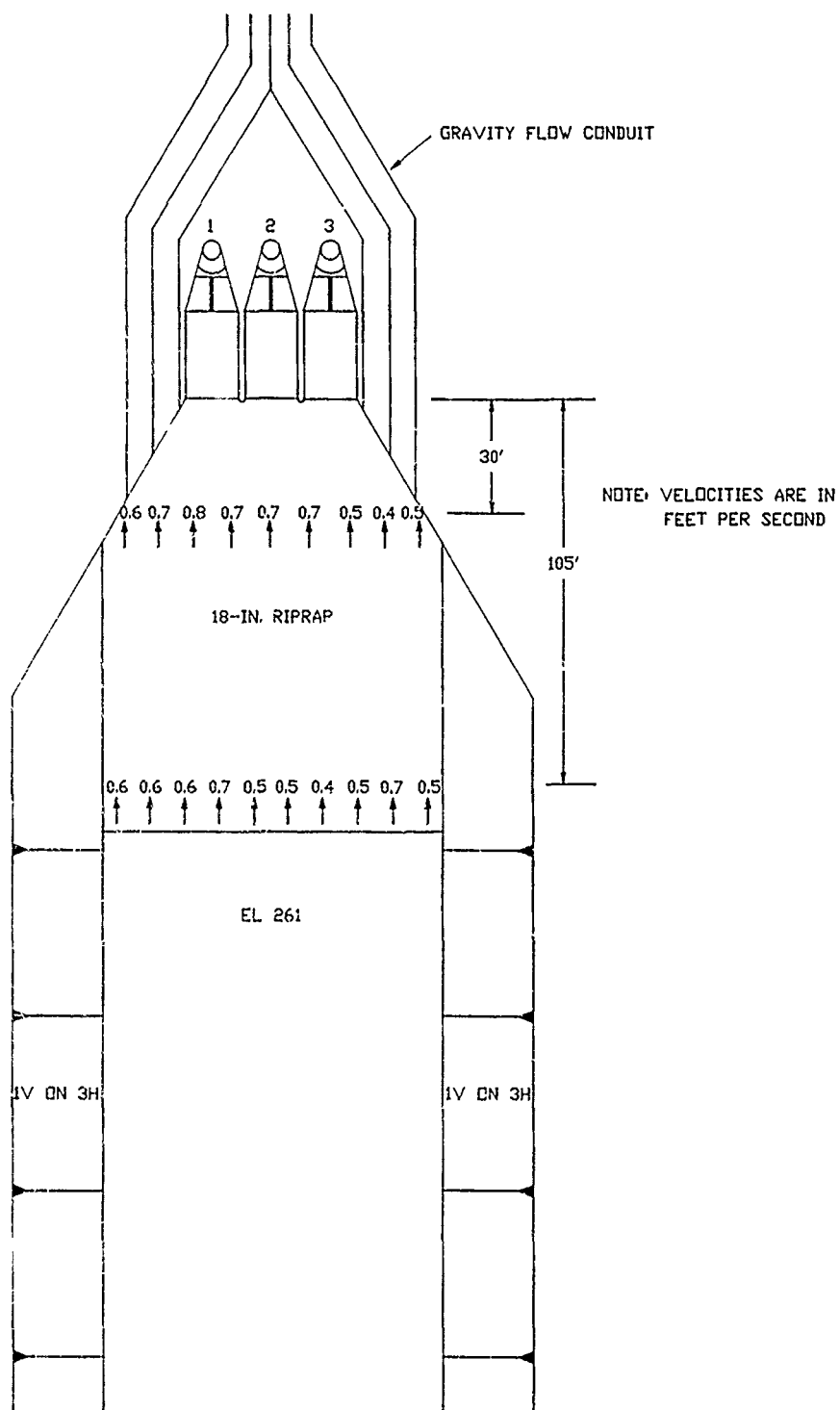
MIDDEPTH VELOCITIES IN CHANNEL WITH GRAVITY FLOW  
5,000-CFS GRAVITY FLOW  
TAILWATER EL 270.3



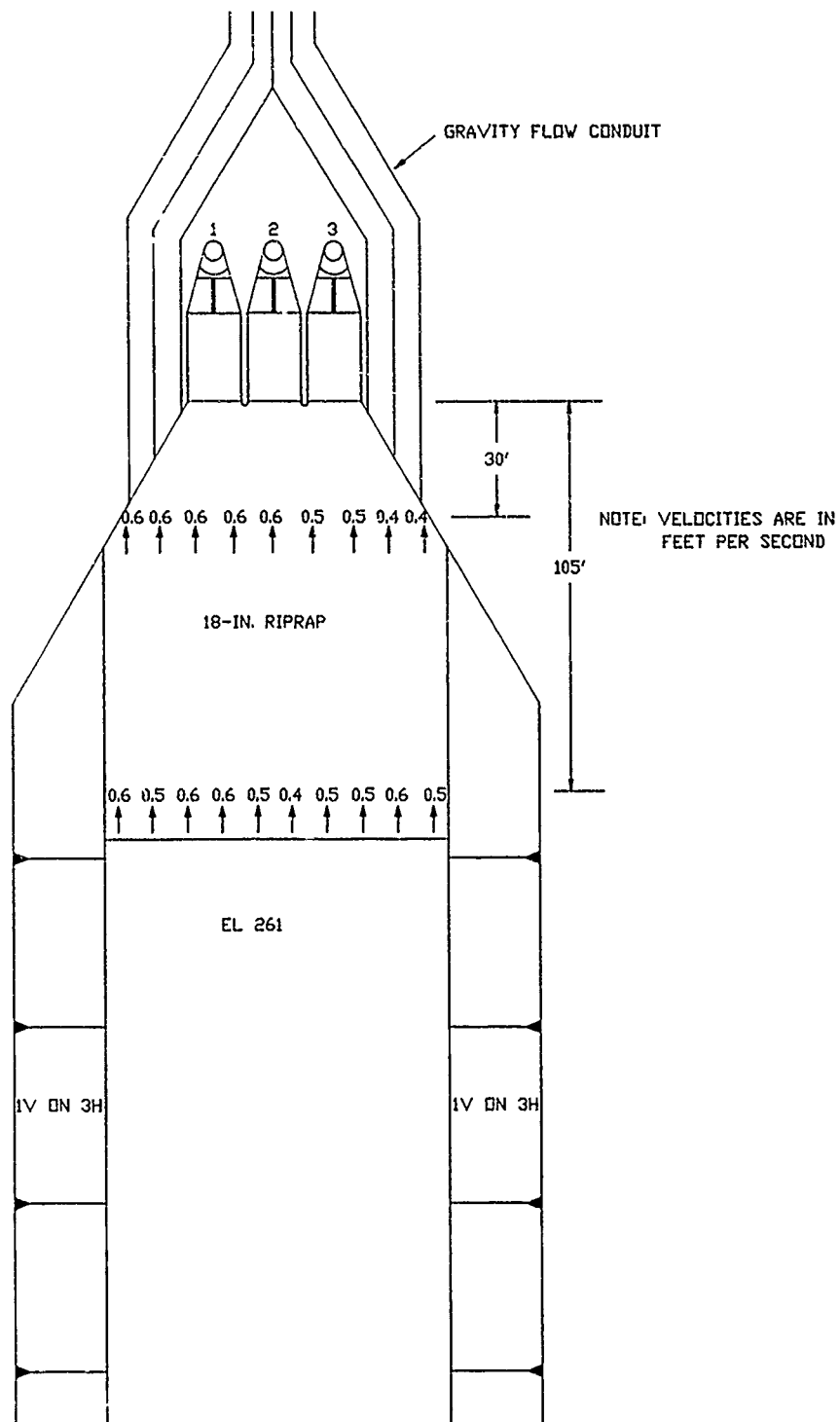
BOTTOM VELOCITIES IN CHANNEL WITH GRAVITY FLOW  
 5,000-CFS GRAVITY FLOW  
 TAILWATER EL 270.3



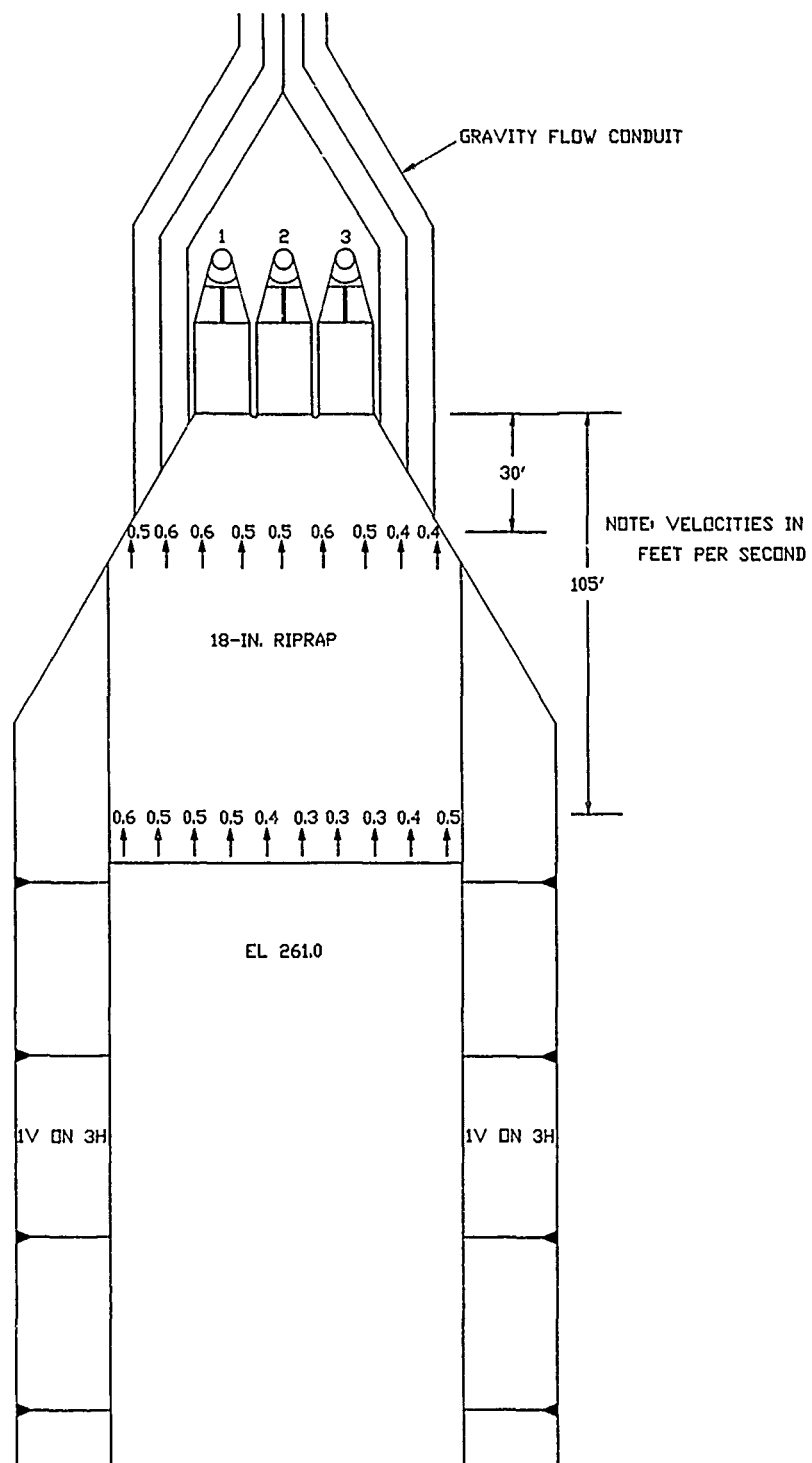
SCOUR SLAB  
APPROACH TO GRAVITY BAYS



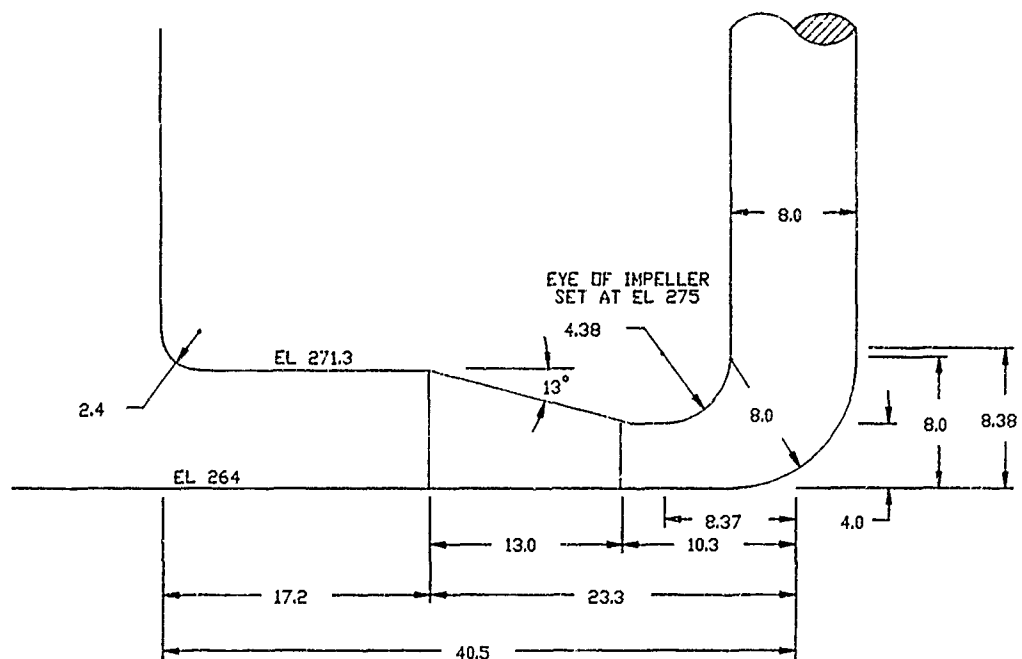
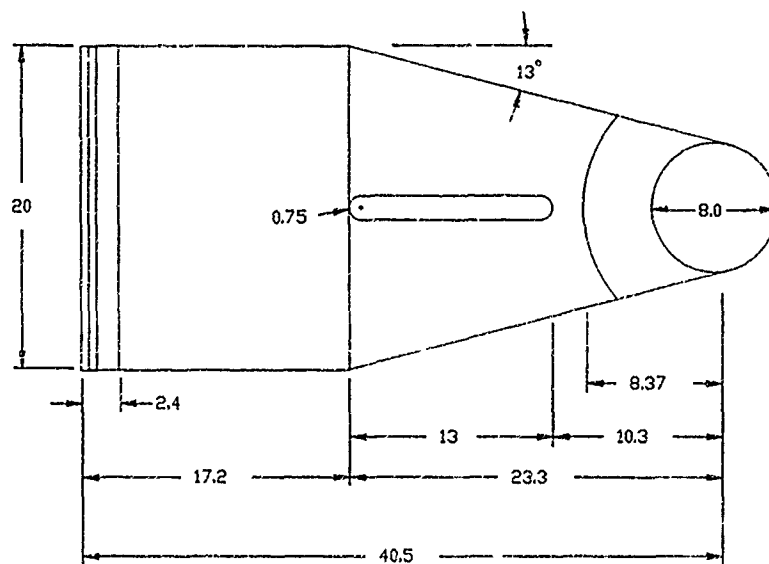
SURFACE VELOCITIES IN APPROACH CHANNEL  
 3 PUMPS OPERATING  
 DISCHARGE PER PUMP 500 CFS  
 POOL EL 275



MIDDEPTH VELOCITIES IN APPROACH CHANNEL  
 3 PUMPS OPERATING  
 DISCHARGE PER PUMP 500 CFS  
 POOL EL 275

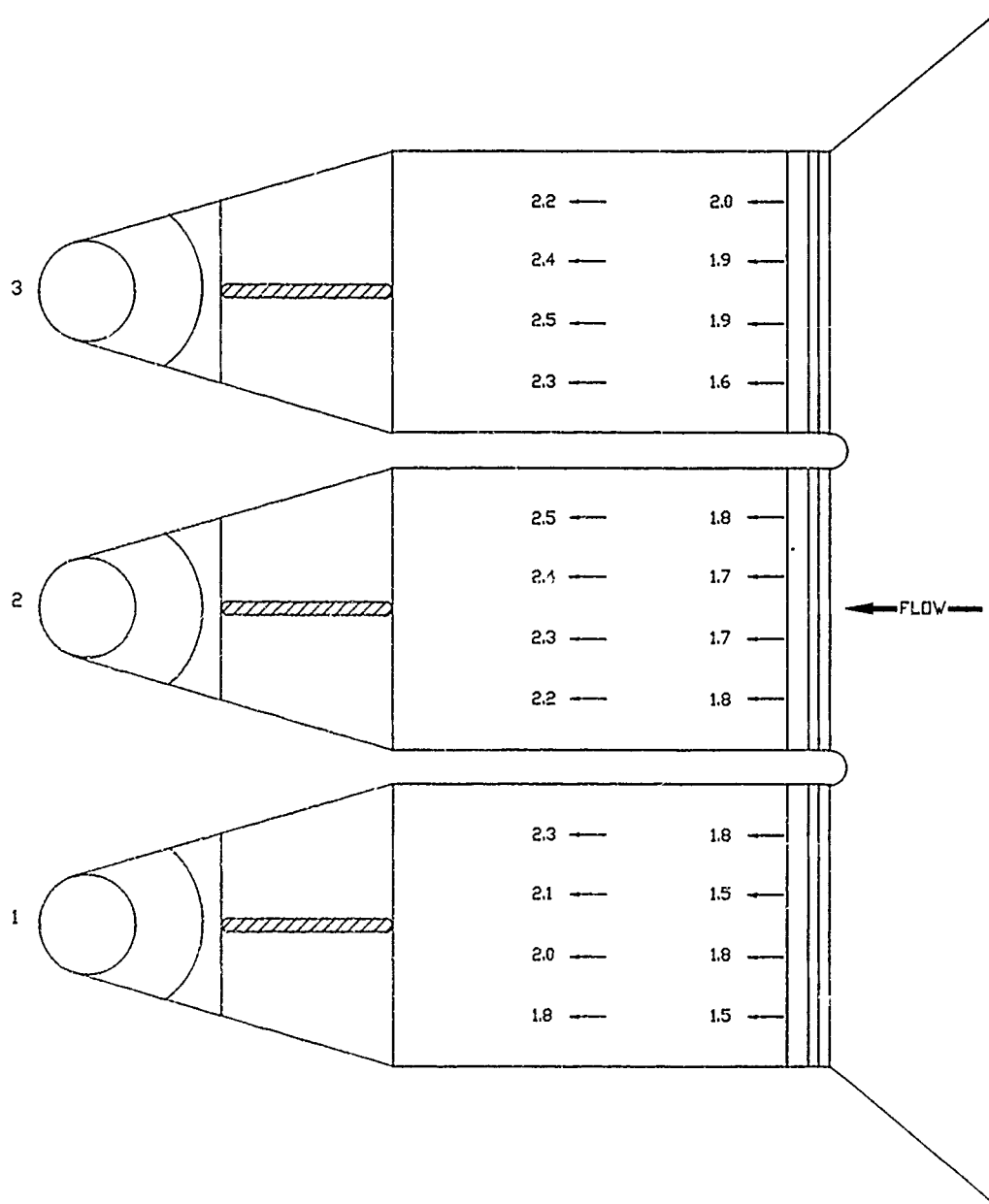


BOTTOM VELOCITIES IN APPROACH CHANNEL  
 3 PUMPS OPERATING  
 DISCHARGE PER PUMP 500 CFS  
 POOL EL 275



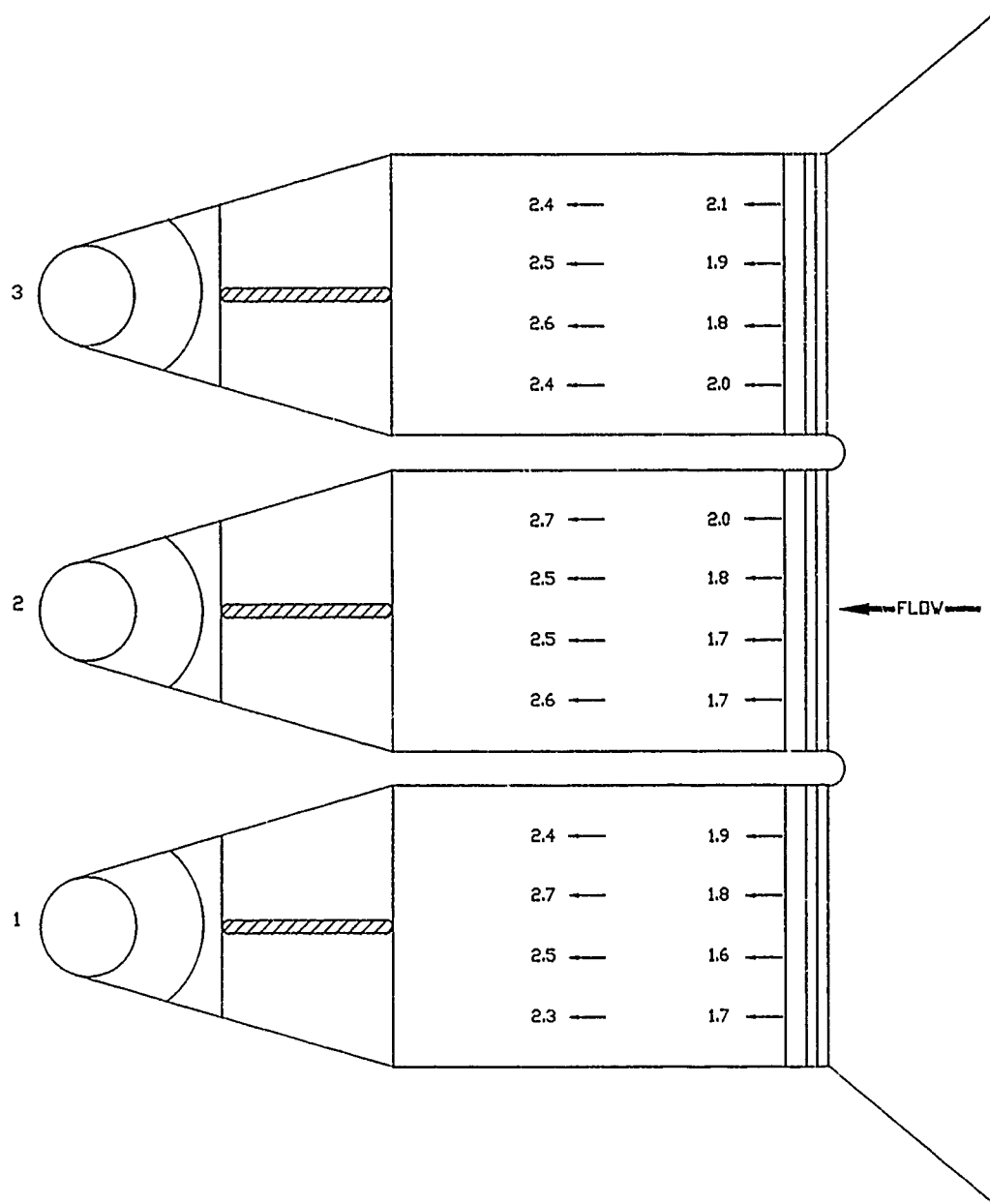
NOTE: ALL DIMENSIONS IN FEET

DESIGN A  
FSI

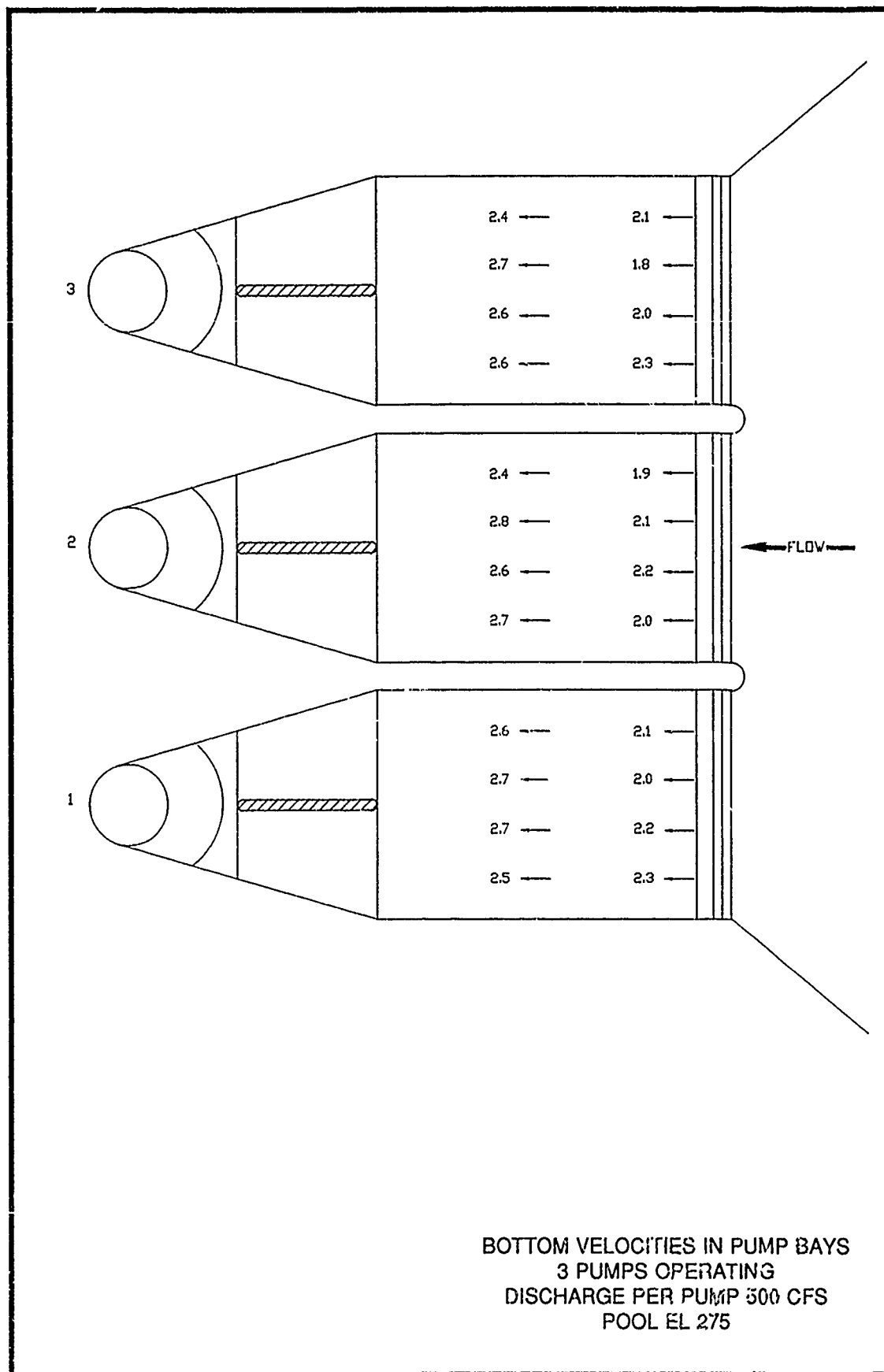


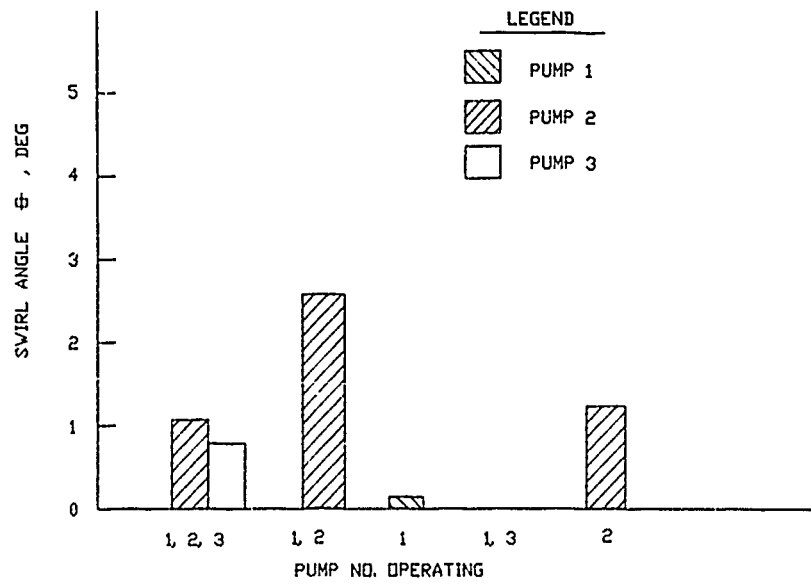
SURFACE VELOCITIES IN PUMP BAYS  
 3 PUMPS OPERATING  
 DISCHARGE PER PUMP 500 CFS  
 POOL EL 275



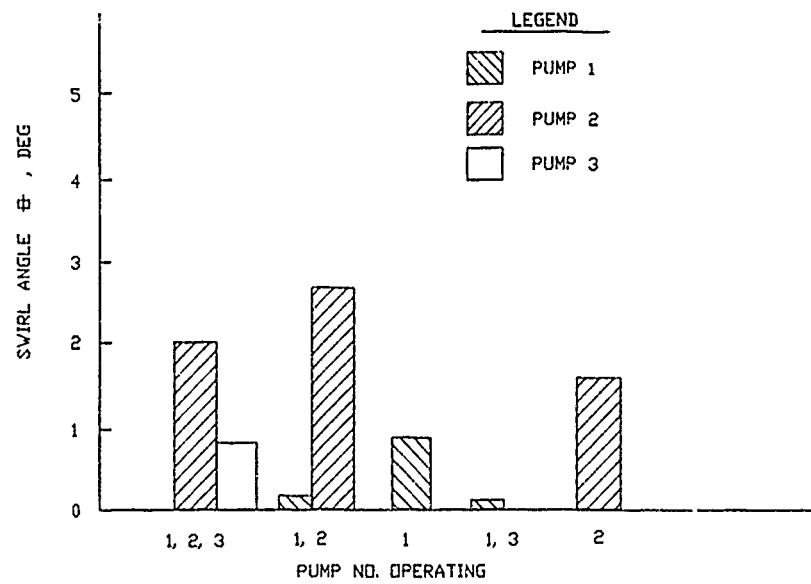


MIDDEPTH VELOCITIES IN PUMP BAYS  
 3 PUMPS OPERATING  
 DISCHARGE PER PUMP 500 CFS  
 POOL EL 275



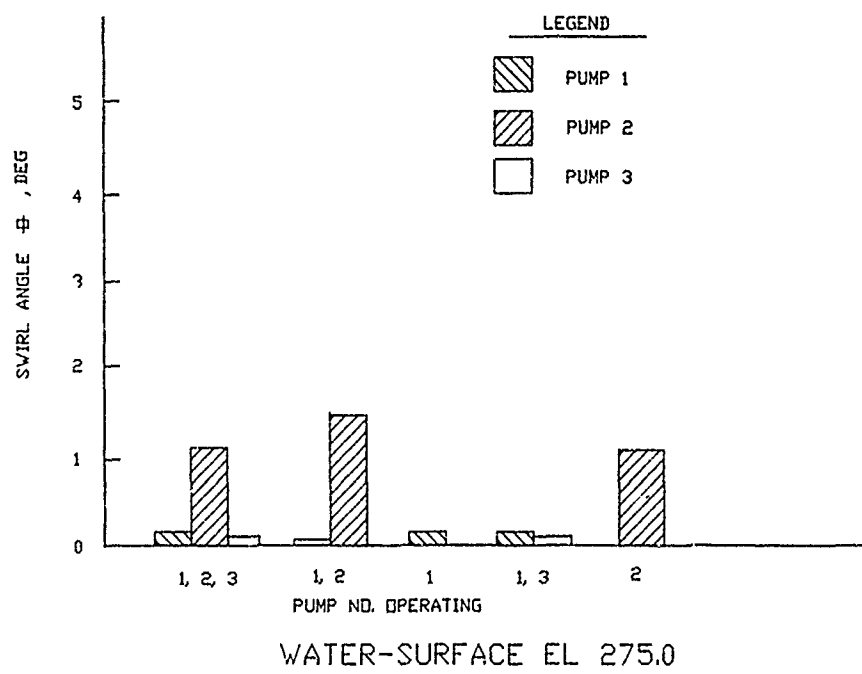
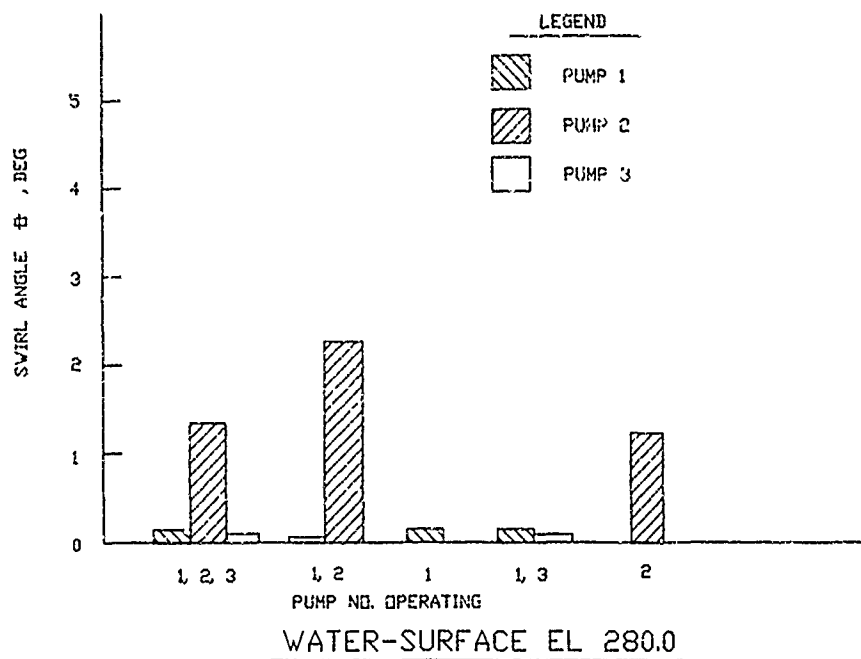


WATER-SURFACE EL 290.0

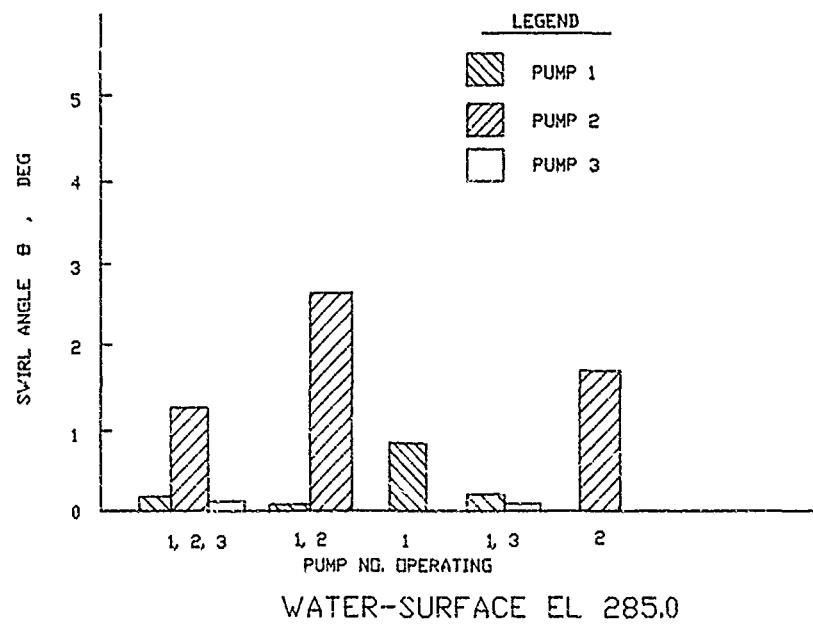
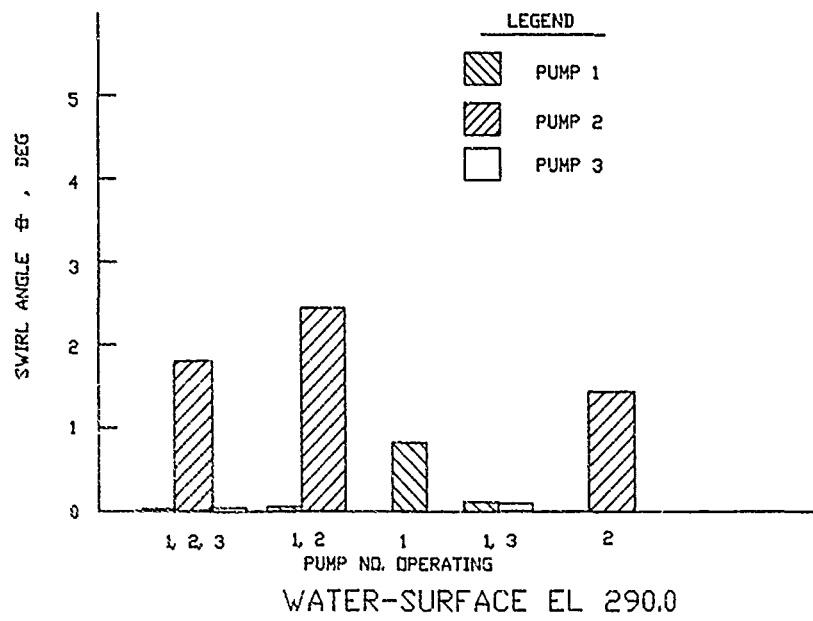


WATER-SURFACE EL 285.0

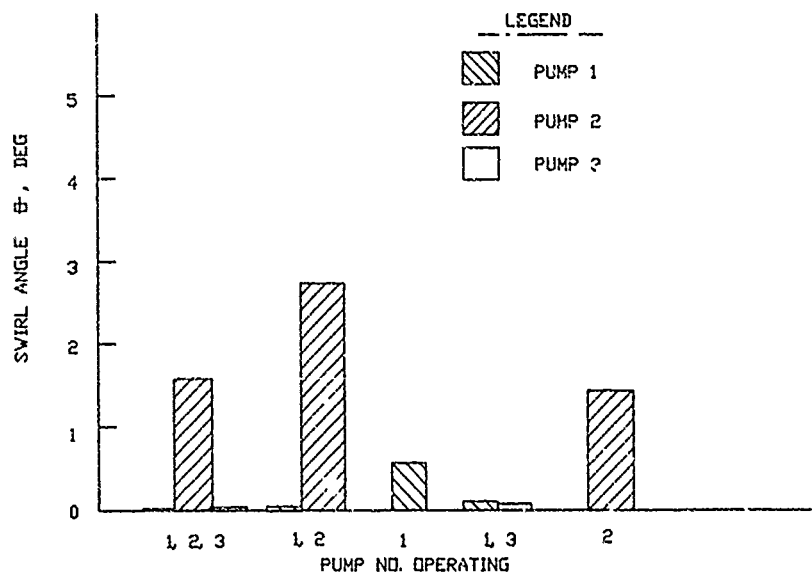
SWIRL ANGLE  
FSI DESIGN A  
DISCHARGE PER PUMP 500 CFS  
WATER-SURFACE EL 290.0 AND 285.0



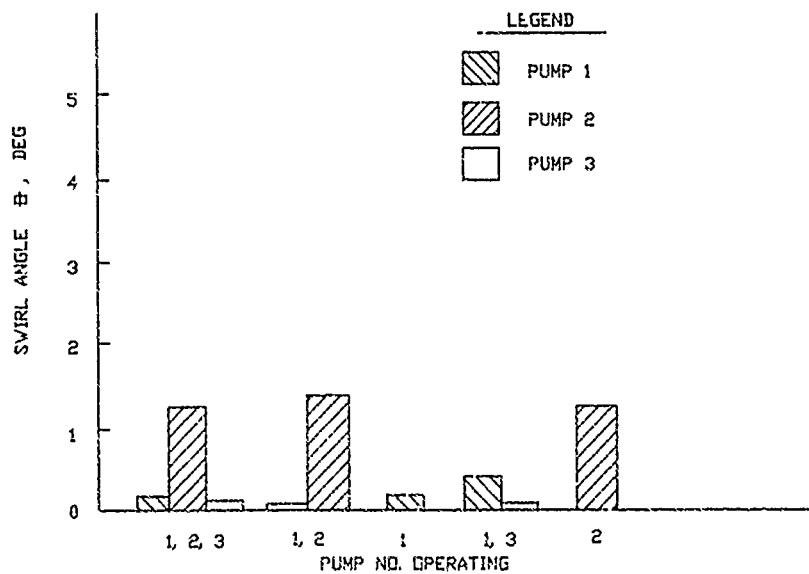
SWIRL ANGLE  
FSI DESIGN A  
DISCHARGE PER PUMP 500 CFS  
WATER-SURFACE EL 280.0 AND 275.0



SWIRL ANGLE  
FSI DESIGN A  
DISCHARGE PER PUMP 650 CFS  
WATER-SURFACE EL 290.0 AND 285.0

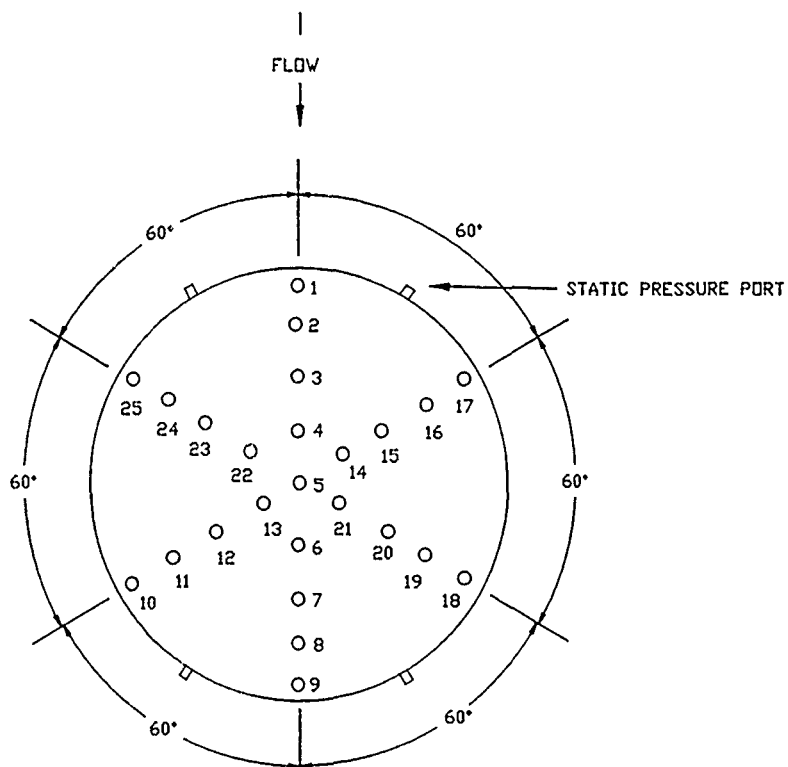


WATER-SURFACE EL 280

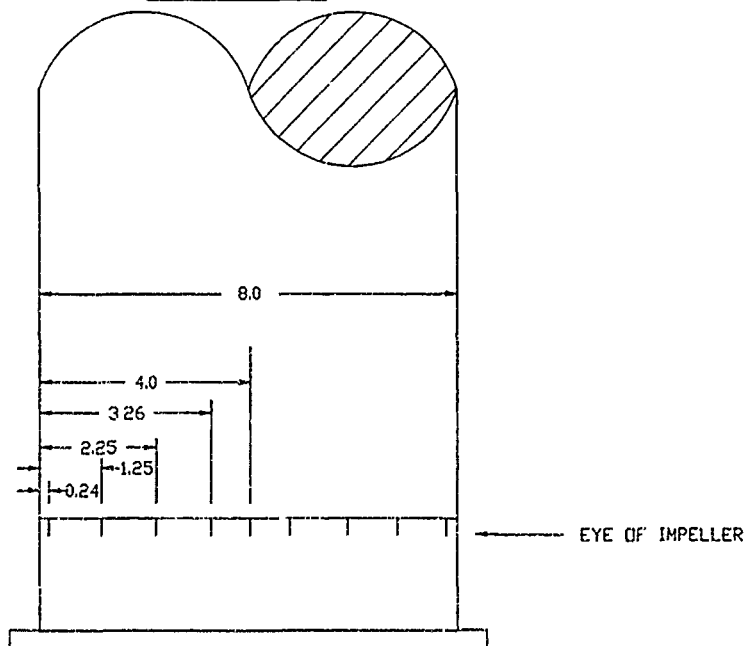


WATER-SURFACE EL 275.0

SWIRL ANGLE  
FSI DESIGN A  
DISCHARGE PER PUMP 650 CFS  
WATER-SURFACE EL 280.0 AND 275.0



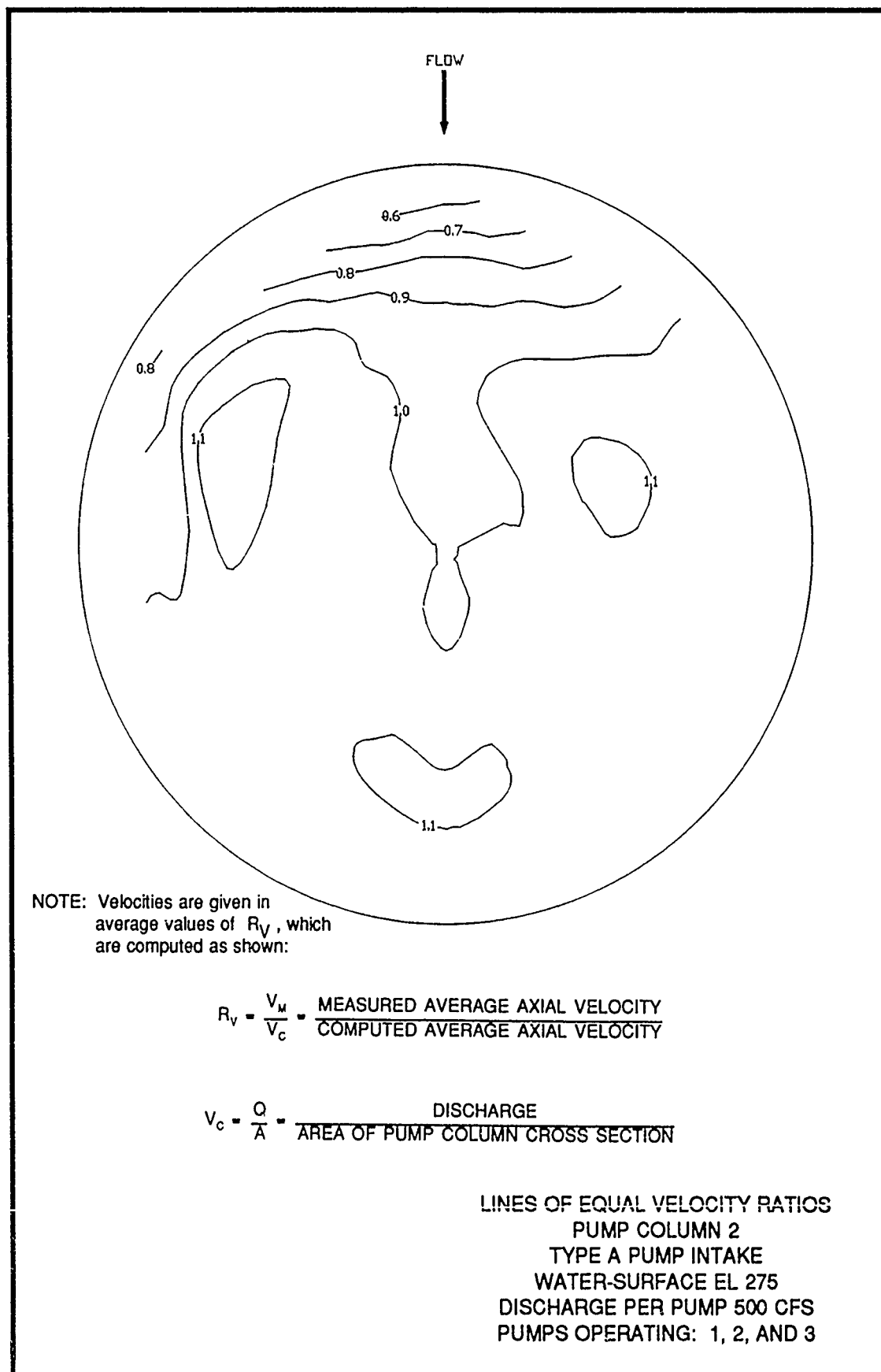
PLAN VIEW



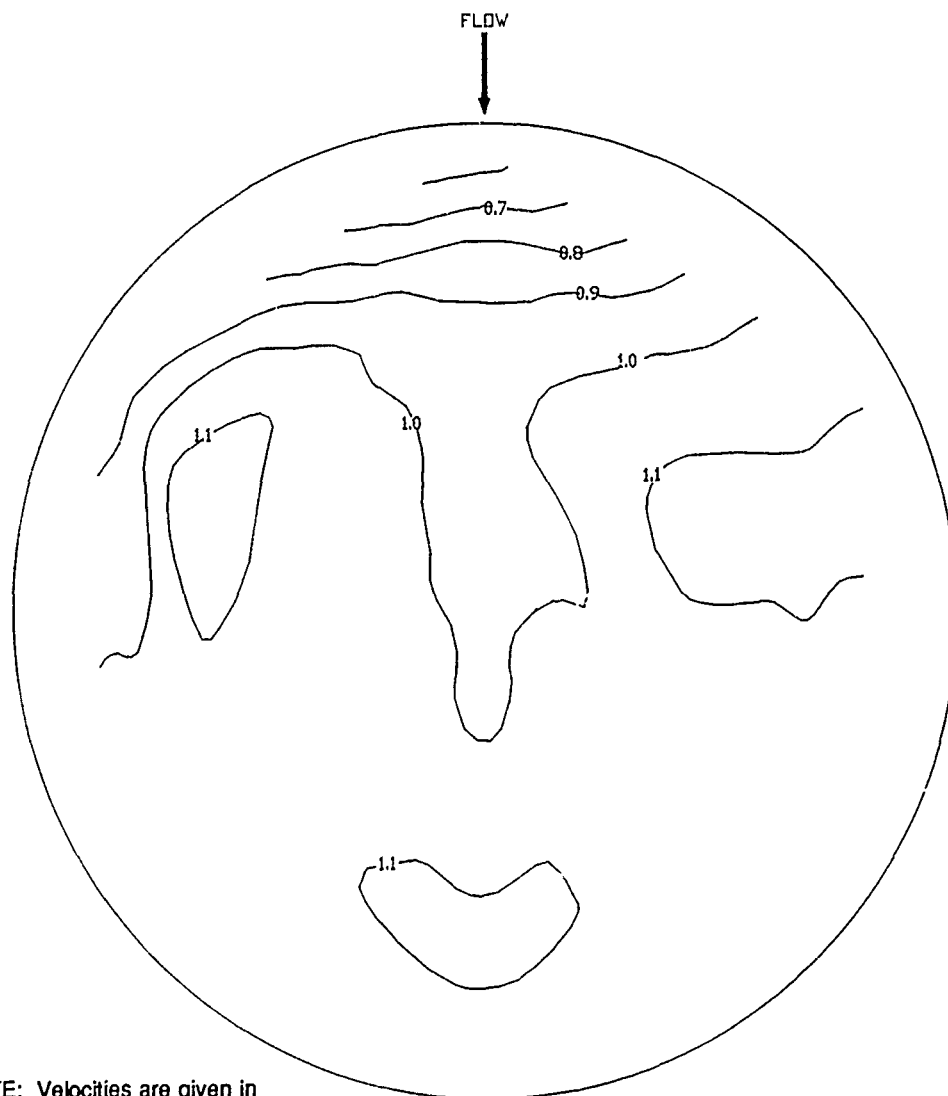
PROFILE

NOTE: ALL DIMENSIONS IN FEET

IMPACT TUBES AND  
STATIC PRESSURE PORTS  
DESIGN A





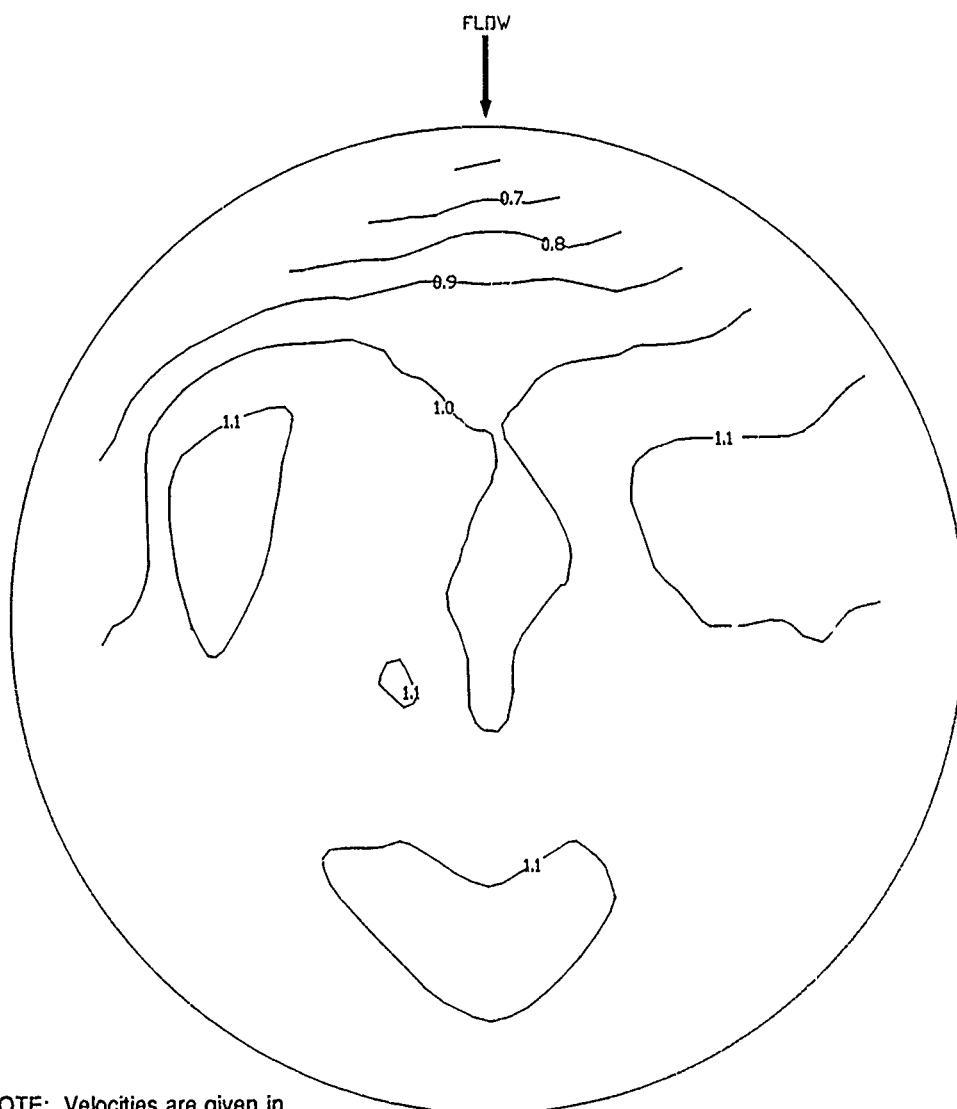


NOTE: Velocities are given in average values of  $R_v$ , which are computed as shown:

$$R_v = \frac{V_m}{V_c} = \frac{\text{MEASURED AVERAGE AXIAL VELOCITY}}{\text{COMPUTED AVERAGE AXIAL VELOCITY}}$$

$$V_c = \frac{Q}{A} = \frac{\text{DISCHARGE}}{\text{AREA OF PUMP COLUMN CROSS SECTION}}$$

LINES OF EQUAL VELOCITY RATIOS  
 PUMP COLUMN 2  
 TYPE A PUMP INTAKE  
 WATER-SURFACE EL 280  
 DISCHARGE PER PUMP 500 CFS  
 PUMPS OPERATING: 1, 2, AND 3

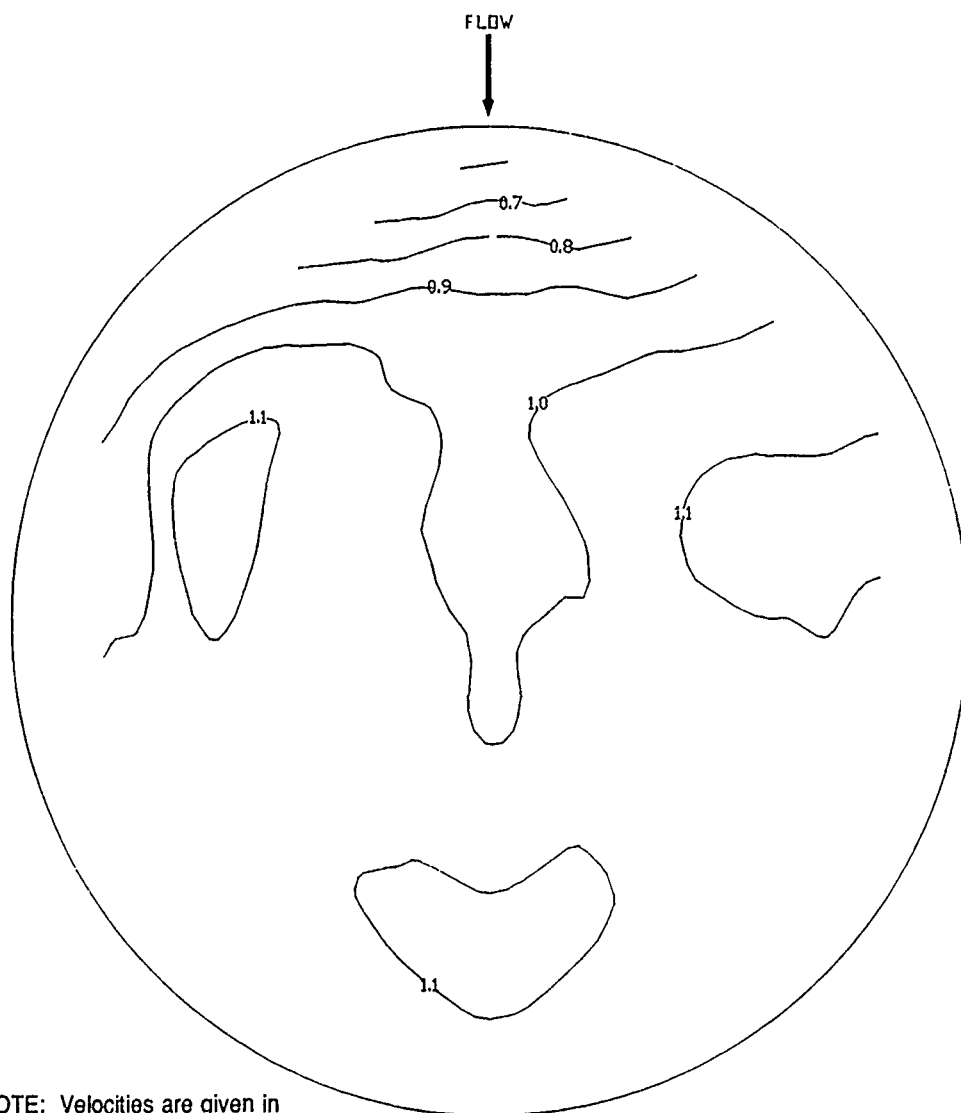


NOTE: Velocities are given in average values of  $R_v$ , which are computed as shown:

$$R_v = \frac{V_M}{V_C} = \frac{\text{MEASURED AVERAGE AXIAL VELOCITY}}{\text{COMPUTED AVERAGE AXIAL VELOCITY}}$$

$$V_C = \frac{Q}{A} = \frac{\text{DISCHARGE}}{\text{AREA OF PUMP COLUMN CROSS SECTION}}$$

LINES OF EQUAL VELOCITY RATIOS  
 PUMP COLUMN 2  
 TYPE A PUMP INTAKE  
 WATER-SURFACE EL 285  
 DISCHARGE PER PUMP 500 CFS  
 PUMPS OPERATING: 1, 2, AND 3

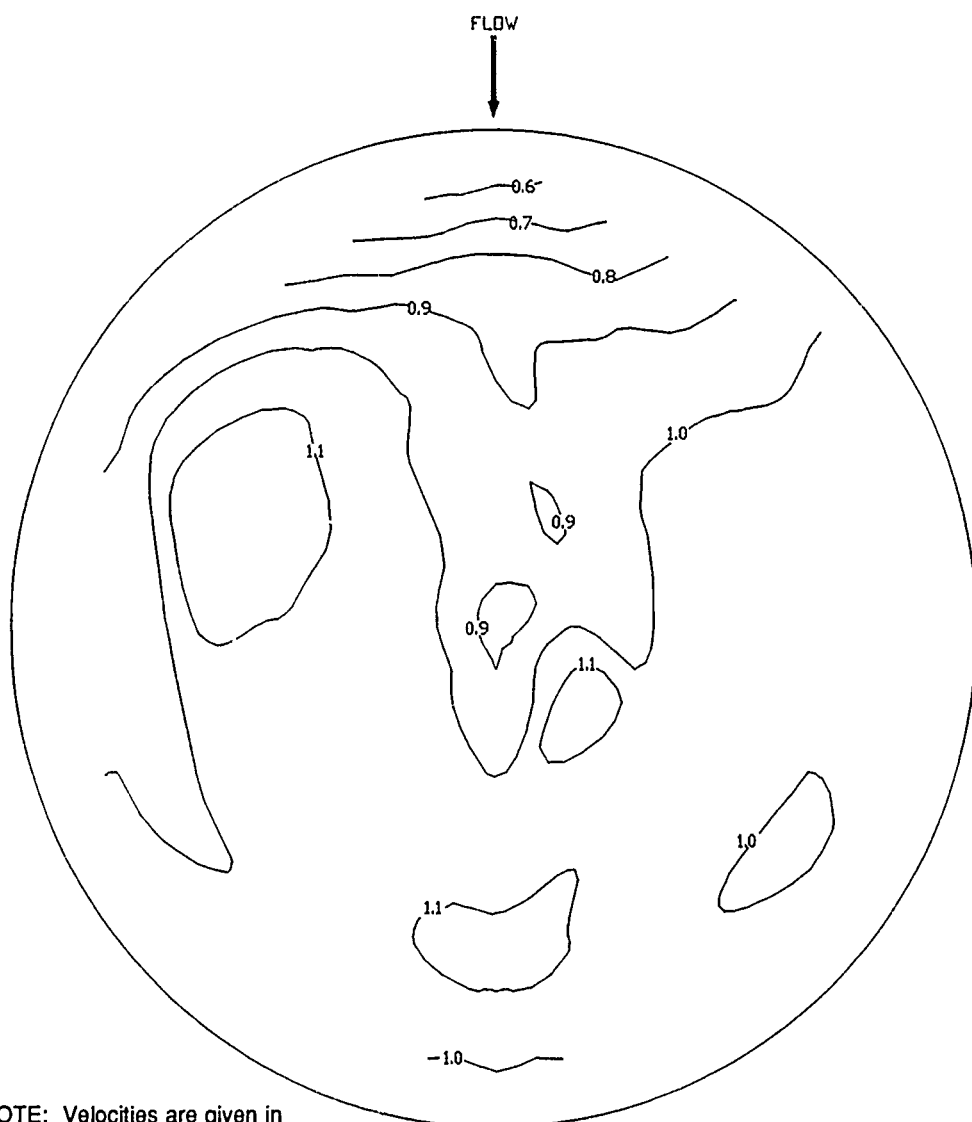


NOTE: Velocities are given in average values of  $R_v$ , which are computed as shown:

$$R_v = \frac{V_m}{V_c} = \frac{\text{MEASURED AVERAGE AXIAL VELOCITY}}{\text{COMPUTED AVERAGE AXIAL VELOCITY}}$$

$$V_c = \frac{Q}{A} = \frac{\text{DISCHARGE}}{\text{AREA OF PUMP COLUMN CROSS SECTION}}$$

LINES OF EQUAL VELOCITY RATIOS  
PUMP COLUMN 2  
TYPE A PUMP INTAKE  
WATER-SURFACE EL 290  
DISCHARGE PER PUMP 500 CFS  
PUMPS OPERATING: 1, 2, AND 3

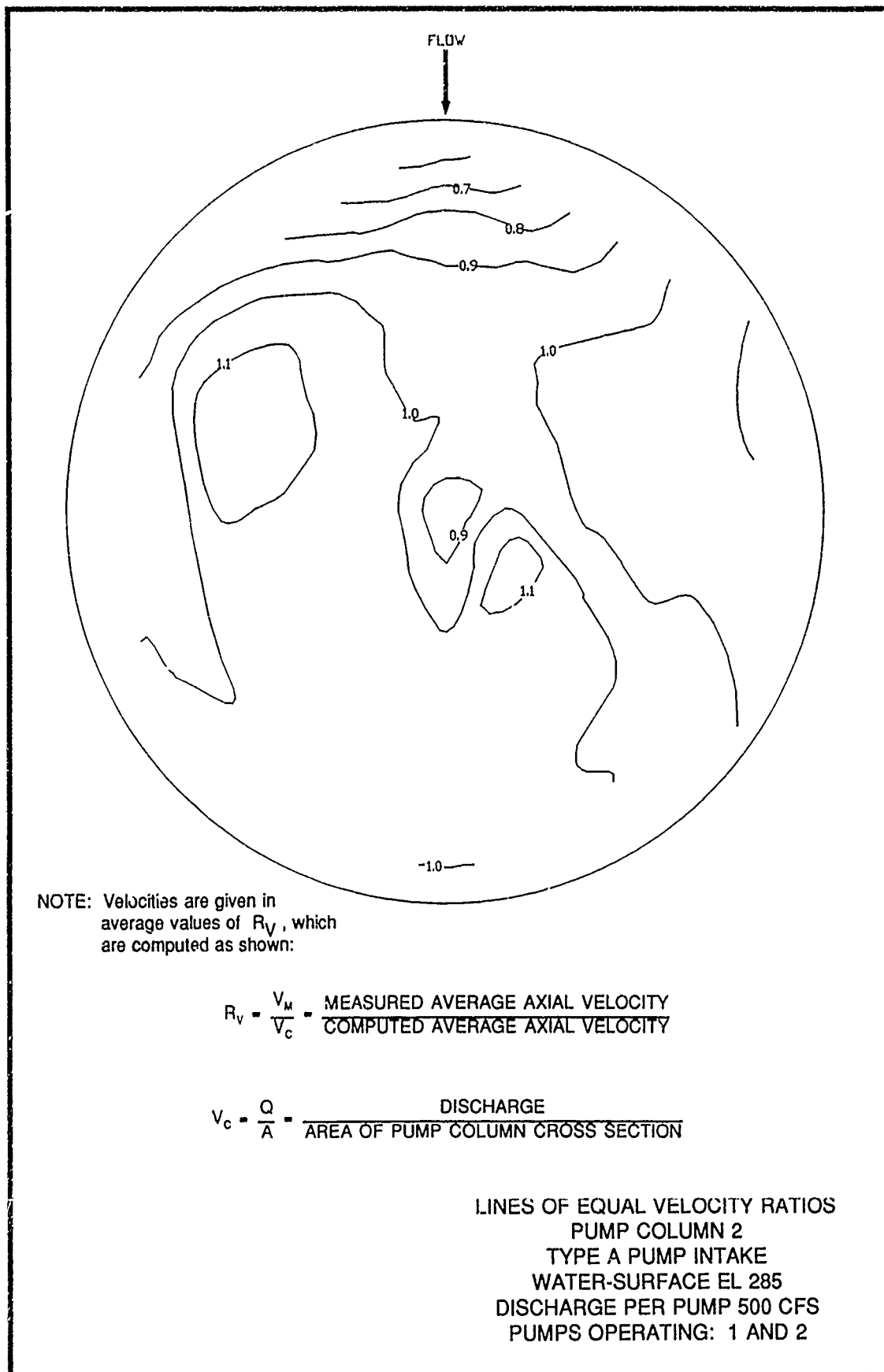


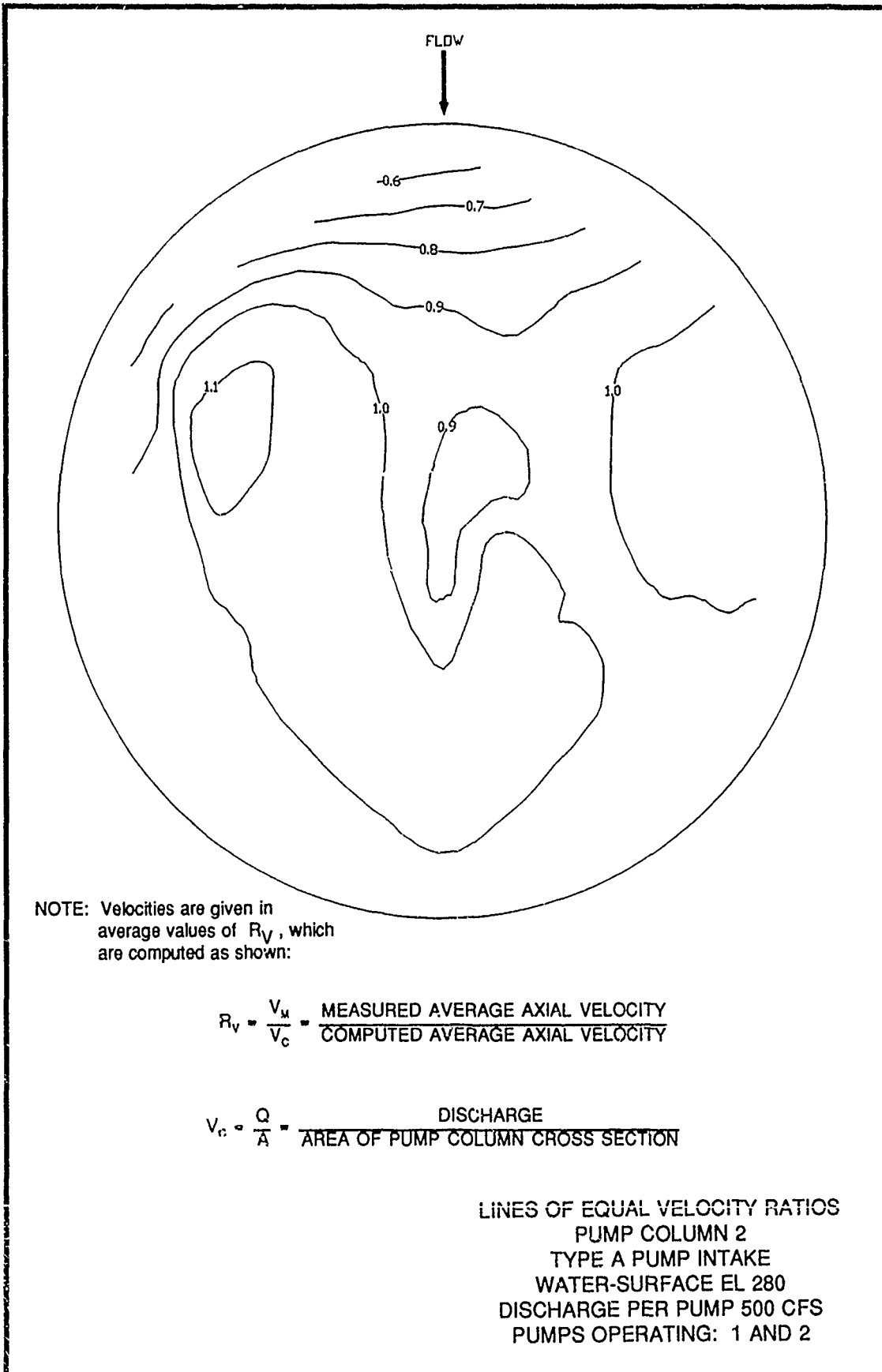
NOTE: Velocities are given in average values of  $R_v$ , which are computed as shown:

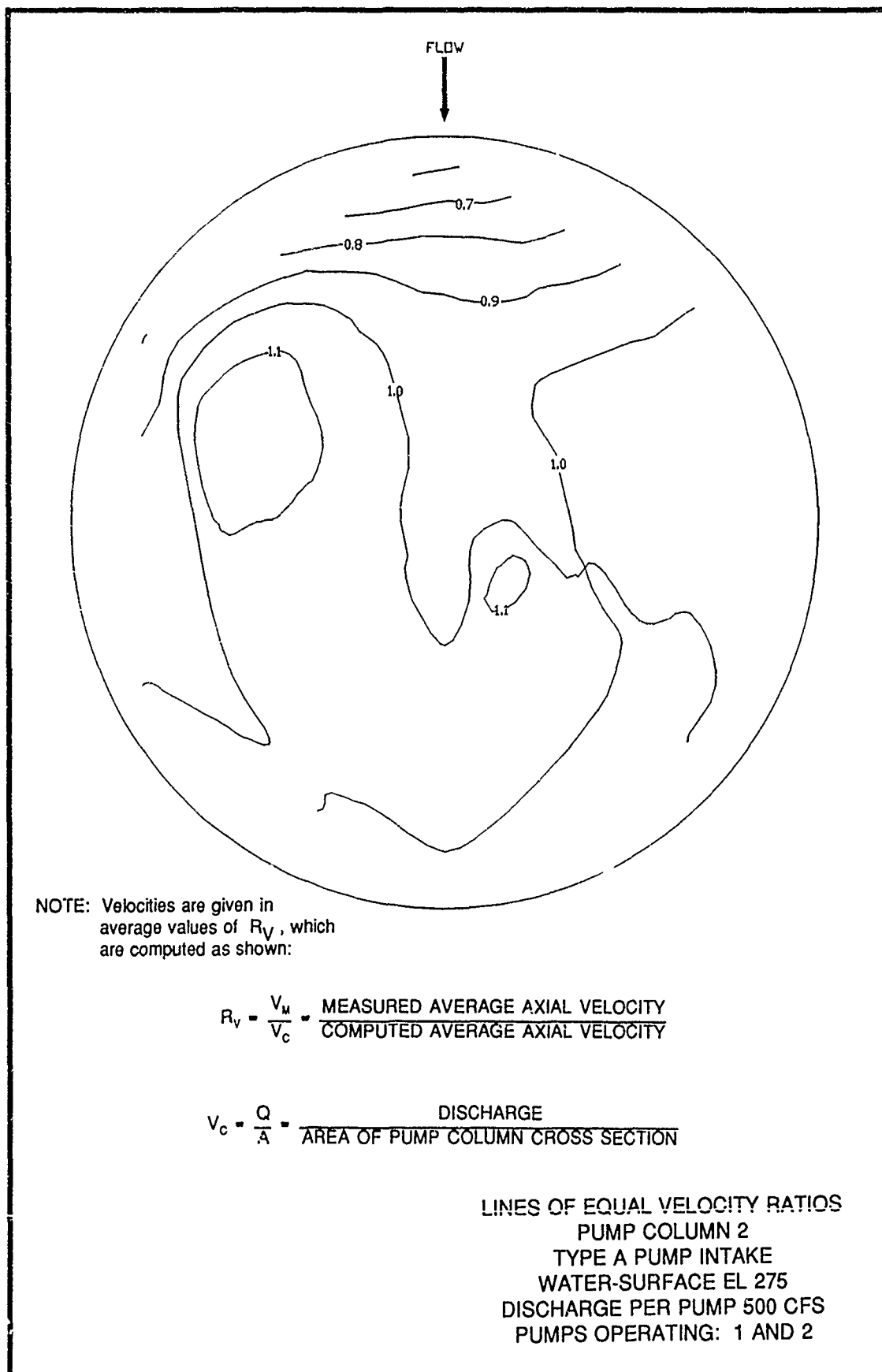
$$R_v = \frac{V_m}{V_c} = \frac{\text{MEASURED AVERAGE AXIAL VELOCITY}}{\text{COMPUTED AVERAGE AXIAL VELOCITY}}$$

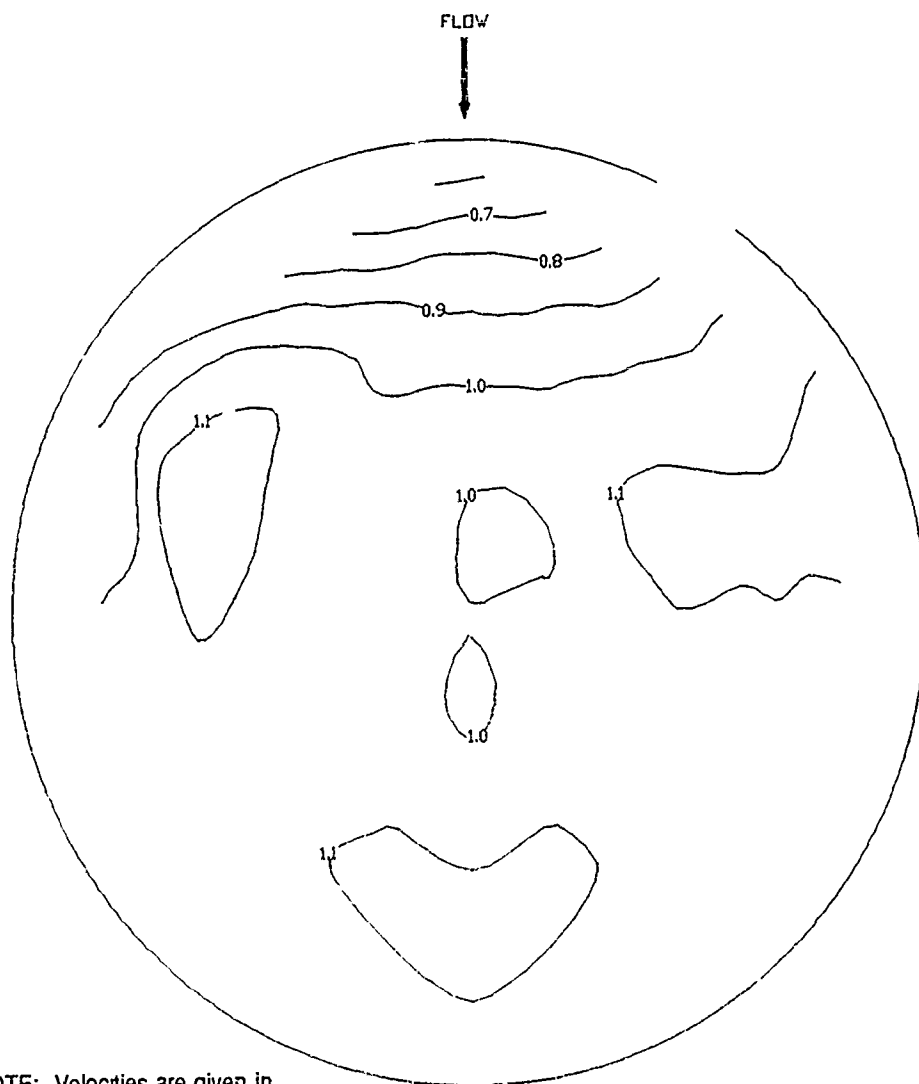
$$V_c = \frac{Q}{A} = \frac{\text{DISCHARGE}}{\text{AREA OF PUMP COLUMN CROSS SECTION}}$$

LINES OF EQUAL VELOCITY RATIOS  
PUMP COLUMN 2  
TYPE A PUMP INTAKE  
WATER-SURFACE EL 290  
DISCHARGE PER PUMP 500 CFS  
PUMPS OPERATING: 1 AND 2









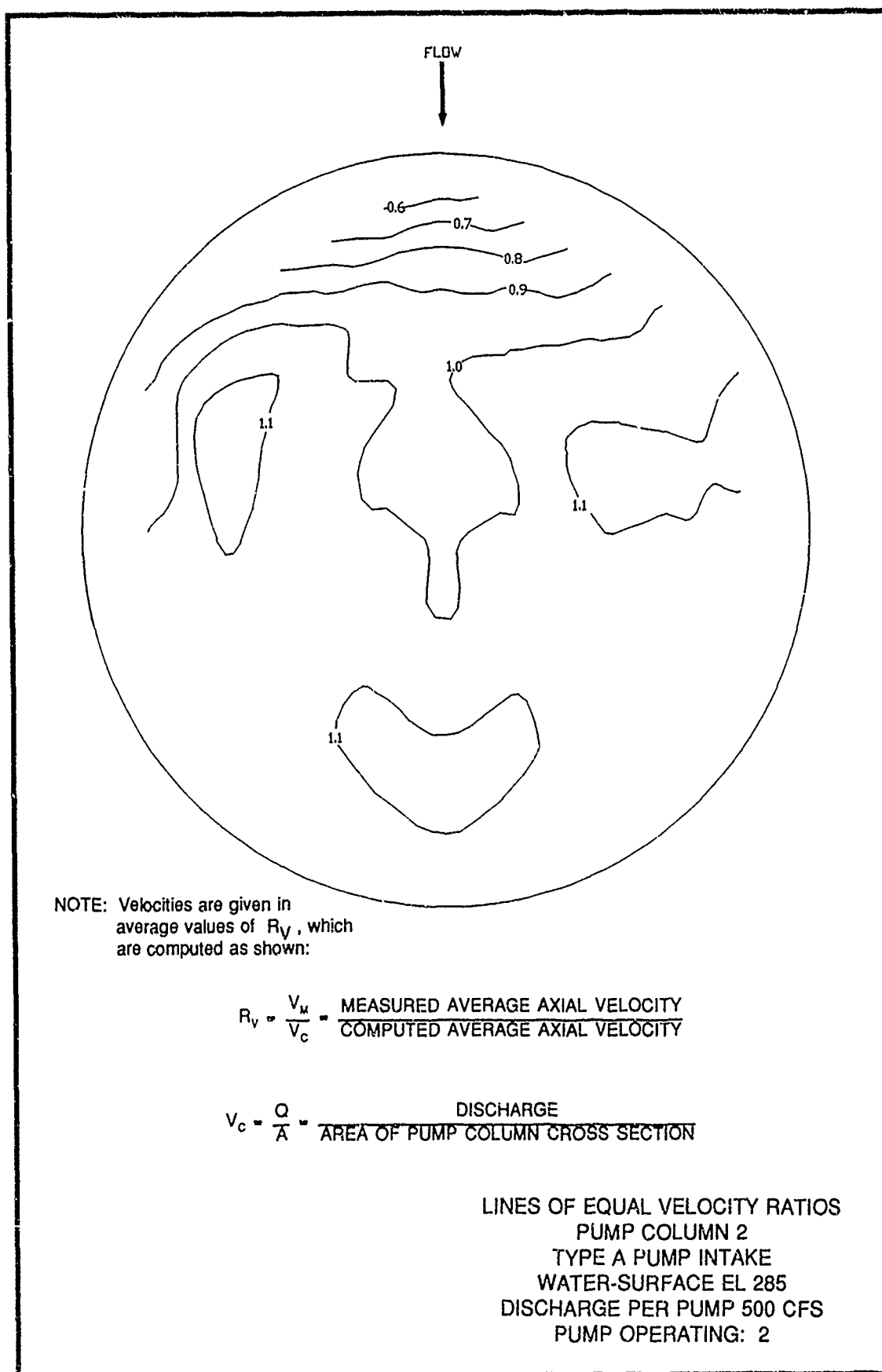
NOTE: Velocities are given in average values of  $R_v$ , which are computed as shown:

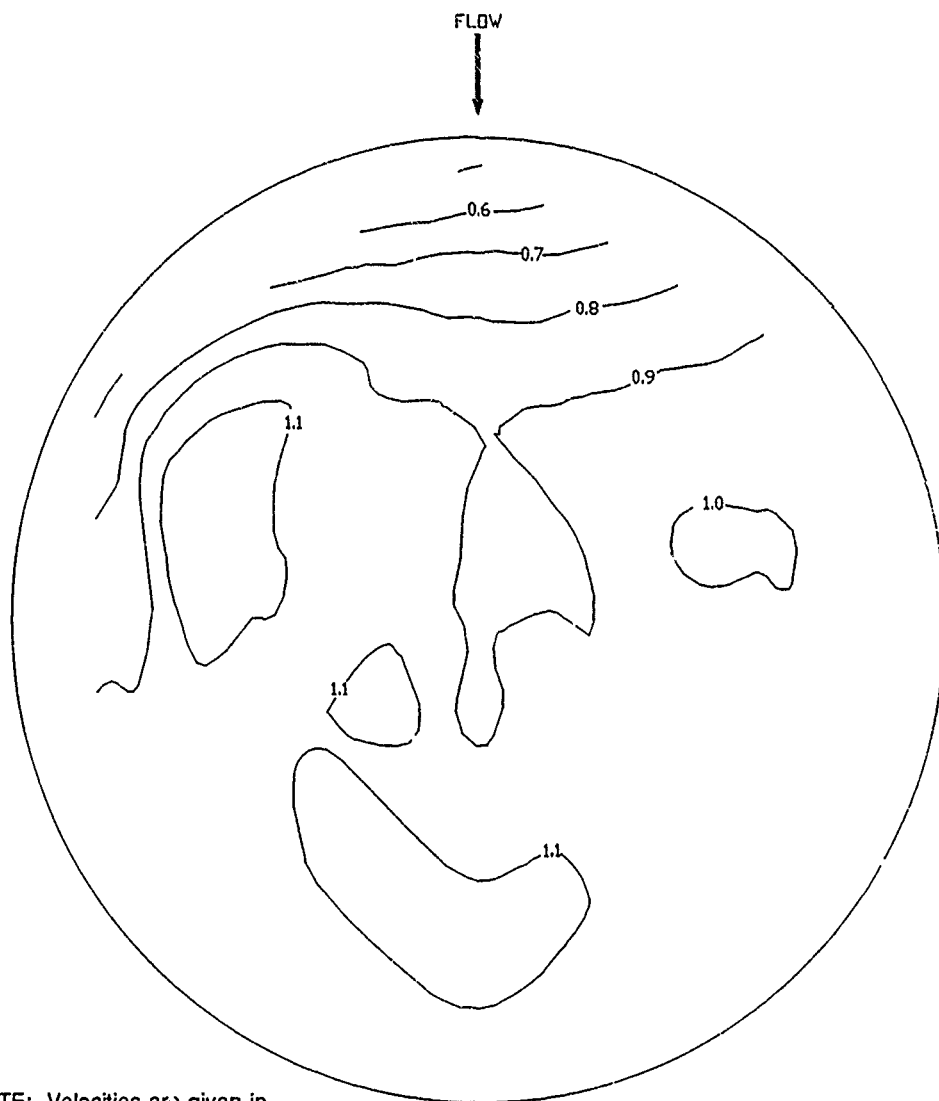
$$R_v = \frac{V_u}{V_c} = \frac{\text{MEASURED AVERAGE AXIAL VELOCITY}}{\text{COMPUTED AVERAGE AXIAL VELOCITY}}$$

$$V_c = \frac{Q}{A} = \frac{\text{DISCHARGE}}{\text{AREA OF PUMP COLUMN CROSS SECTION}}$$

LINES OF EQUAL VELOCITY RATIOS  
PUMP COLUMN 2  
TYPE A PUMP INTAKE  
WATER-SURFACE EL 290  
DISCHARGE PER PUMP 500 CFS  
PUMP OPERATING: 2





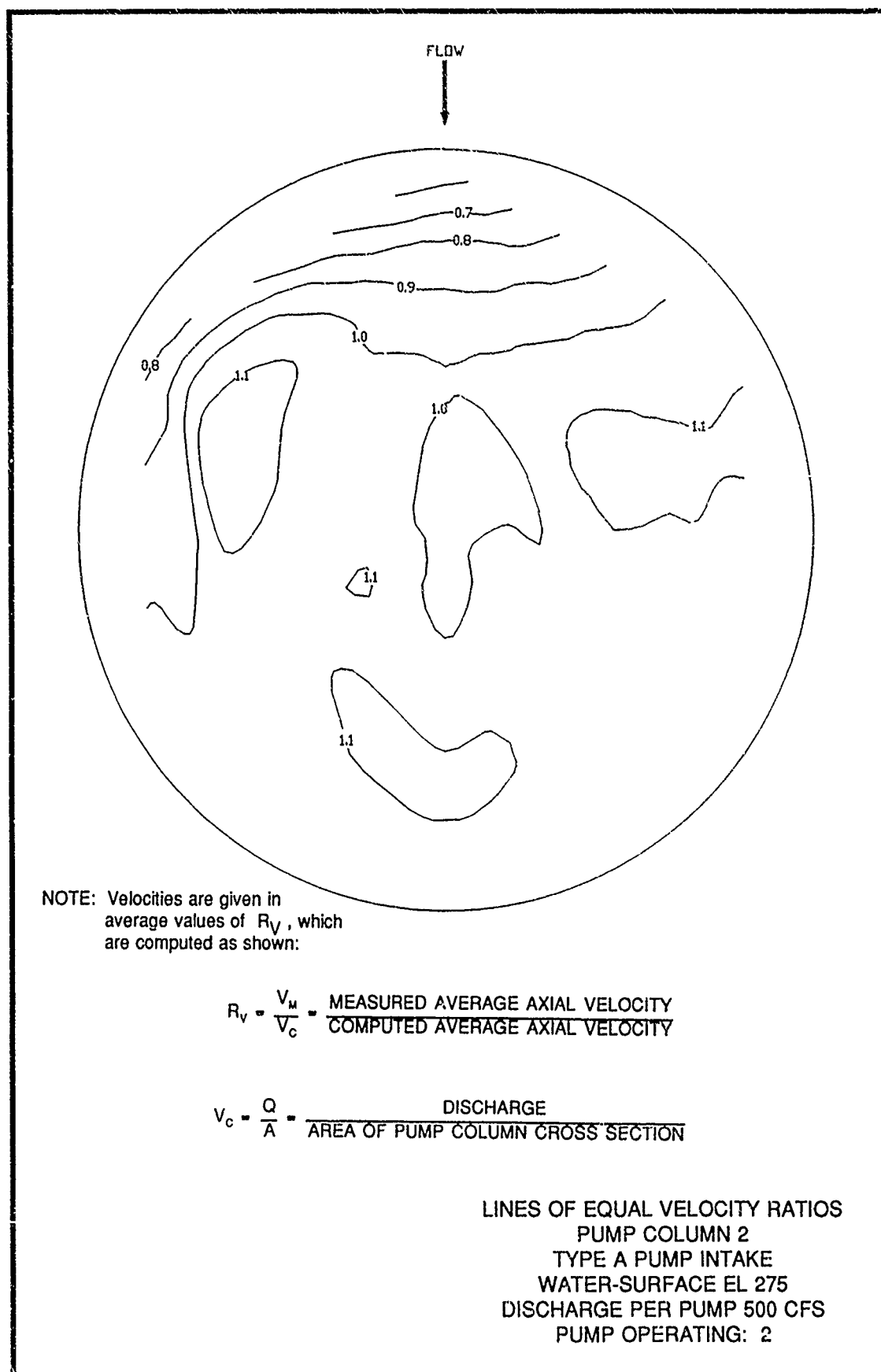


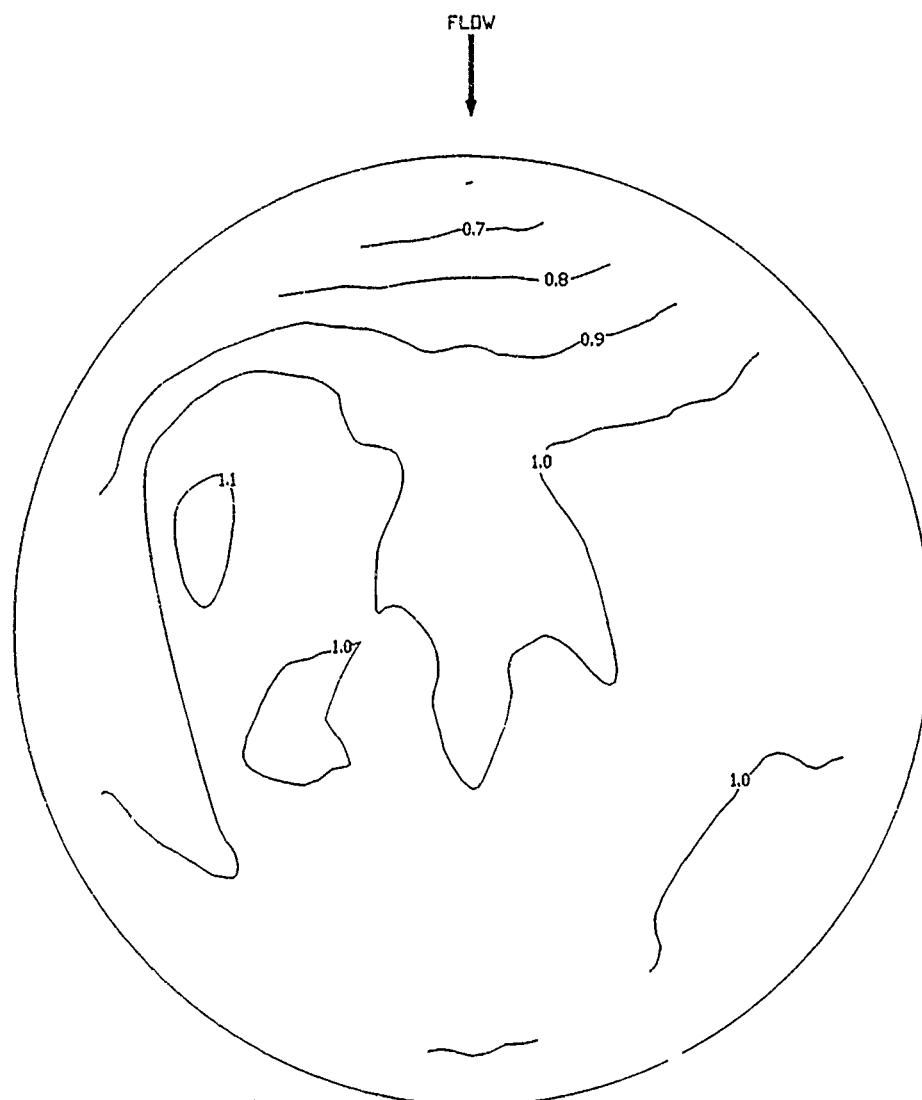
NOTE: Velocities are given in average values of  $R_v$ , which are computed as shown:

$$R_v = \frac{V_m}{V_c} = \frac{\text{MEASURED AVERAGE AXIAL VELOCITY}}{\text{COMPUTED AVERAGE AXIAL VELOCITY}}$$

$$V_c = \frac{Q}{A} = \frac{\text{DISCHARGE}}{\text{AREA OF PUMP COLUMN CROSS SECTION}}$$

LINES OF EQUAL VELOCITY RATIOS  
PUMP COLUMN 2  
TYPE A PUMP INTAKE  
WATER-SURFACE EL 280  
DISCHARGE PER PUMP 500 CFS  
PUMP OPERATING: 2



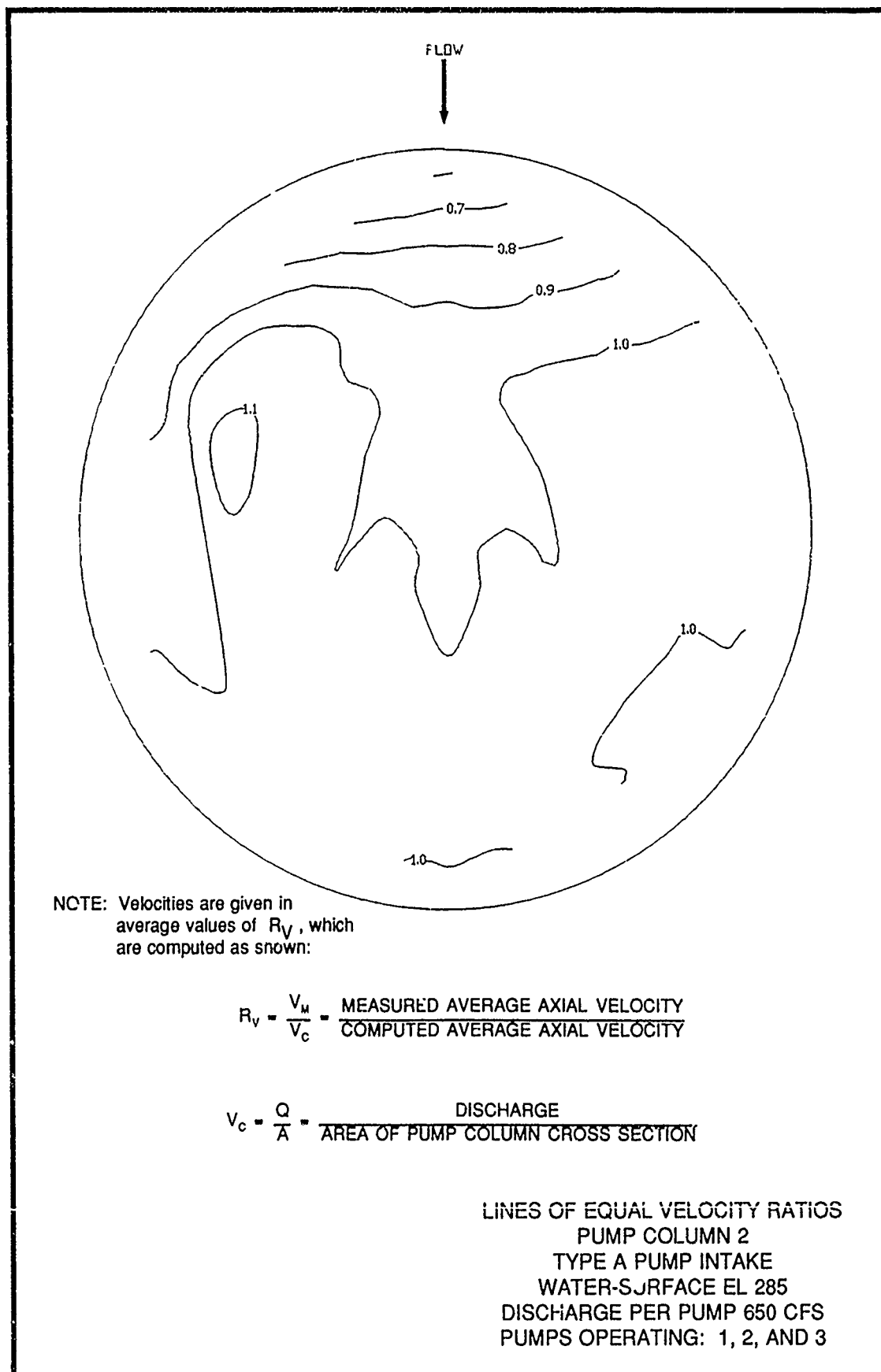


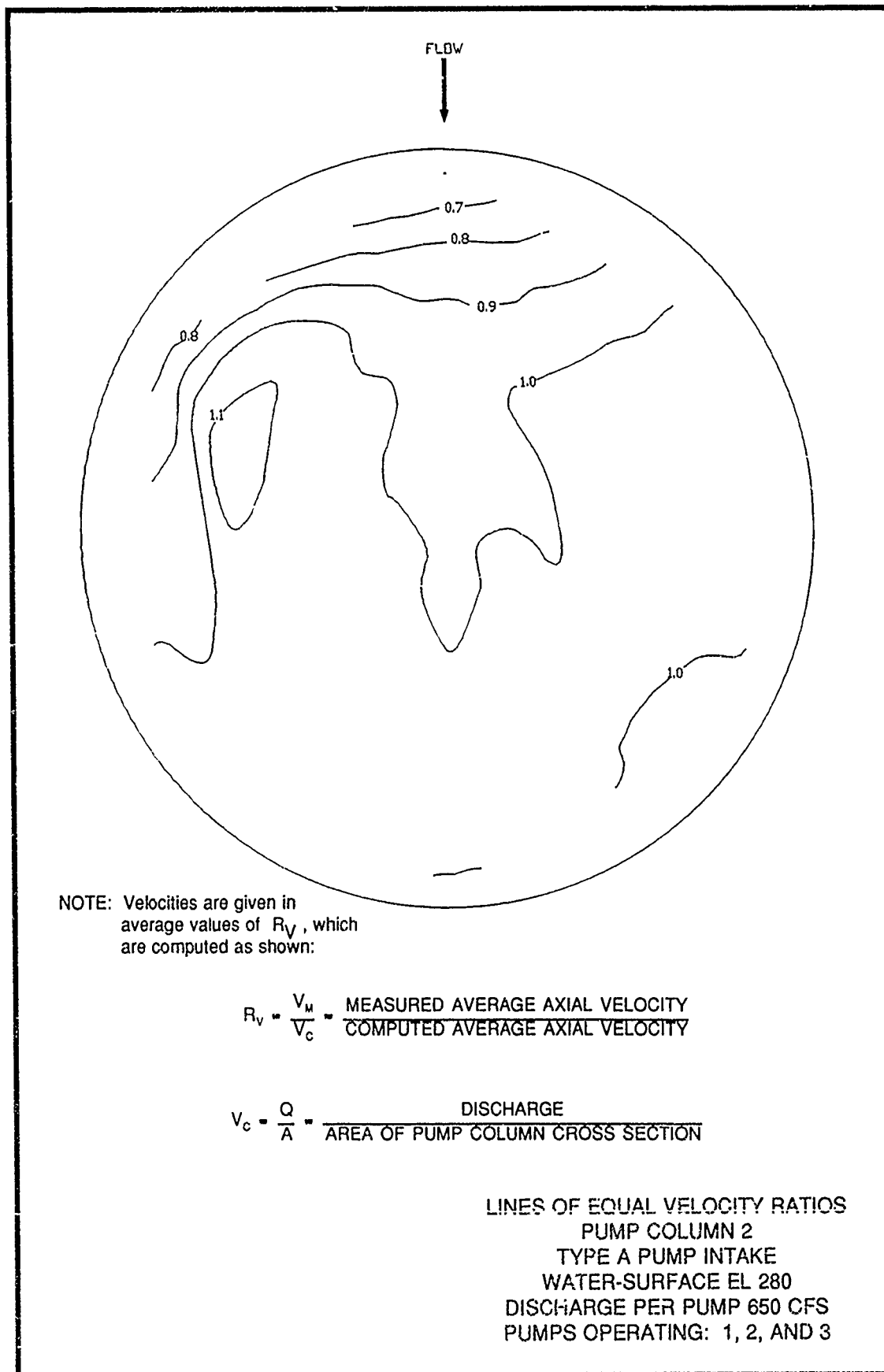
NOTE: Velocities are given in average values of  $R_v$ , which are computed as shown:

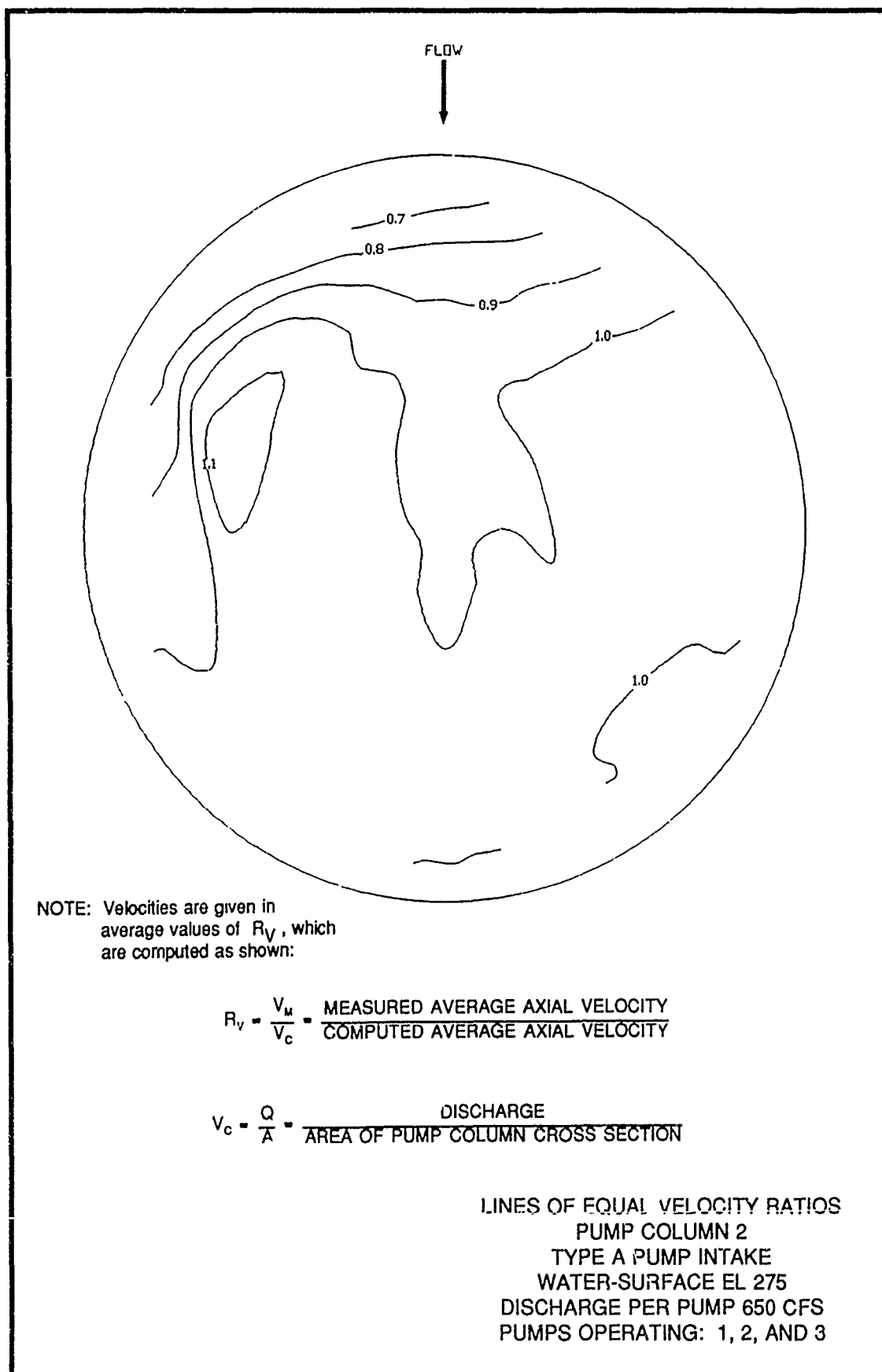
$$R_v = \frac{V_m}{V_c} = \frac{\text{MEASURED AVERAGE AXIAL VELOCITY}}{\text{COMPUTED AVERAGE AXIAL VELOCITY}}$$

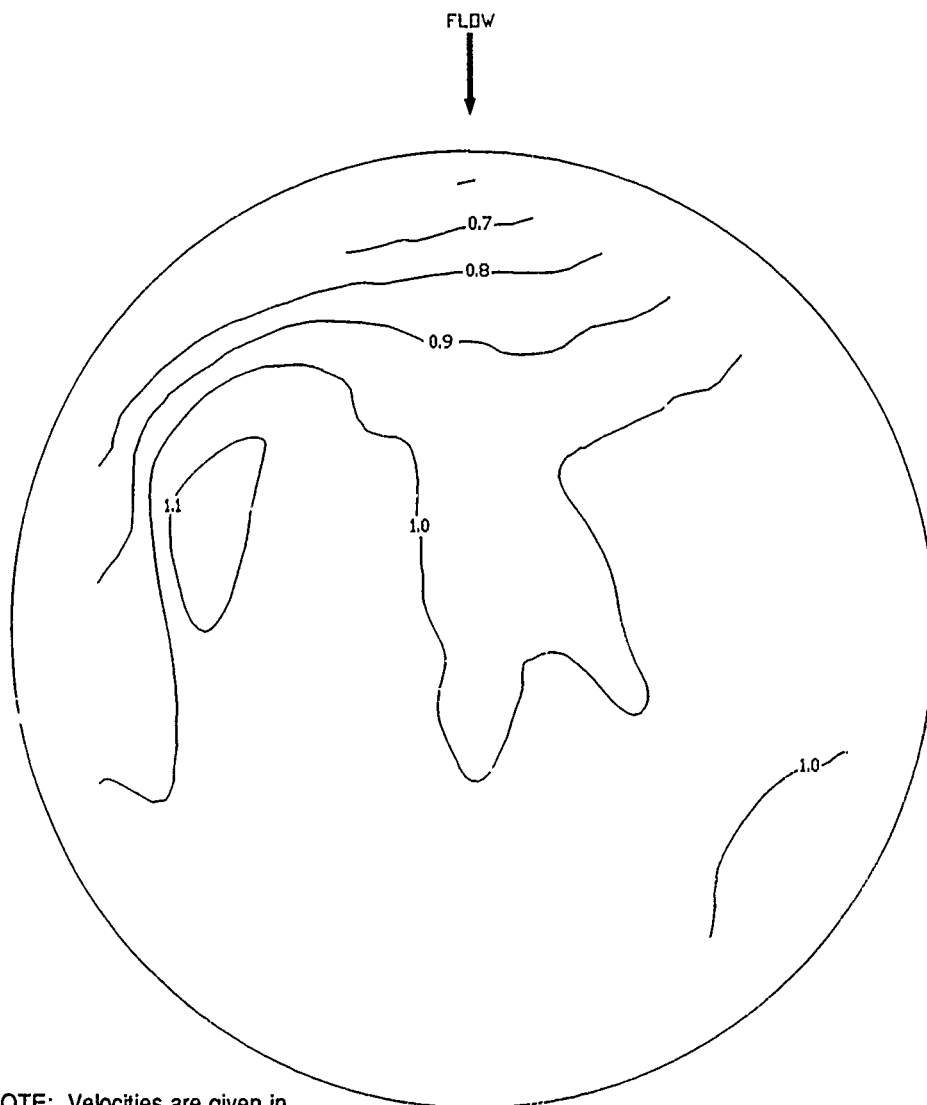
$$V_c = \frac{Q}{A} = \frac{\text{DISCHARGE}}{\text{AREA OF PUMP COLUMN CROSS SECTION}}$$

LINES OF EQUAL VELOCITY RATIOS  
 PUMP COLUMN 2  
 TYPE A PUMP INTAKE  
 WATER-SURFACE EL 290  
 DISCHARGE PER PUMP 650 CFS  
 PUMPS OPERATING: 1, 2, AND 3









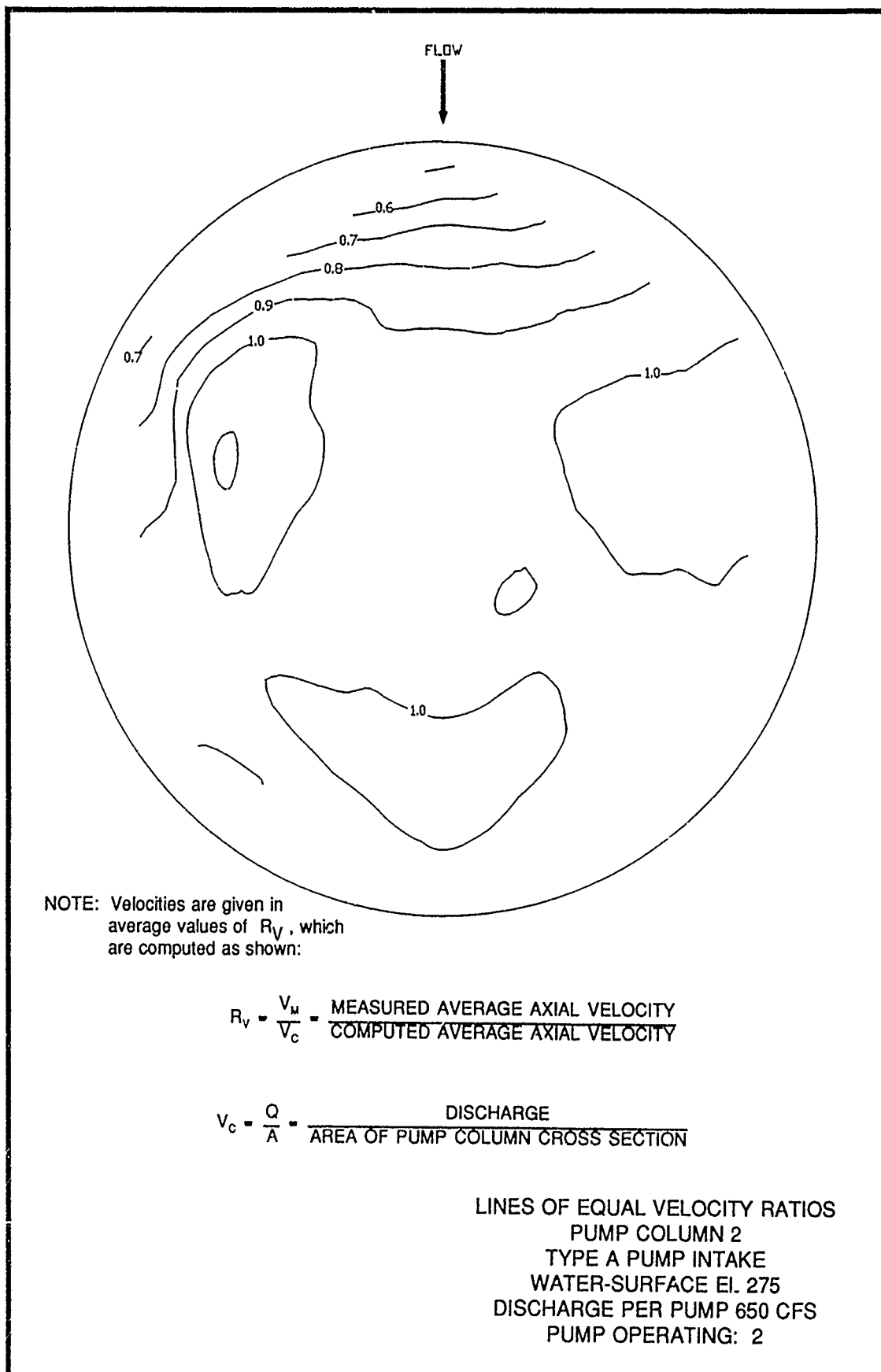
NOTE: Velocities are given in average values of  $R_v$ , which are computed as shown:

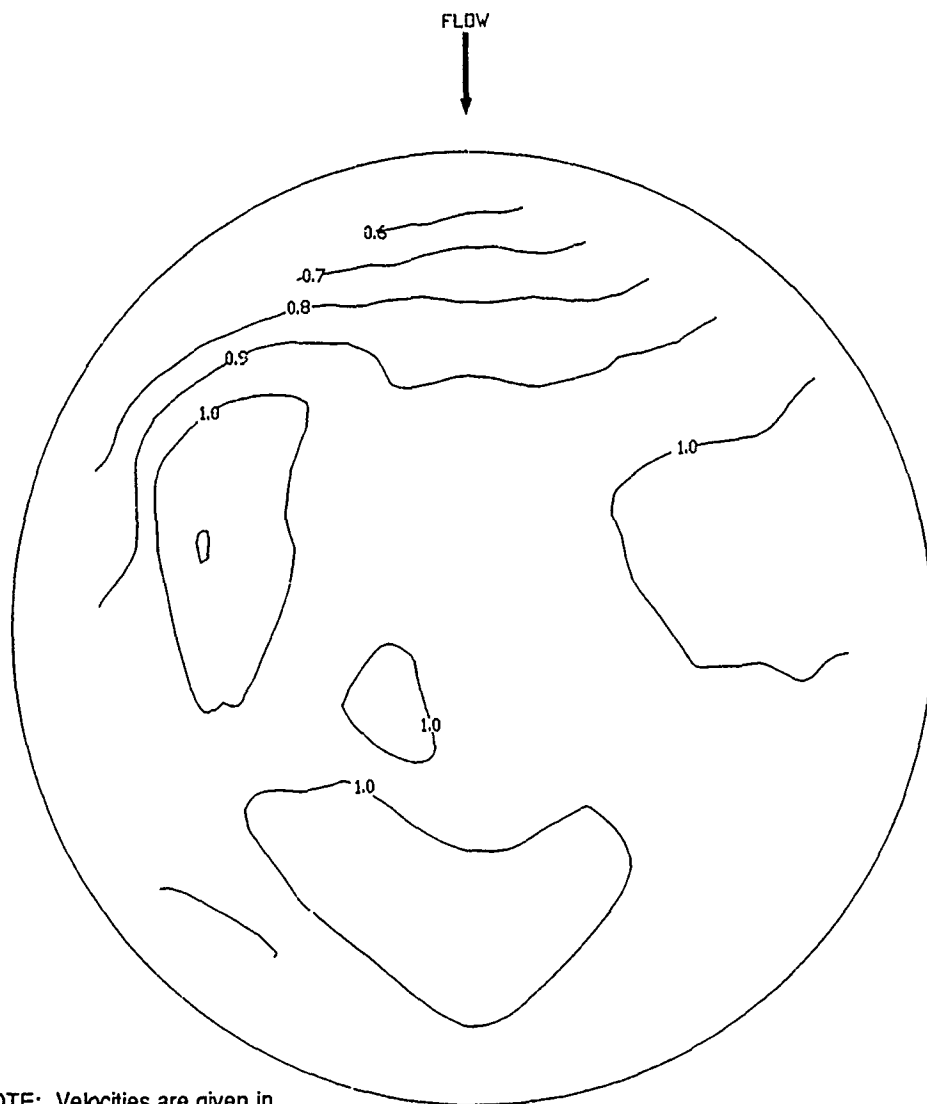
$$R_v = \frac{V_m}{V_c} = \frac{\text{MEASURED AVERAGE AXIAL VELOCITY}}{\text{COMPUTED AVERAGE AXIAL VELOCITY}}$$

$$V_c = \frac{Q}{A} = \frac{\text{DISCHARGE}}{\text{AREA OF PUMP COLUMN CROSS SECTION}}$$

LINES OF EQUAL VELOCITY RATIOS  
PUMP COLUMN 2  
TYPE A PUMP INTAKE  
WATER-SURFACE EL 280  
DISCHARGE PER PUMP 650 CFS  
PUMPS OPERATING: 1 AND 2





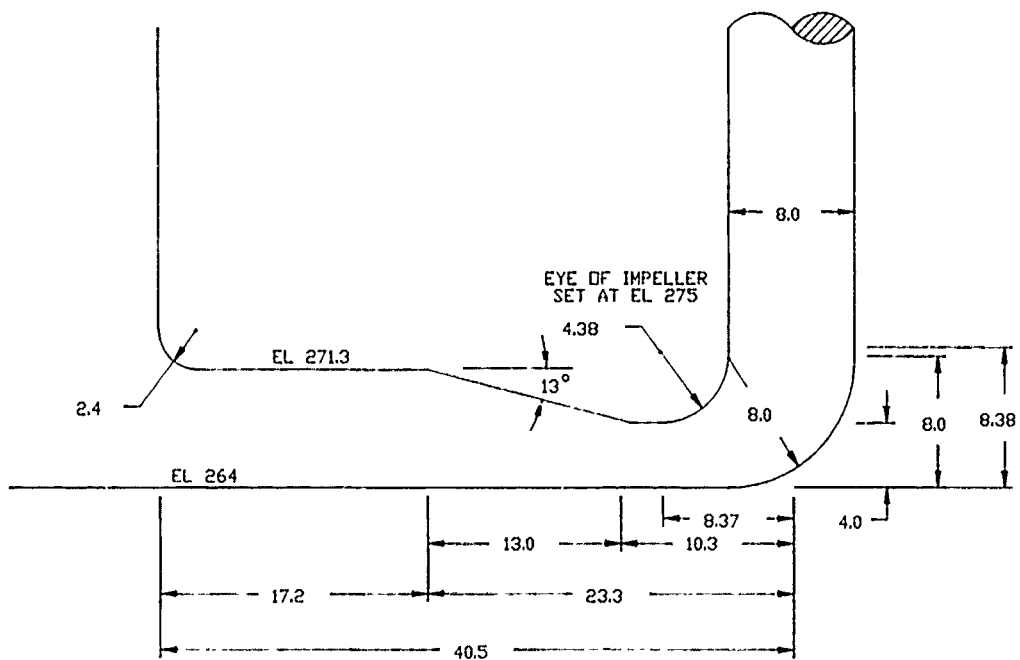
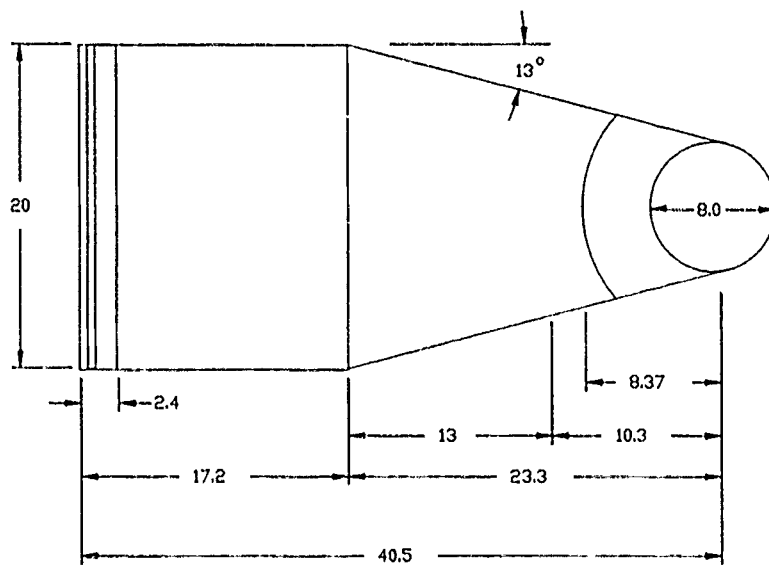


NOTE: Velocities are given in average values of  $R_v$ , which are computed as shown:

$$R_v = \frac{V_m}{V_c} = \frac{\text{MEASURED AVERAGE AXIAL VELOCITY}}{\text{COMPUTED AVERAGE AXIAL VELOCITY}}$$

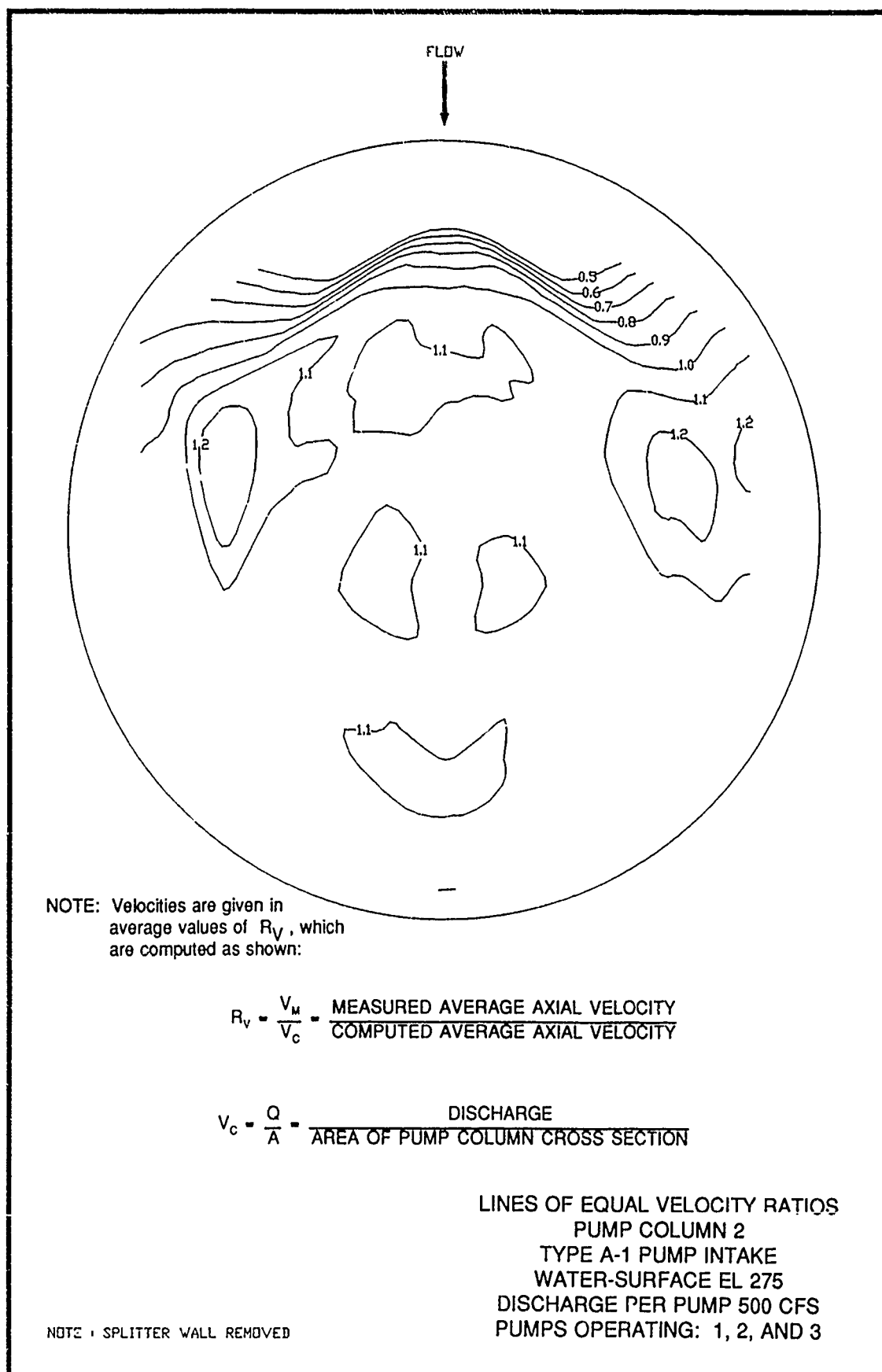
$$V_c = \frac{Q}{A} = \frac{\text{DISCHARGE}}{\text{AREA OF PUMP COLUMN CROSS SECTION}}$$

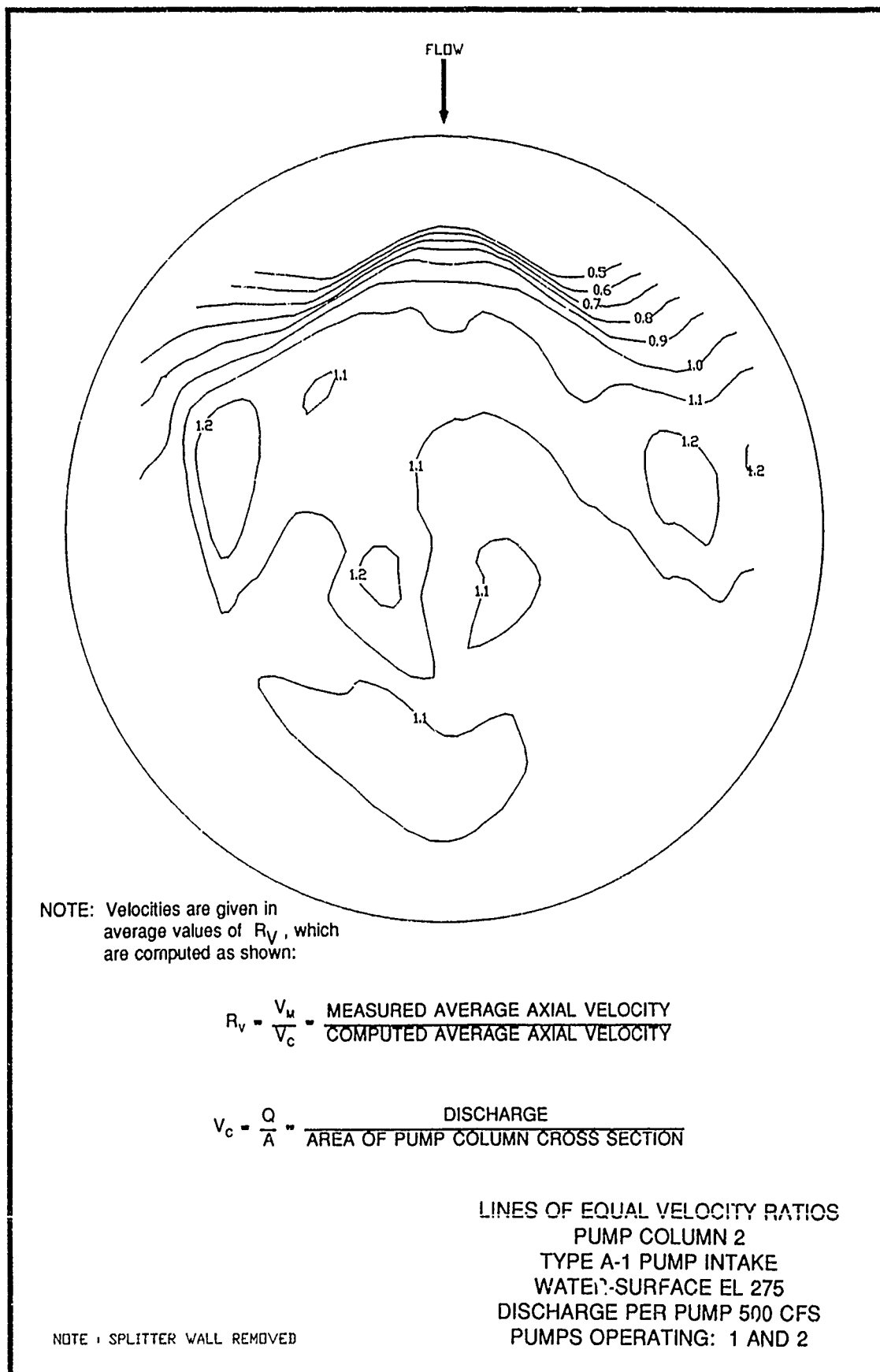
LINES OF EQUAL VELOCITY RATIOS  
PUMP COLUMN 2  
TYPE A PUMP INTAKE  
WATER-SURFACE EL 280  
DISCHARGE PER PUMP 650 CFS  
PUMP OPERATING: 2

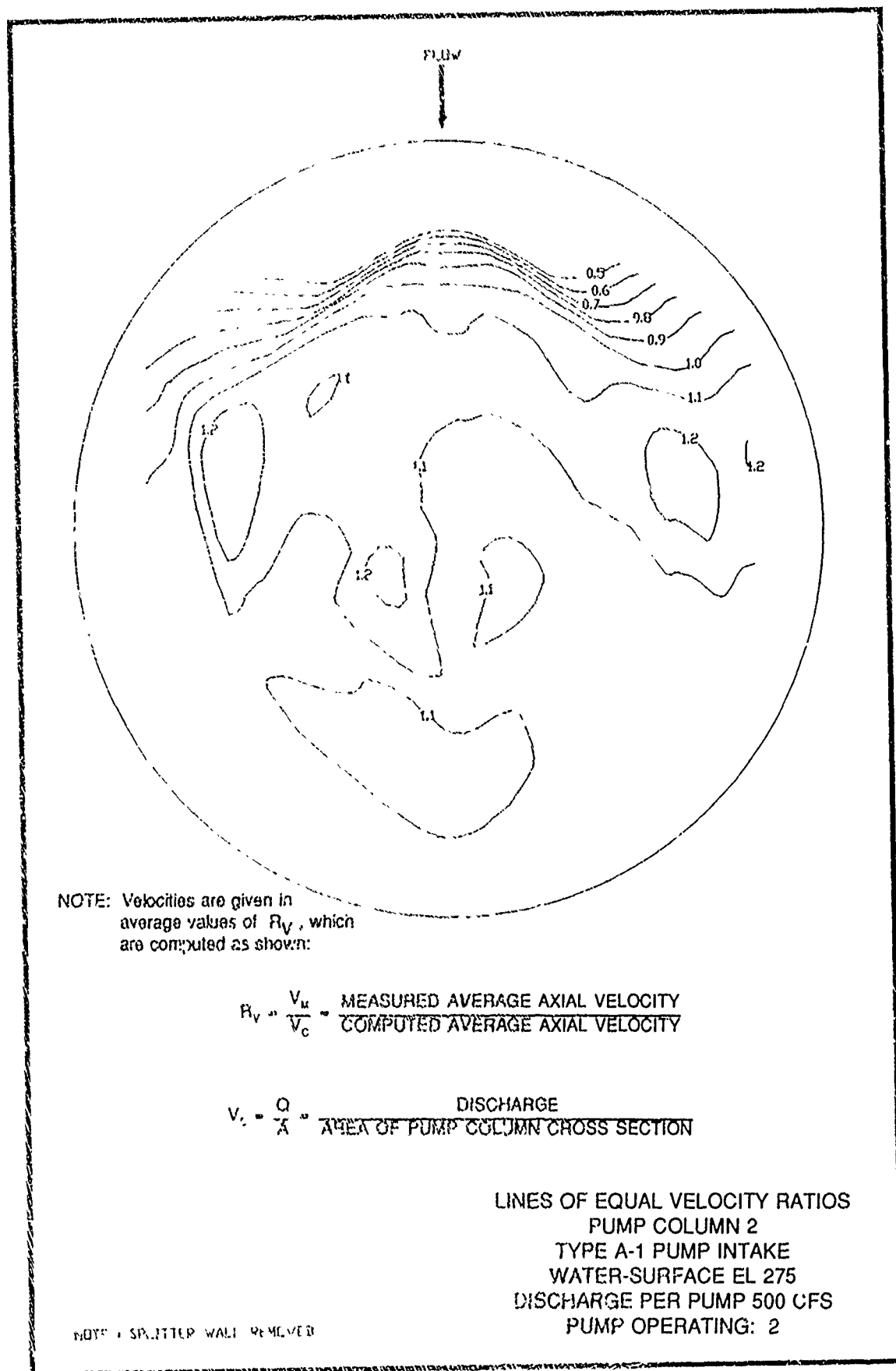


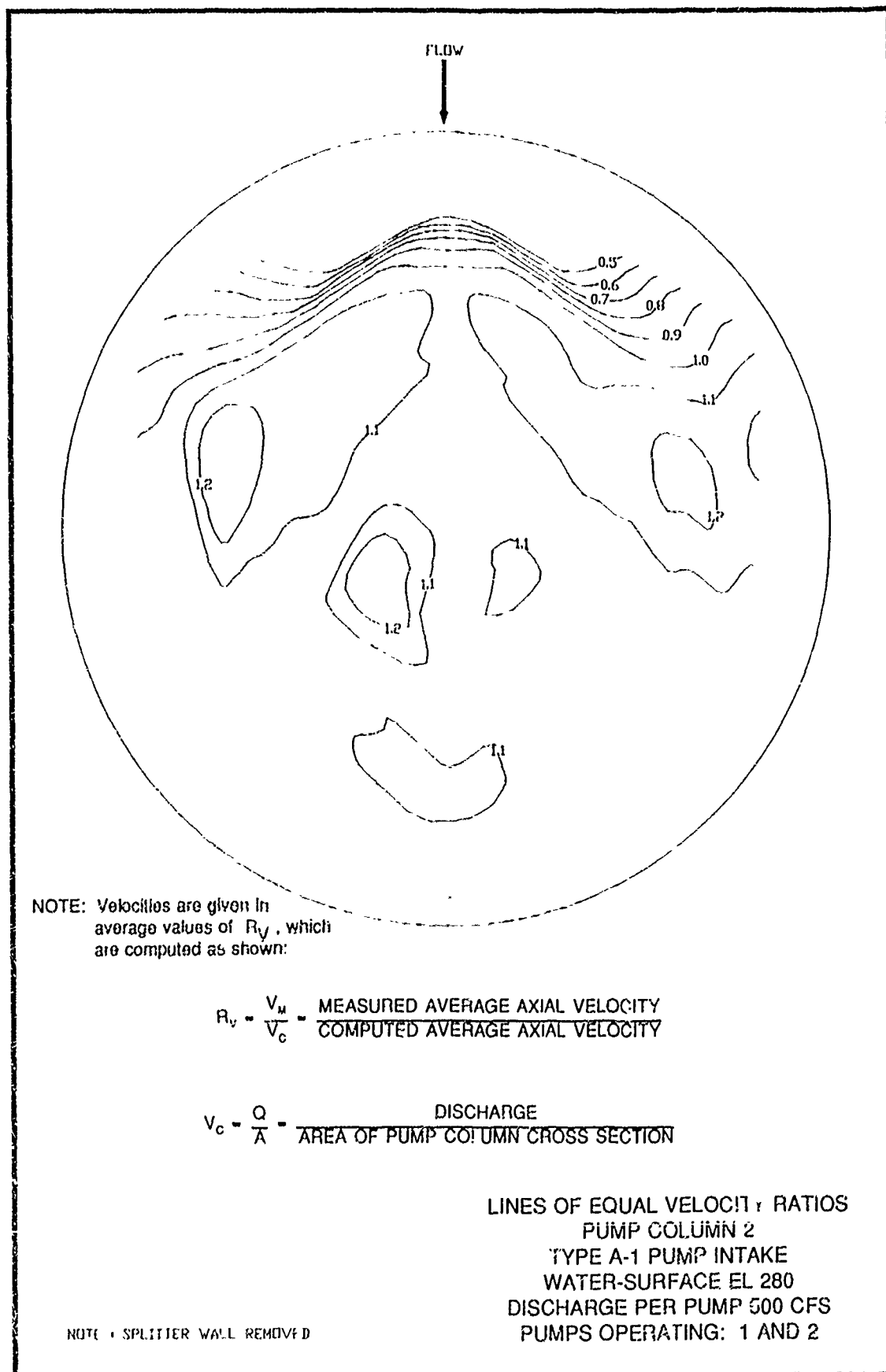
NOTE: ALL DIMENSIONS IN FEET

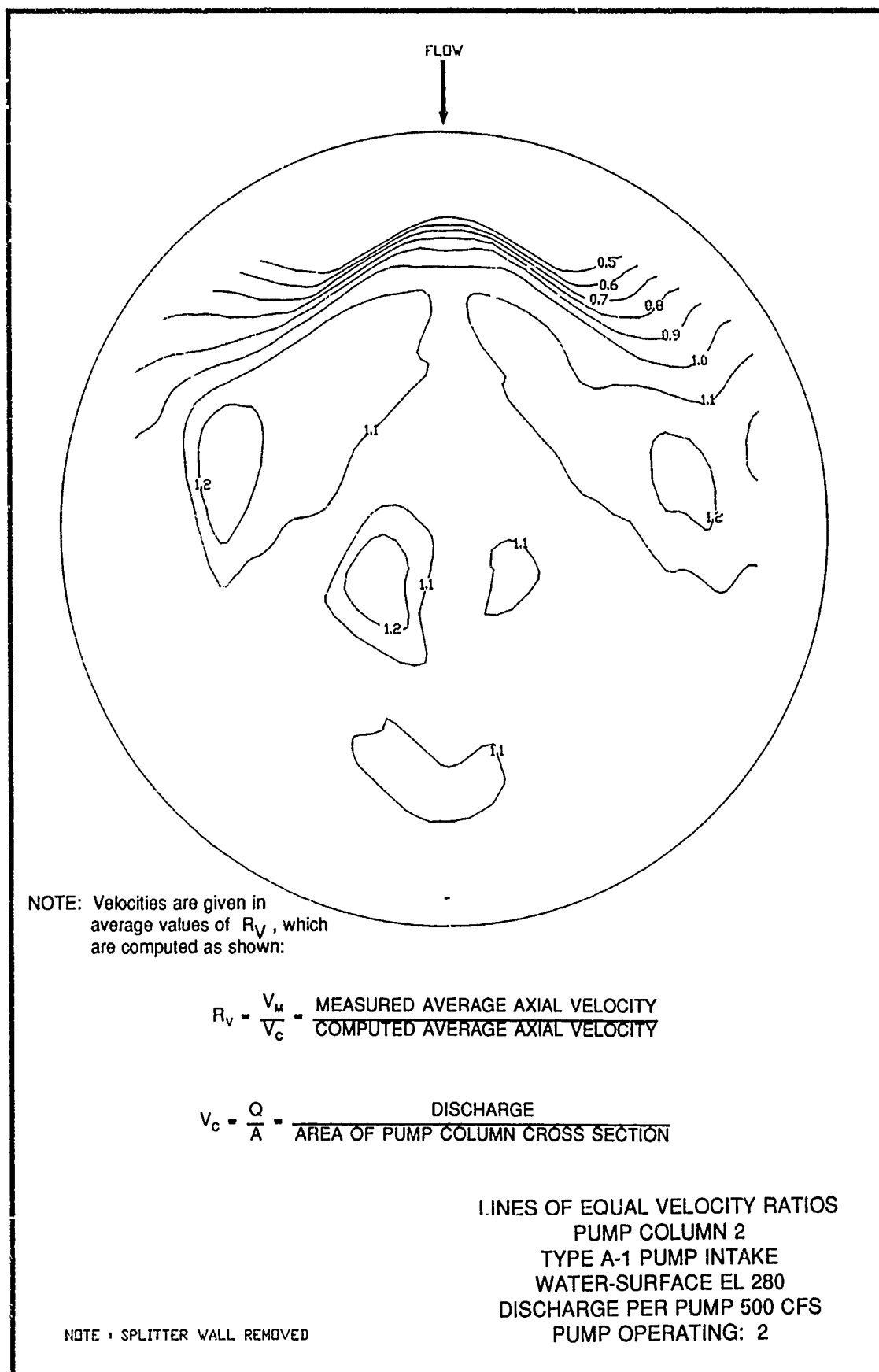
DESIGN A-1  
FSI  
SPLITTER WALL REMOVED



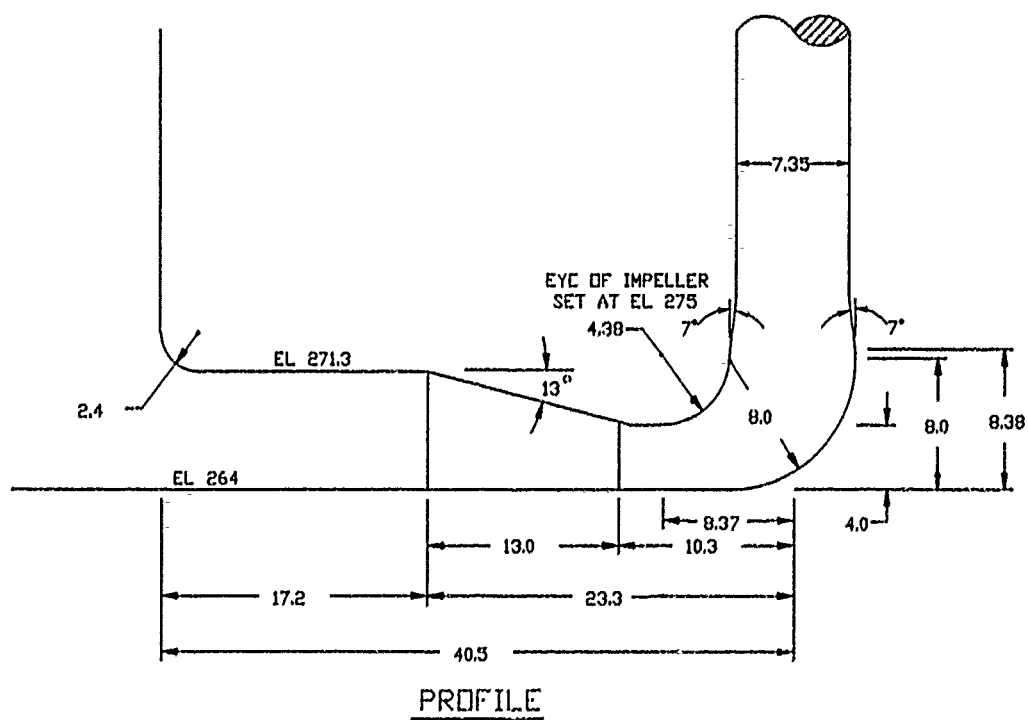
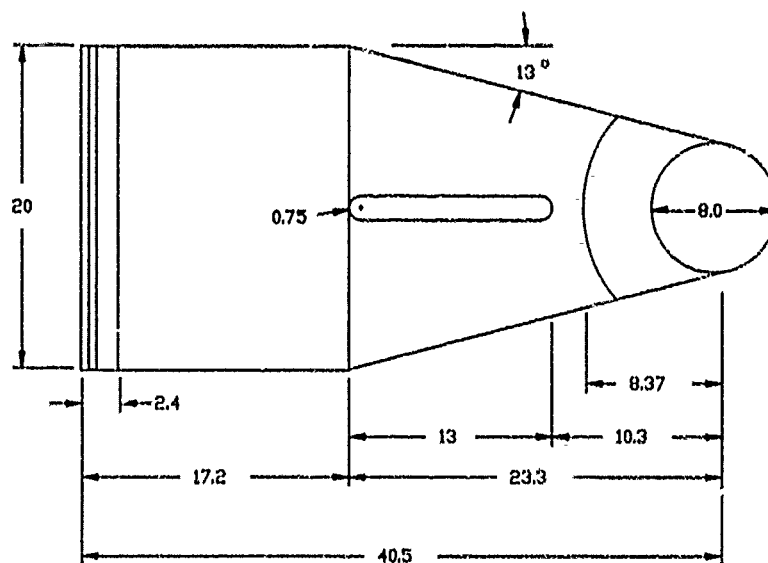






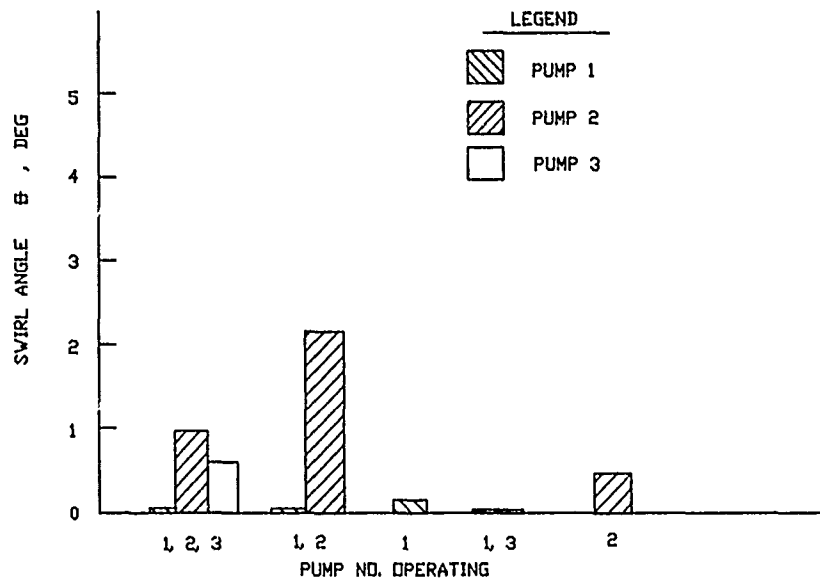




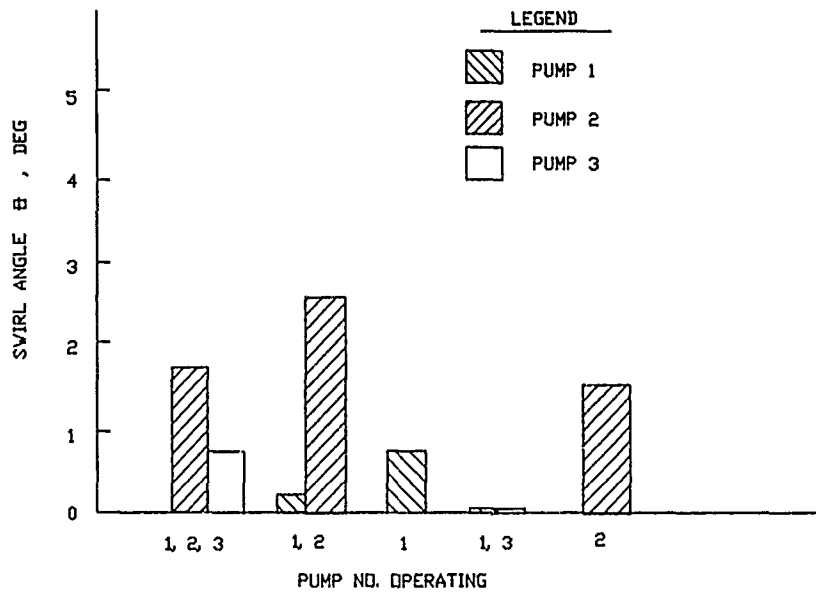


NOTE: ALL DIMENSIONS IN FEET

DESIGN B  
FSI

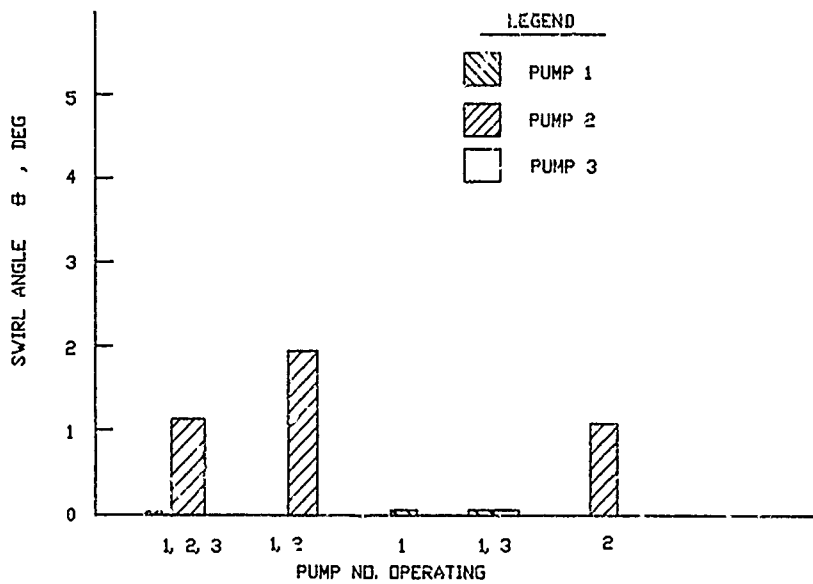


WATER-SURFACE EL 290.0

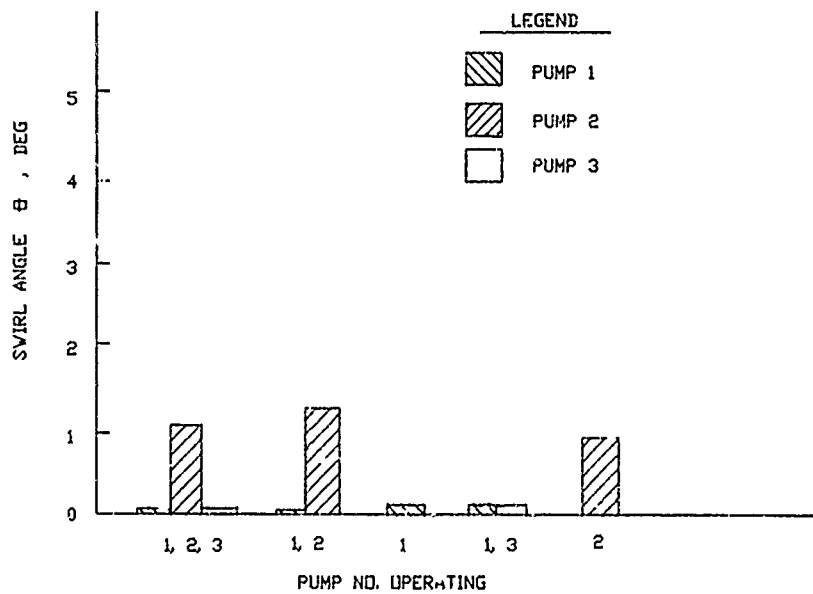


WATER-SURFACE EL 285.0

SWIRL ANGLE  
FSI DESIGN B  
DISCHARGE PER PUMP 500 CFS  
WATER-SURFACE EL 290.0 AND 285.0

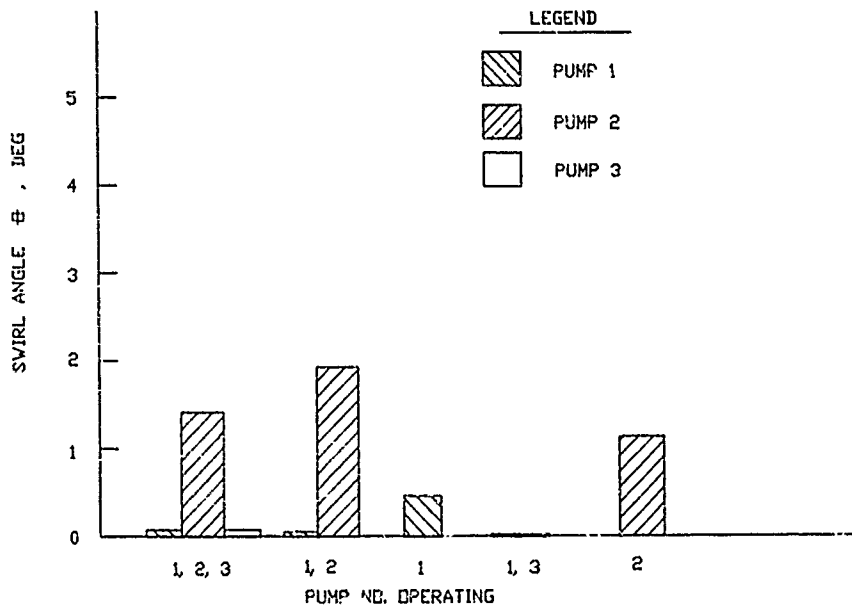


WATER-SURFACE EL 280.0

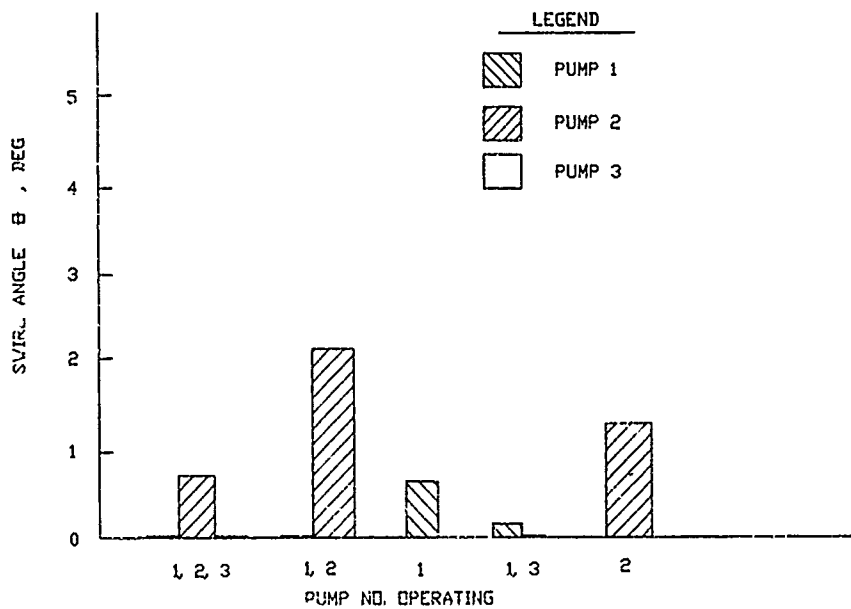


WATER-SURFACE EL 275.0

SWIRL ANGLE  
FSI DESIGN B  
DISCHARGE PER PUMP 500 CFS  
WATER-SURFACE EL 280.0 AND 275.0

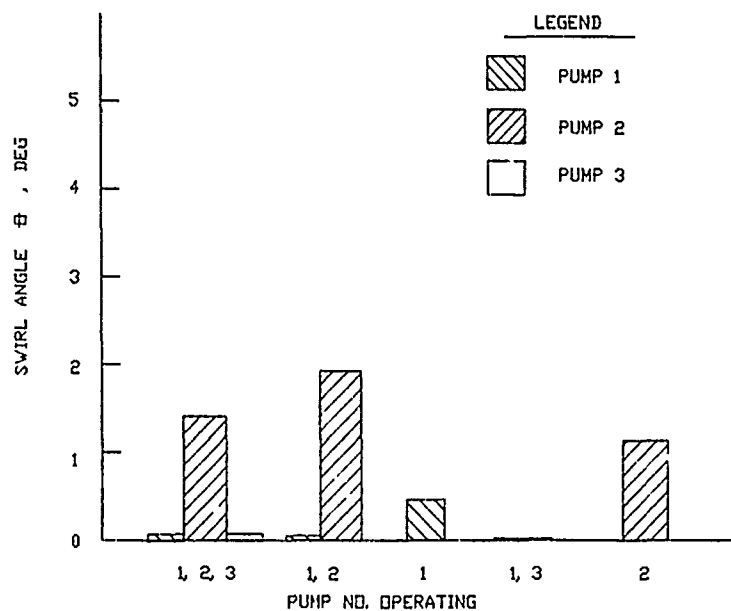


WATER-SURFACE EL 290.0

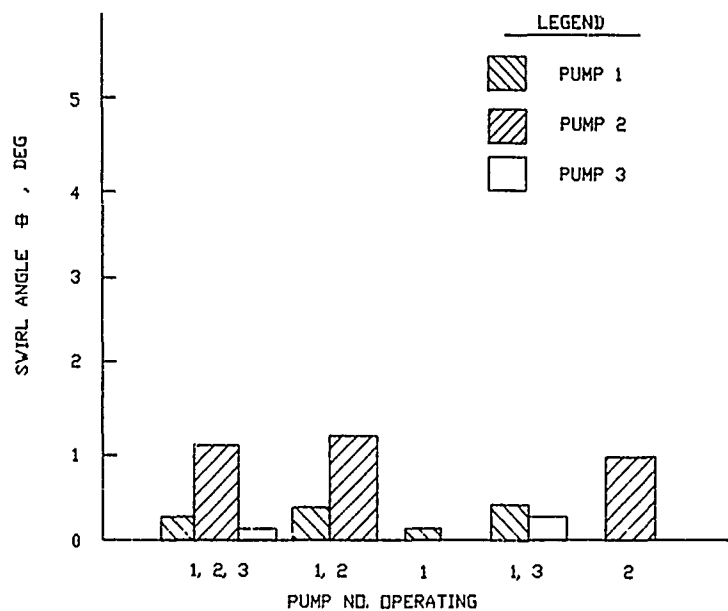


WATER-SURFACE EL 285.0

SWIRL ANGLE  
FSI DESIGN B  
DISCHARGE PER PUMP 650 CFS  
WATER-SURFACE EL 290.0 AND 285.0

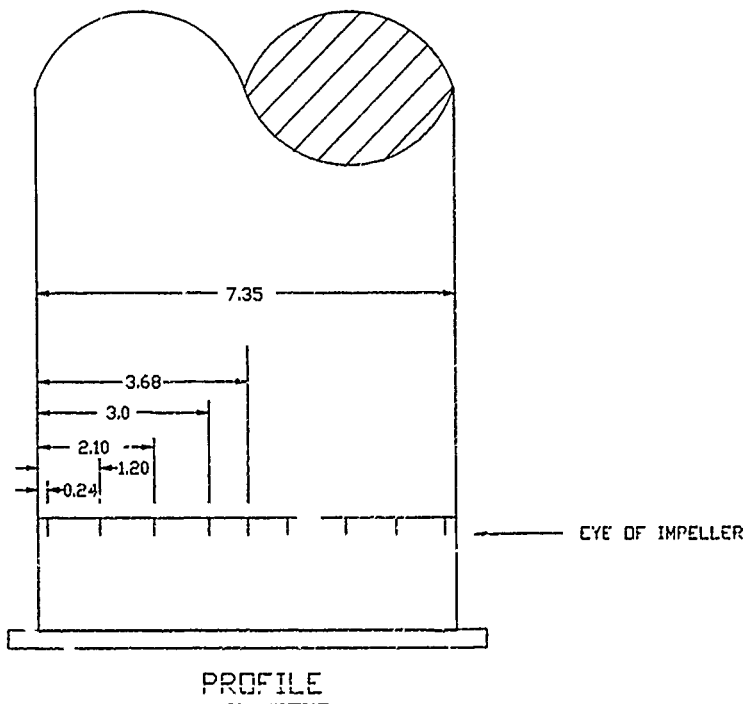
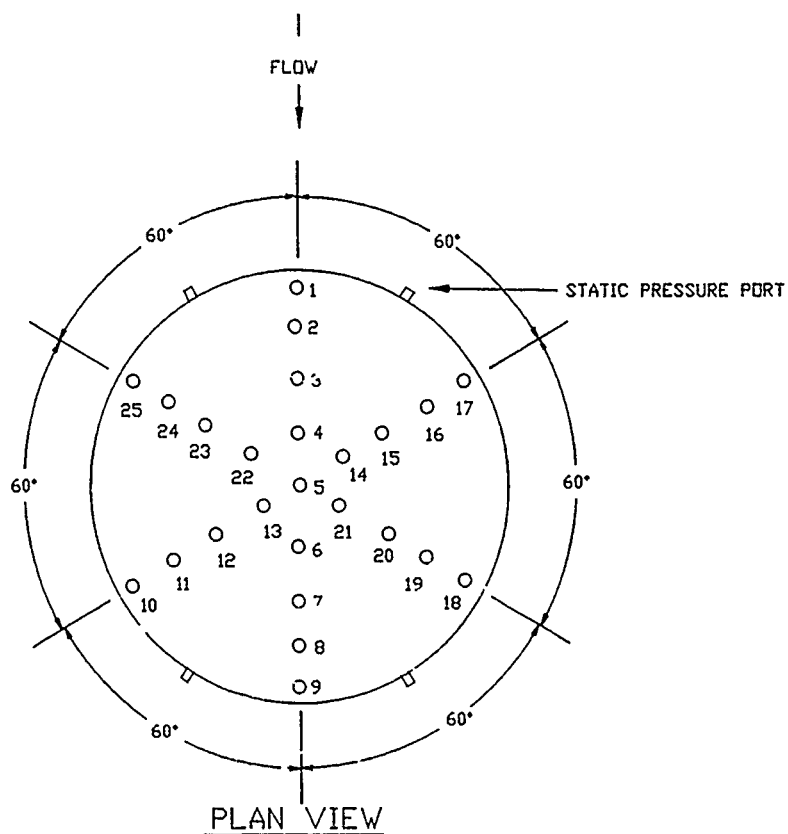


WATER-SURFACE EL 280.0



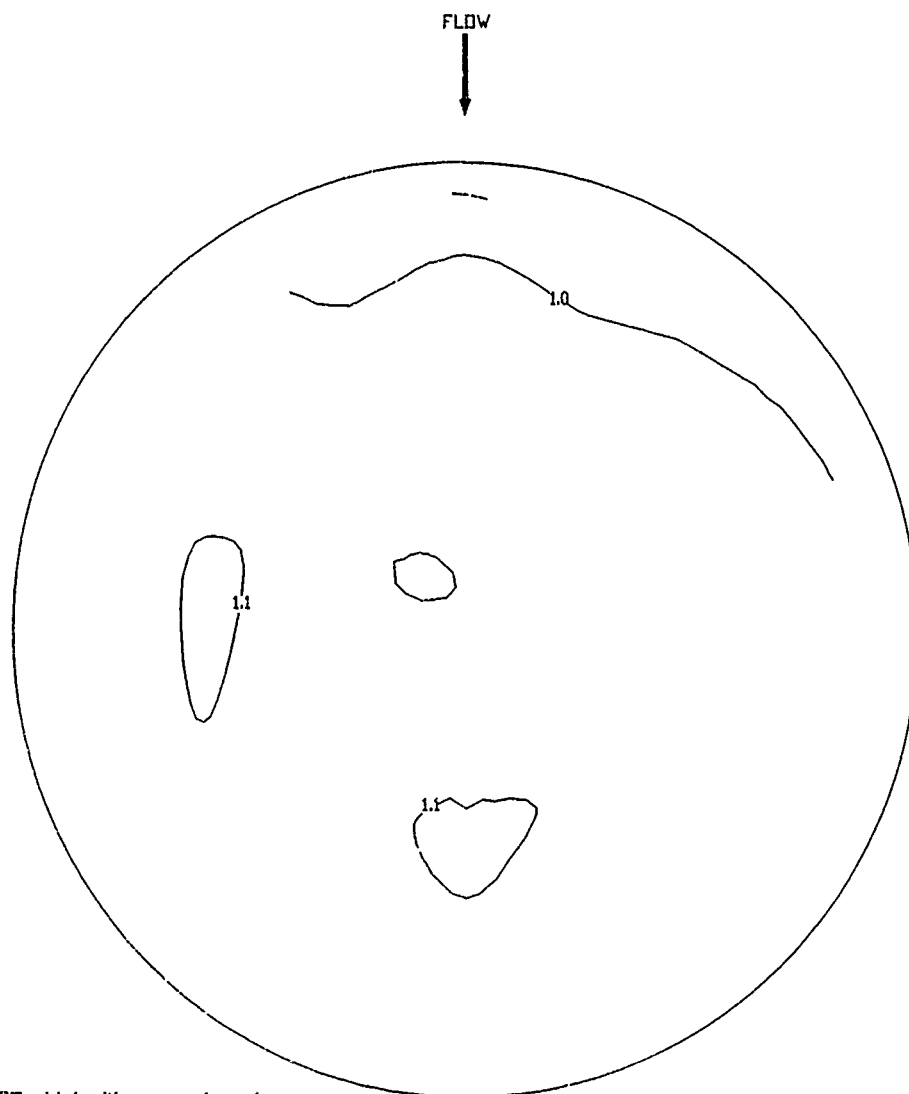
WATER-SURFACE EL 275.0

SWIRL ANGLE  
FSI DESIGN B  
DISCHARGE PER PUMP 650 CFS  
WATER-SURFACE EL 280.0 AND 275.0



NOTE: ALL DIMENSIONS IN FEET

### IMPACT TUBES AND STATIC PRESSURE PORTS DESIGN B

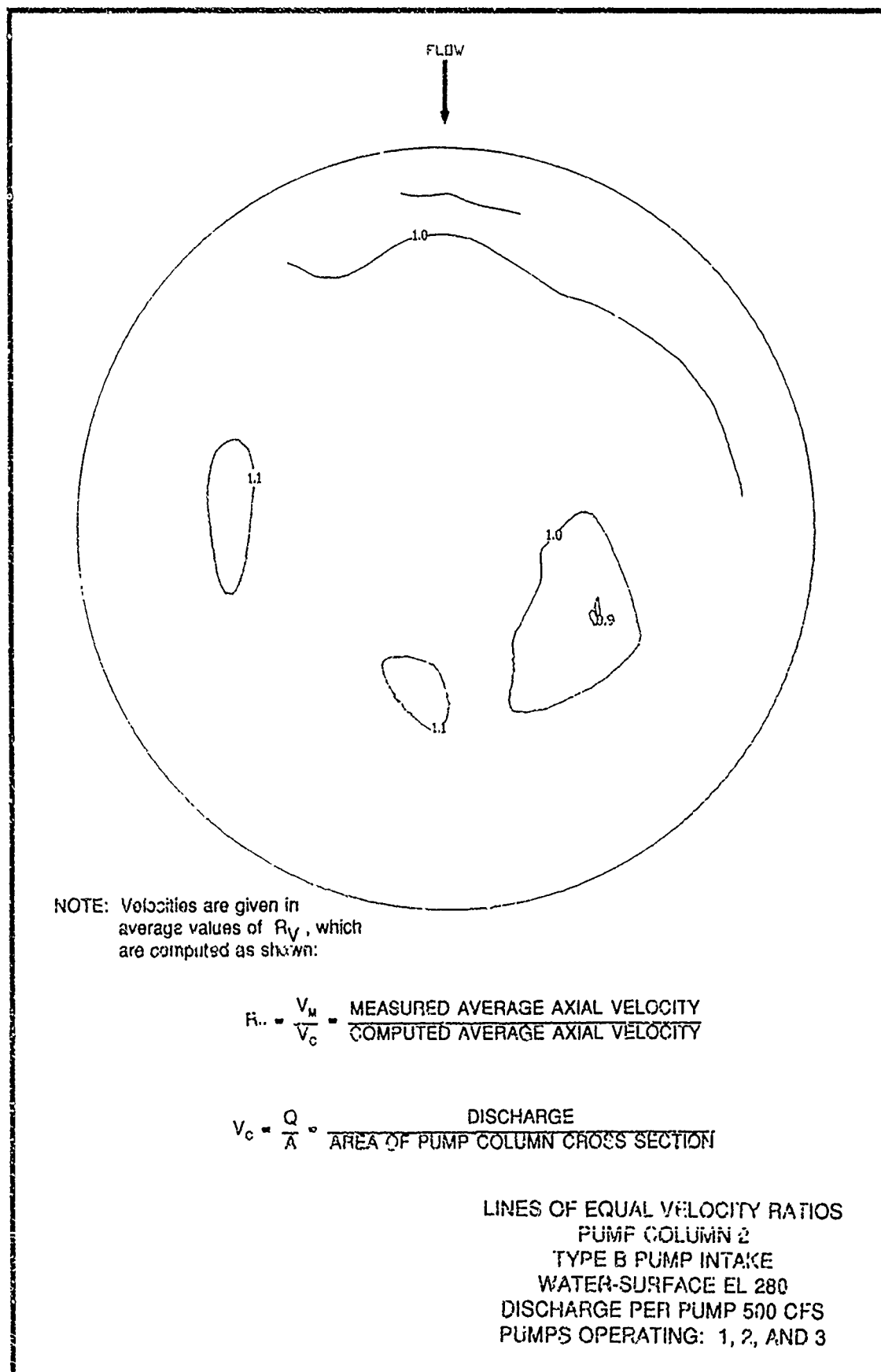


NOTE: Velocities are given in average values of  $R_v$ , which are computed as shown:

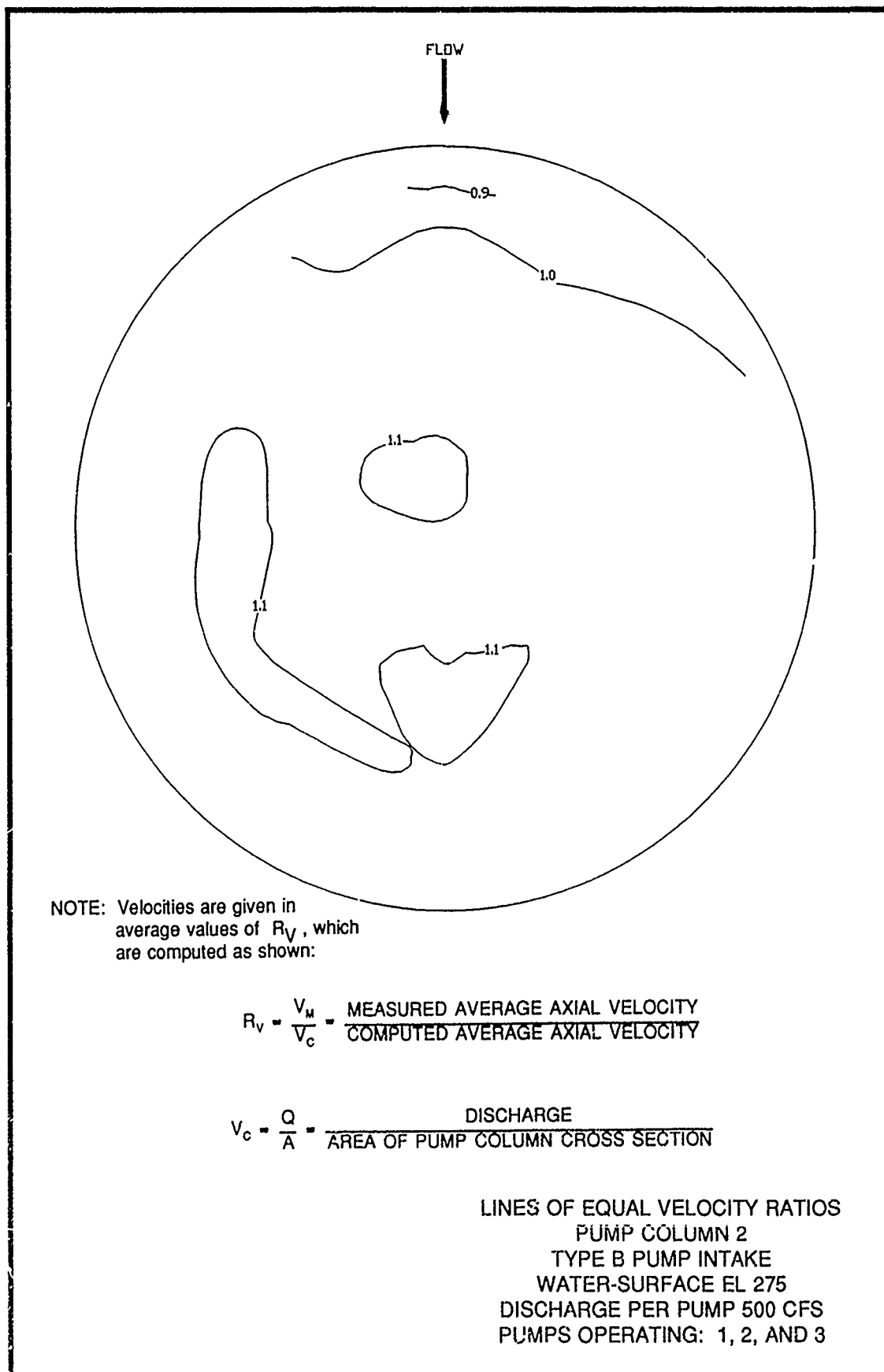
$$R_v = \frac{V_m}{V_c} = \frac{\text{MEASURED AVERAGE AXIAL VELOCITY}}{\text{COMPUTED AVERAGE AXIAL VELOCITY}}$$

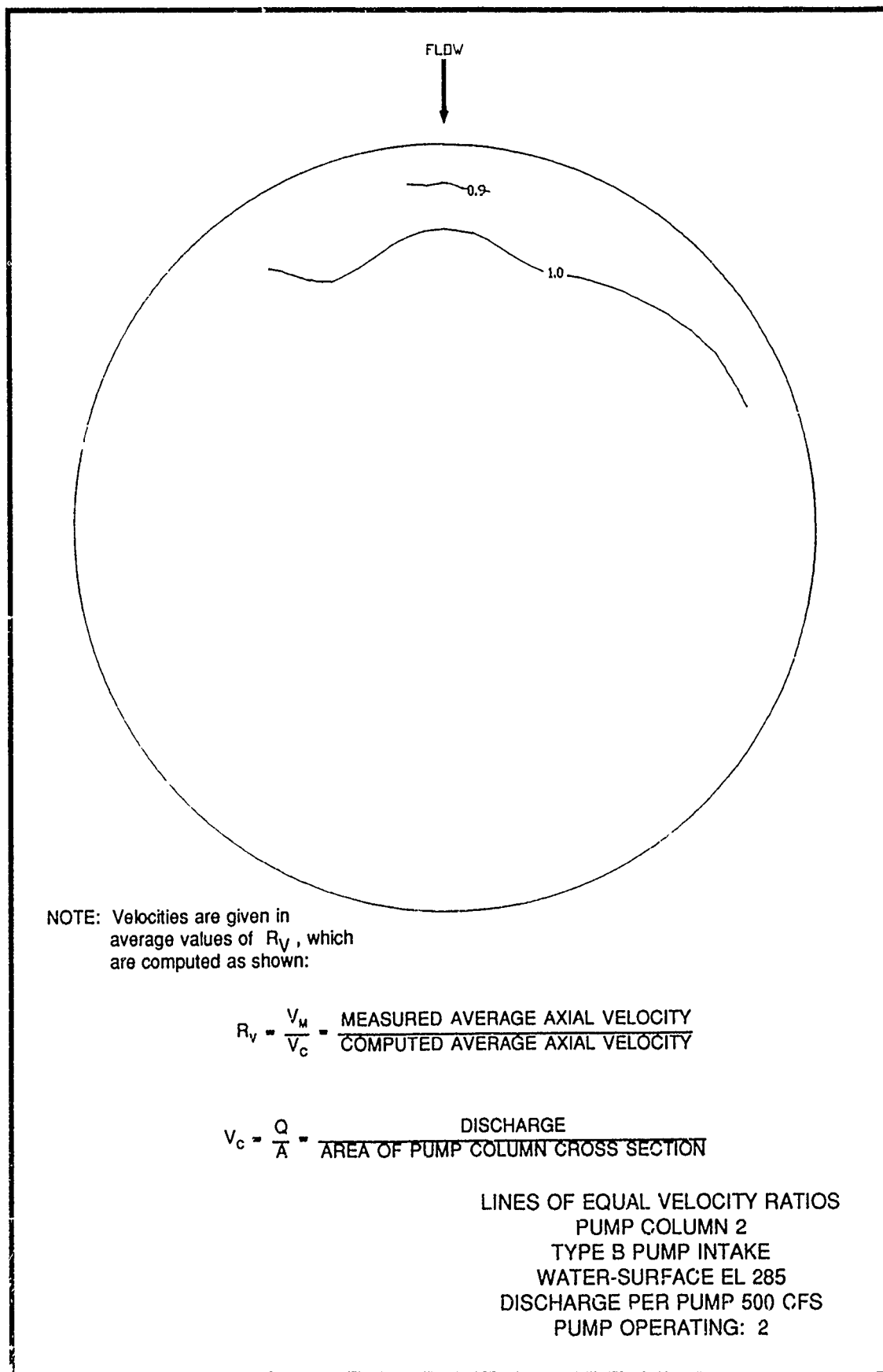
$$V_c = \frac{Q}{A} = \frac{\text{DISCHARGE}}{\text{AREA OF PUMP COLUMN CROSS SECTION}}$$

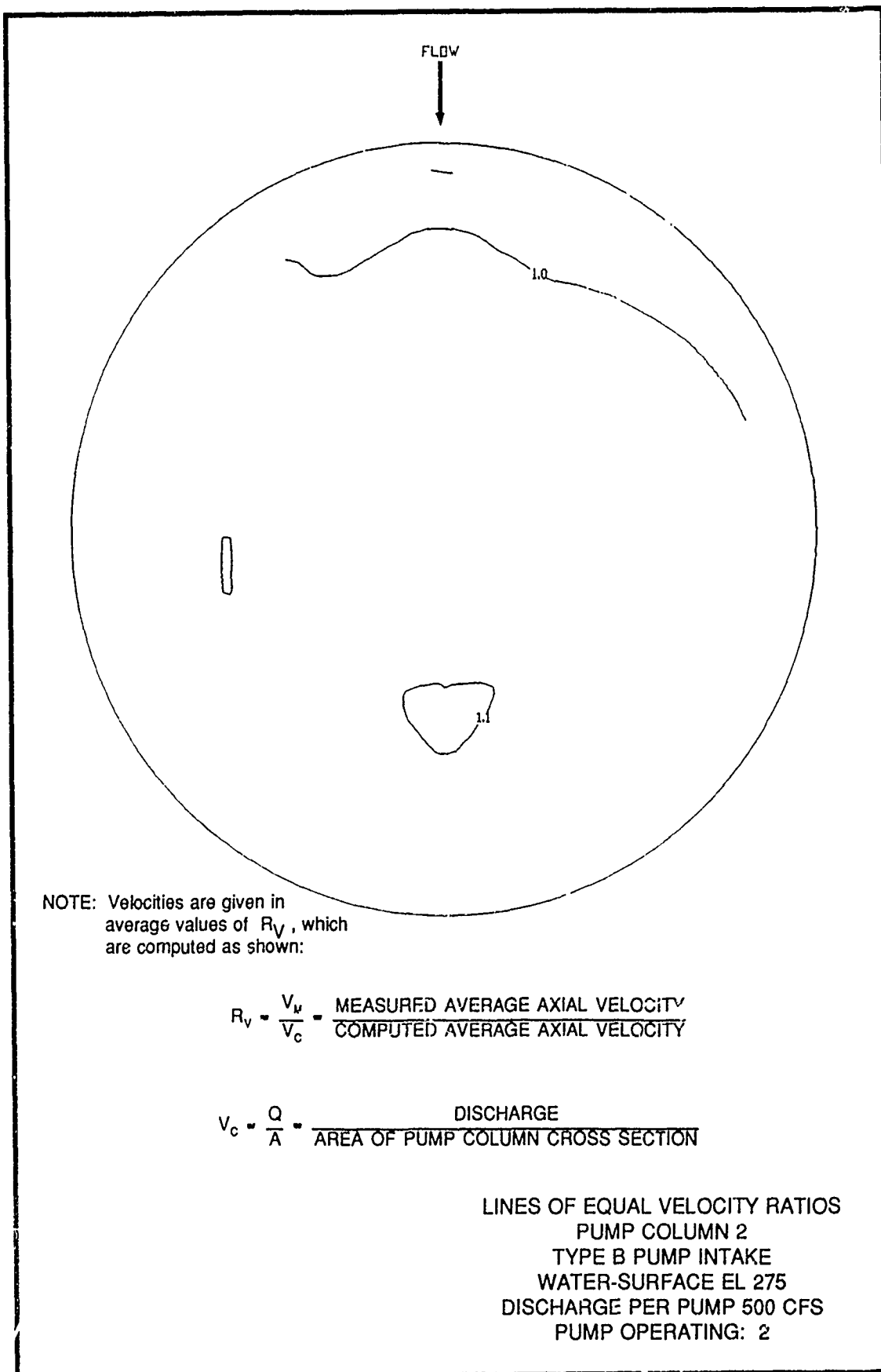
LINES OF EQUAL VELOCITY RATIOS  
PUMP COLUMN 2  
TYPE B PUMP INTAKE  
WATER-SURFACE EL 285  
DISCHARGE PER PUMP 500 CFS  
PUMPS OPERATING: 1, 2, AND 3

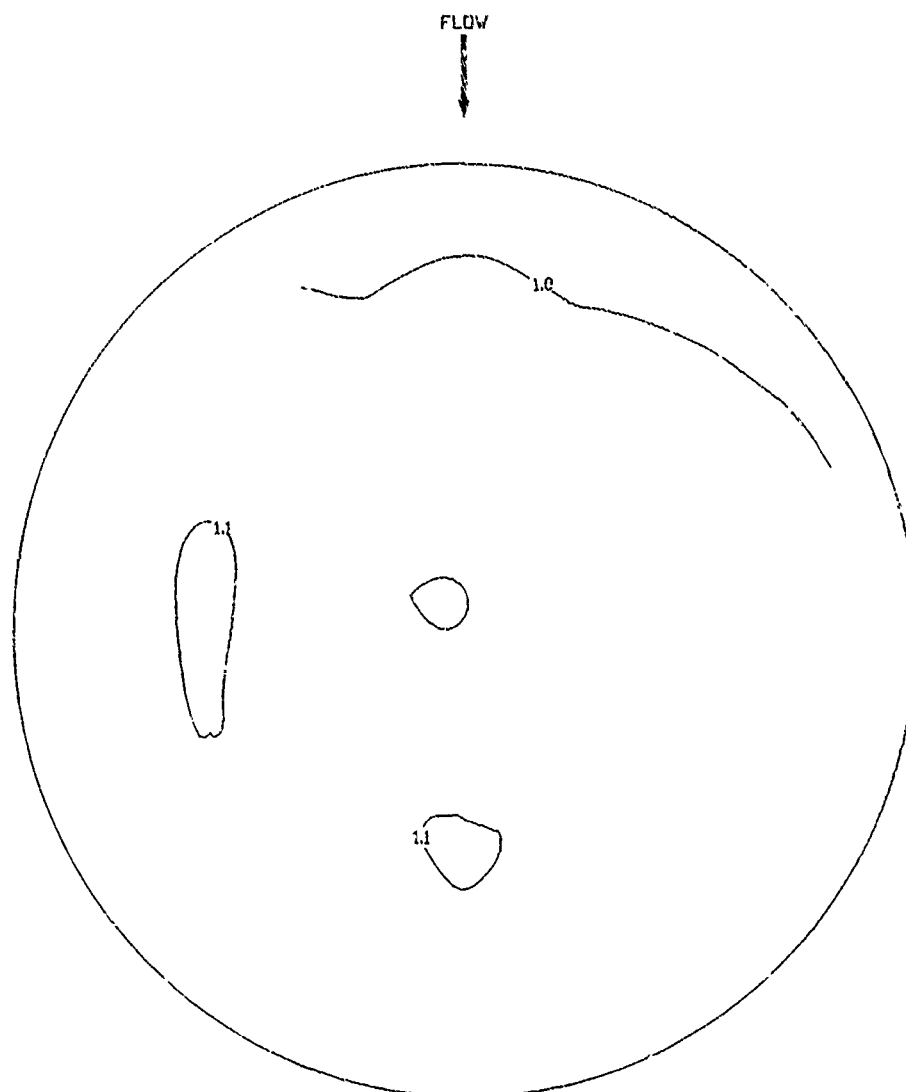










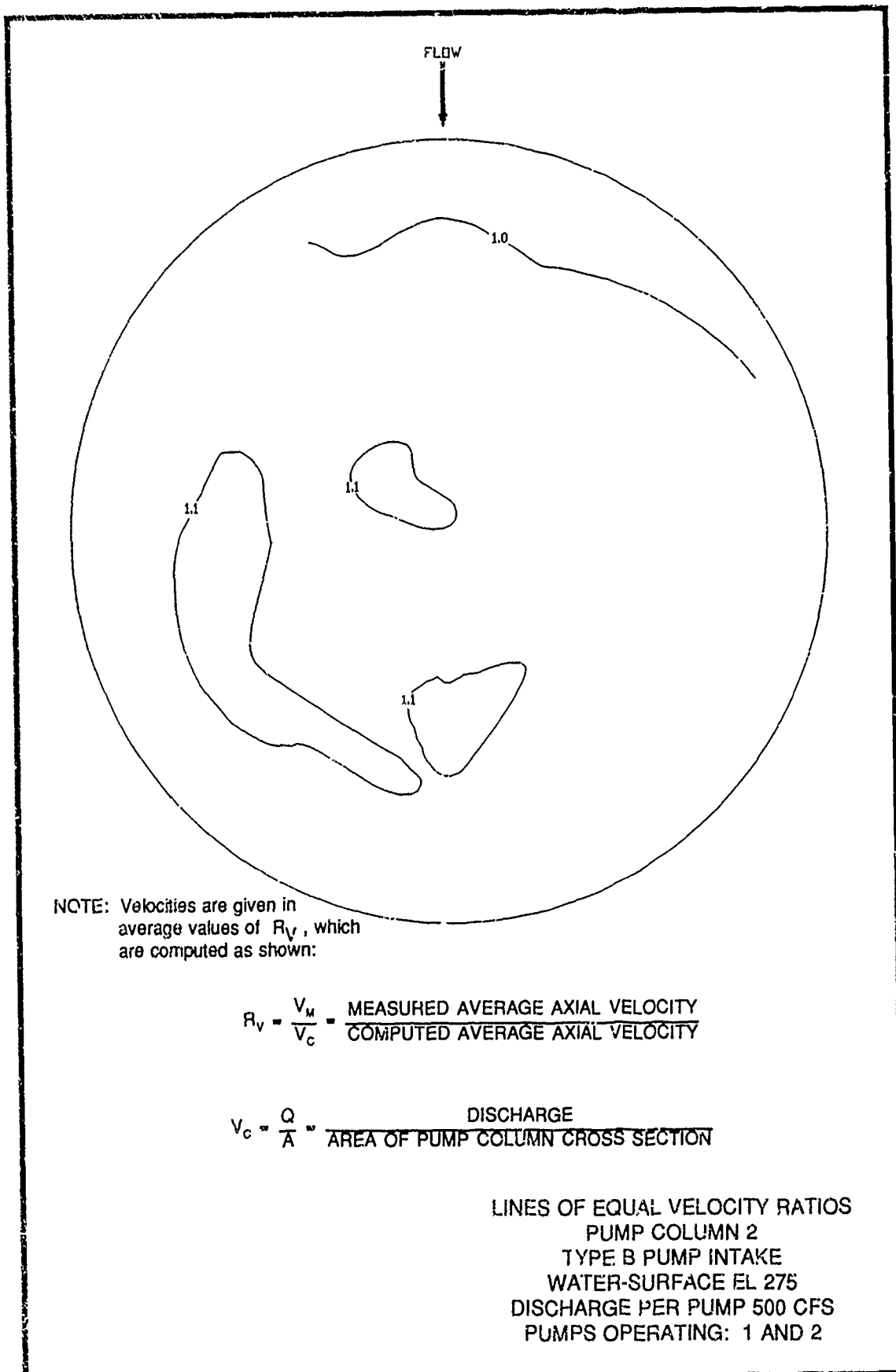


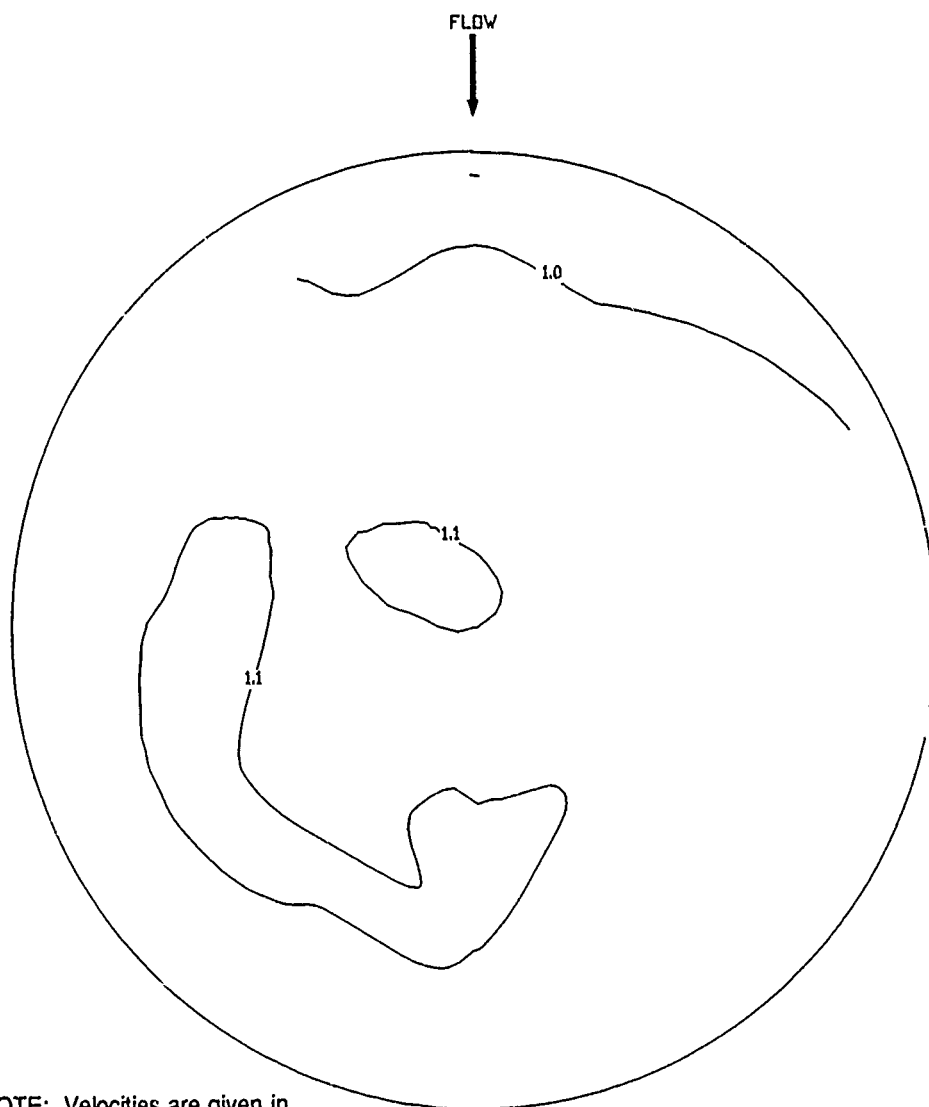
NOTE: Velocities are given in average values of  $R_v$ , which are computed as shown:

$$R_v = \frac{V_m}{V_c} = \frac{\text{MEASURED AVERAGE AXIAL VELOCITY}}{\text{COMPUTED AVERAGE AXIAL VELOCITY}}$$

$$V_c = \frac{Q}{A} = \frac{\text{DISCHARGE}}{\text{AREA OF PUMP COLUMN CROSS SECTION}}$$

LINES OF EQUAL VELOCITY RATIOS  
PUMP COLUMN 2  
TYPE B PUMP INTAKE  
WATER-SURFACE EL 285  
DISCHARGE PER PUMP 500 CFS  
PUMPS OPERATING: 1 AND 2



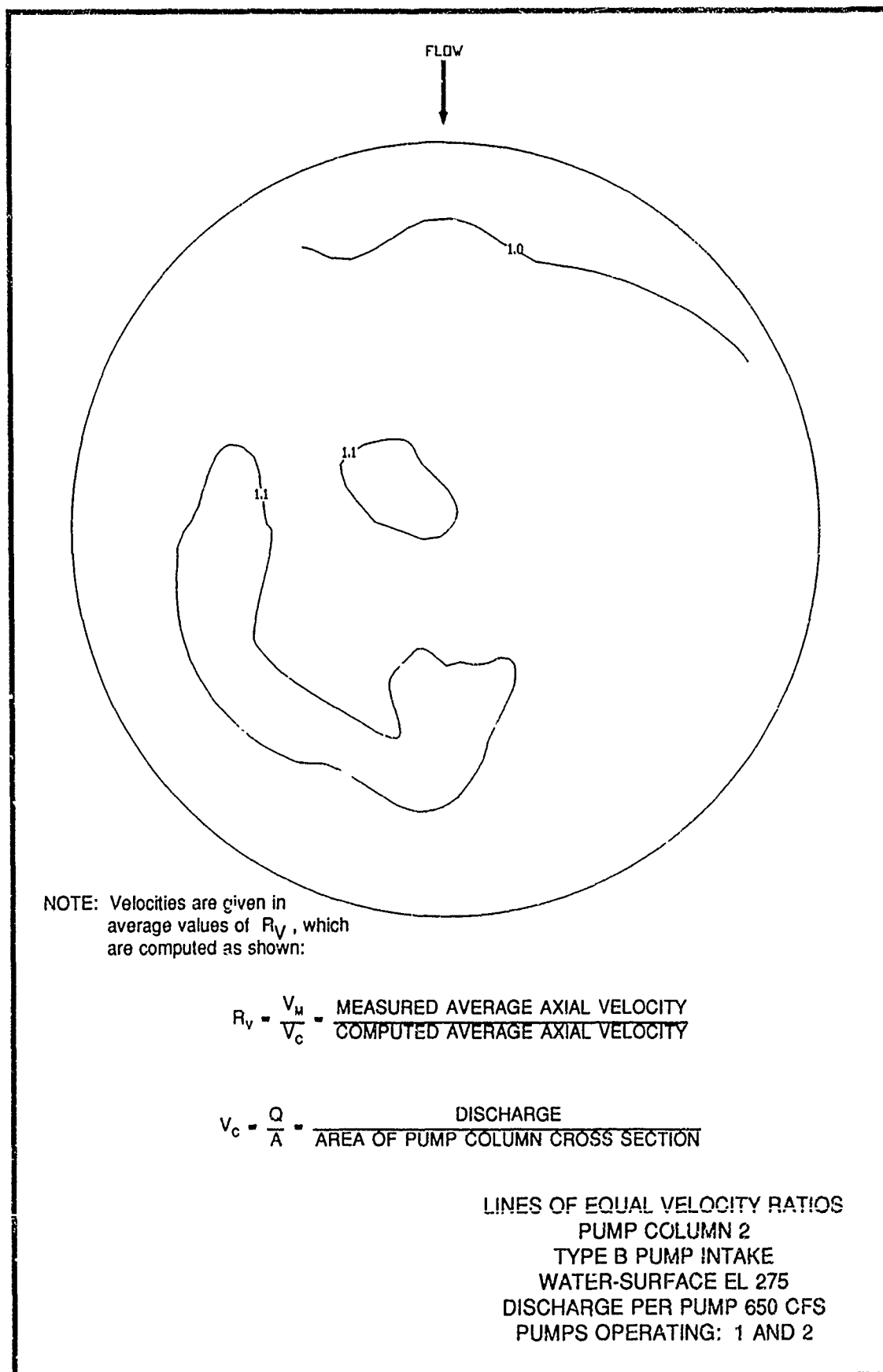


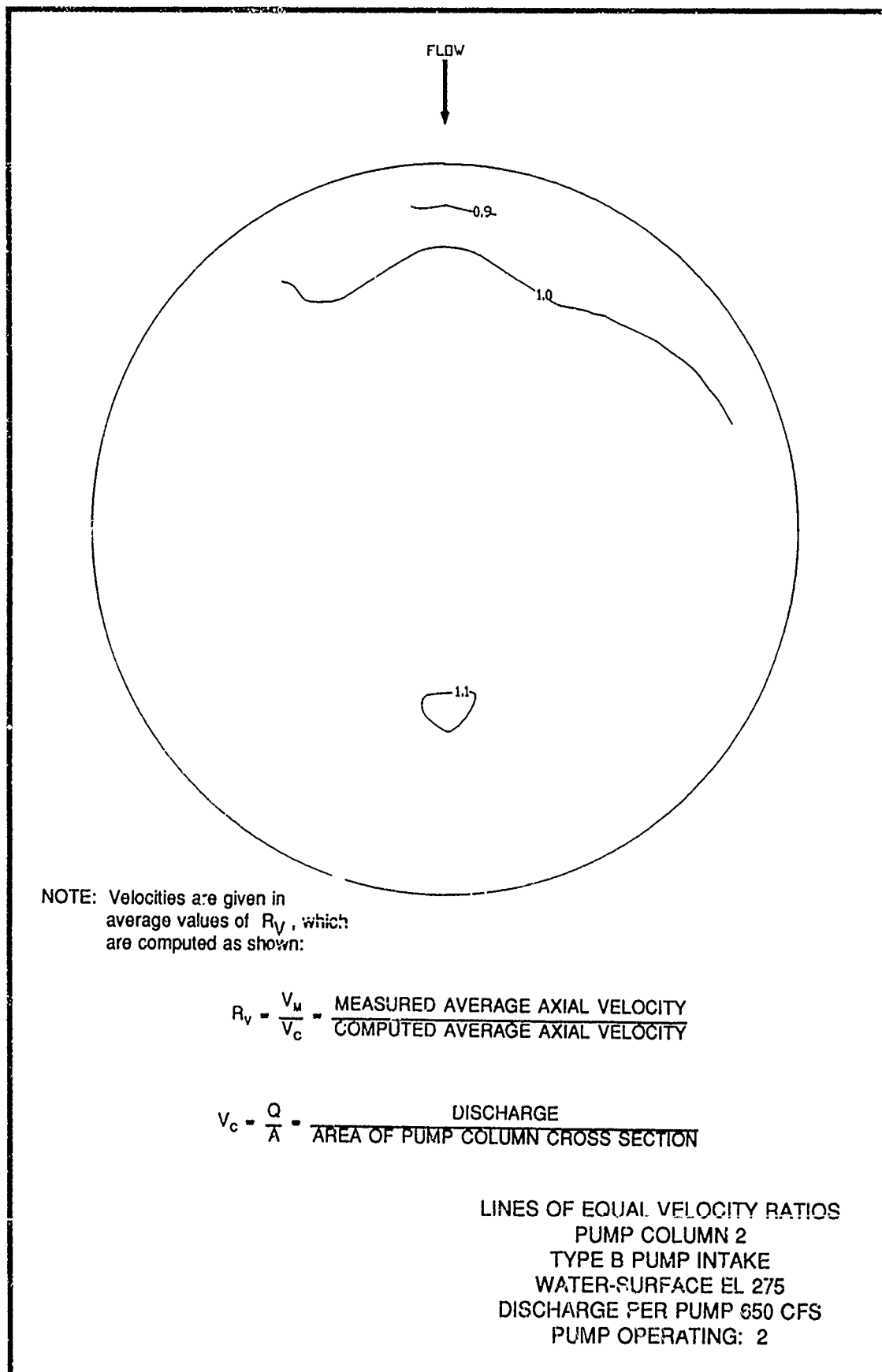
NOTE: Velocities are given in average values of  $R_v$ , which are computed as shown:

$$R_v = \frac{V_m}{V_c} = \frac{\text{MEASURED AVERAGE AXIAL VELOCITY}}{\text{COMPUTED AVERAGE AXIAL VELOCITY}}$$

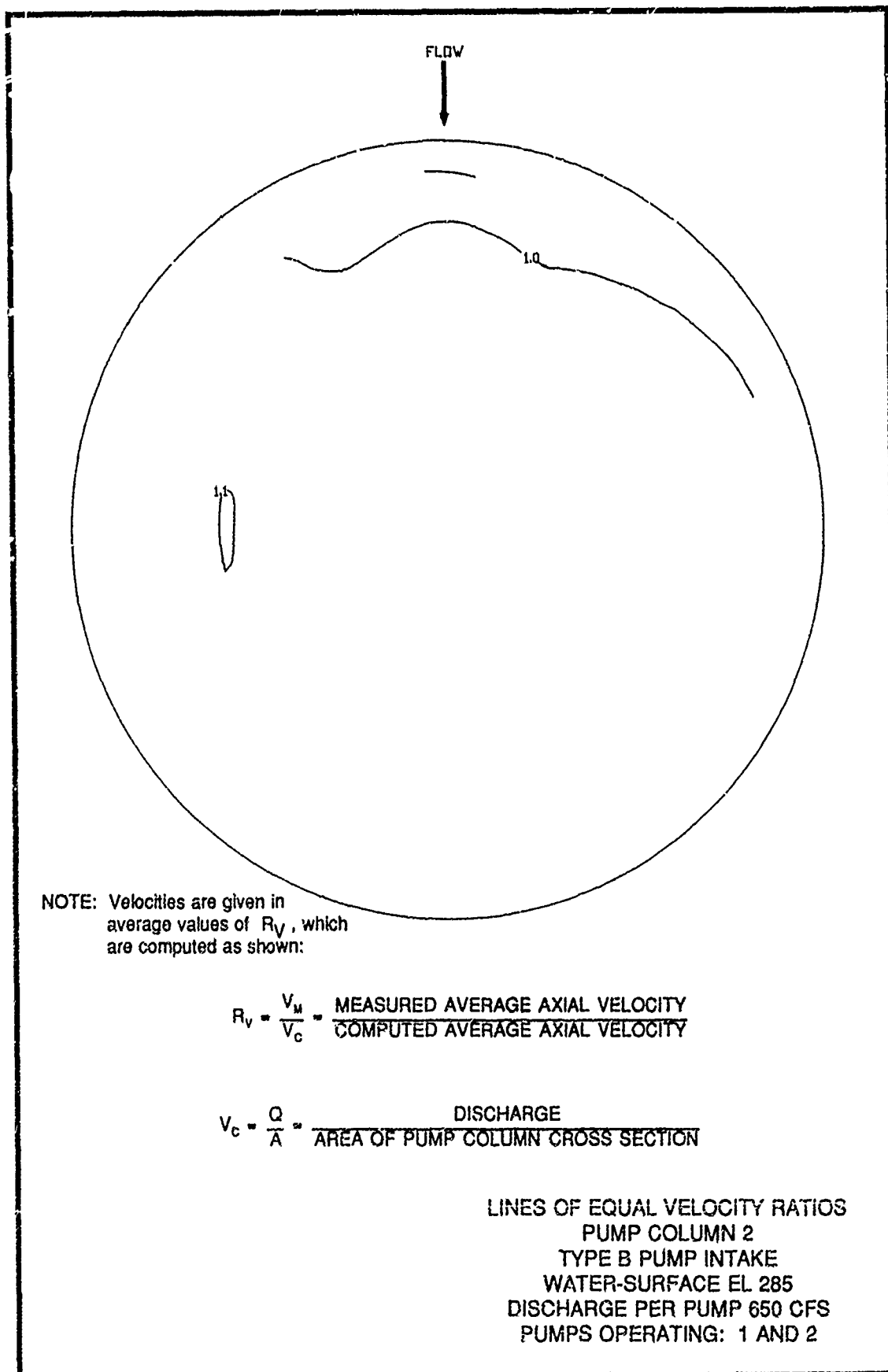
$$V_c = \frac{Q}{A} = \frac{\text{DISCHARGE}}{\text{AREA OF PUMP COLUMN CROSS SECTION}}$$

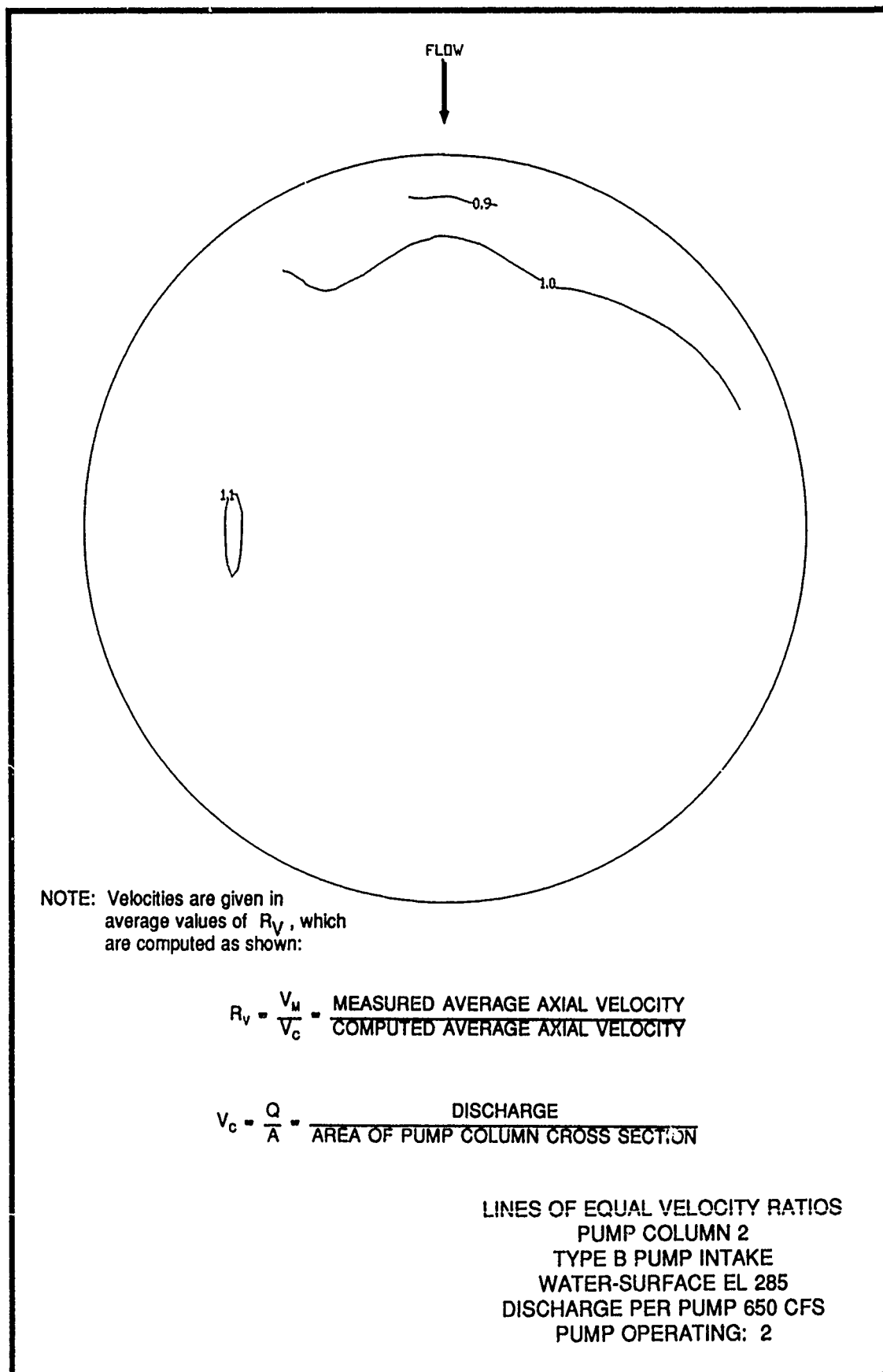
LINES OF EQUAL VELOCITY RATIOS  
PUMP COLUMN 2  
TYPE B PUMP INTAKE  
WATER-SURFACE EL 275  
DISCHARGE PER PUMP 650 CFS  
PUMPS OPERATING: 1, 2, AND 3









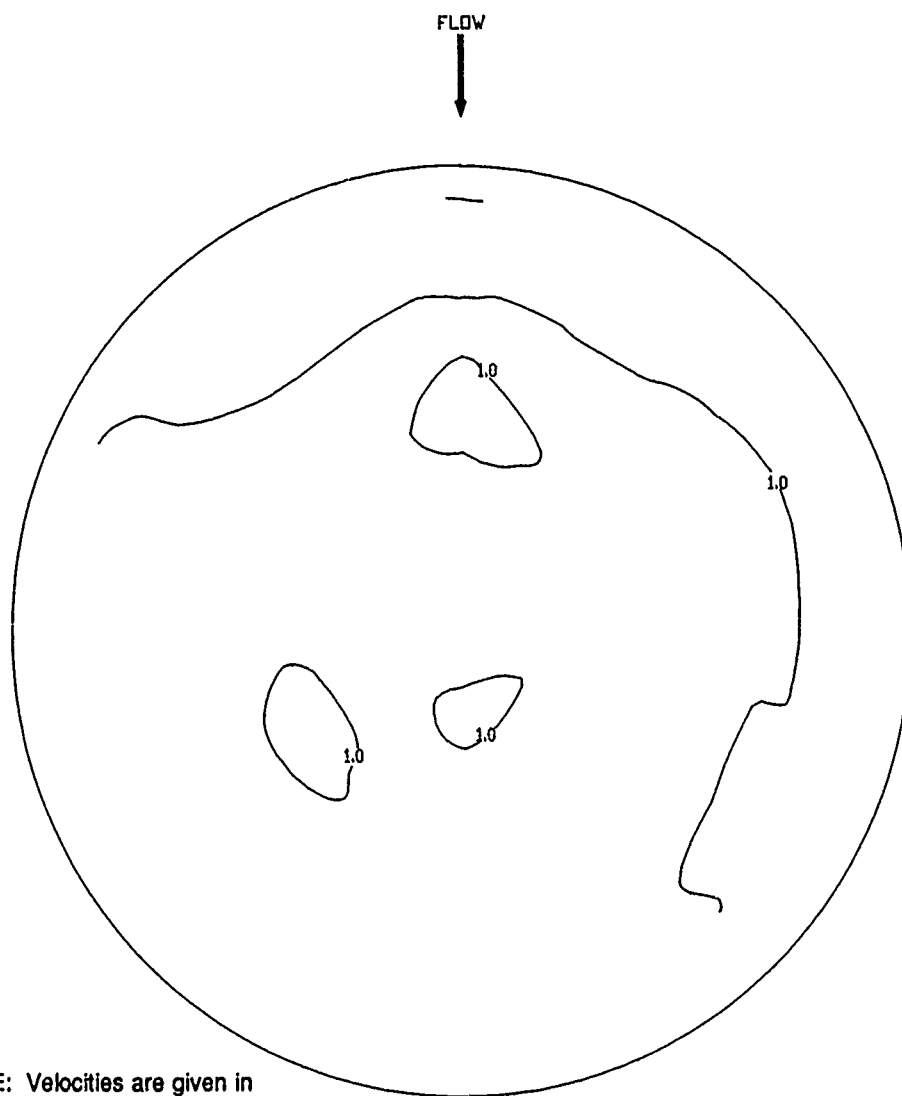


NOTE: Velocities are given in average values of  $R_v$ , which are computed as shown:

$$R_v = \frac{V_m}{V_c} = \frac{\text{MEASURED AVERAGE AXIAL VELOCITY}}{\text{COMPUTED AVERAGE AXIAL VELOCITY}}$$

$$V_c = \frac{Q}{A} = \frac{\text{DISCHARGE}}{\text{AREA OF PUMP COLUMN CROSS SECTION}}$$

LINES OF EQUAL VELOCITY RATIOS  
 PUMP COLUMN 2  
 TYPE B PUMP INTAKE  
 WATER-SURFACE EL 285  
 DISCHARGE PER PUMP 650 CFS  
 PUMP OPERATING: 2

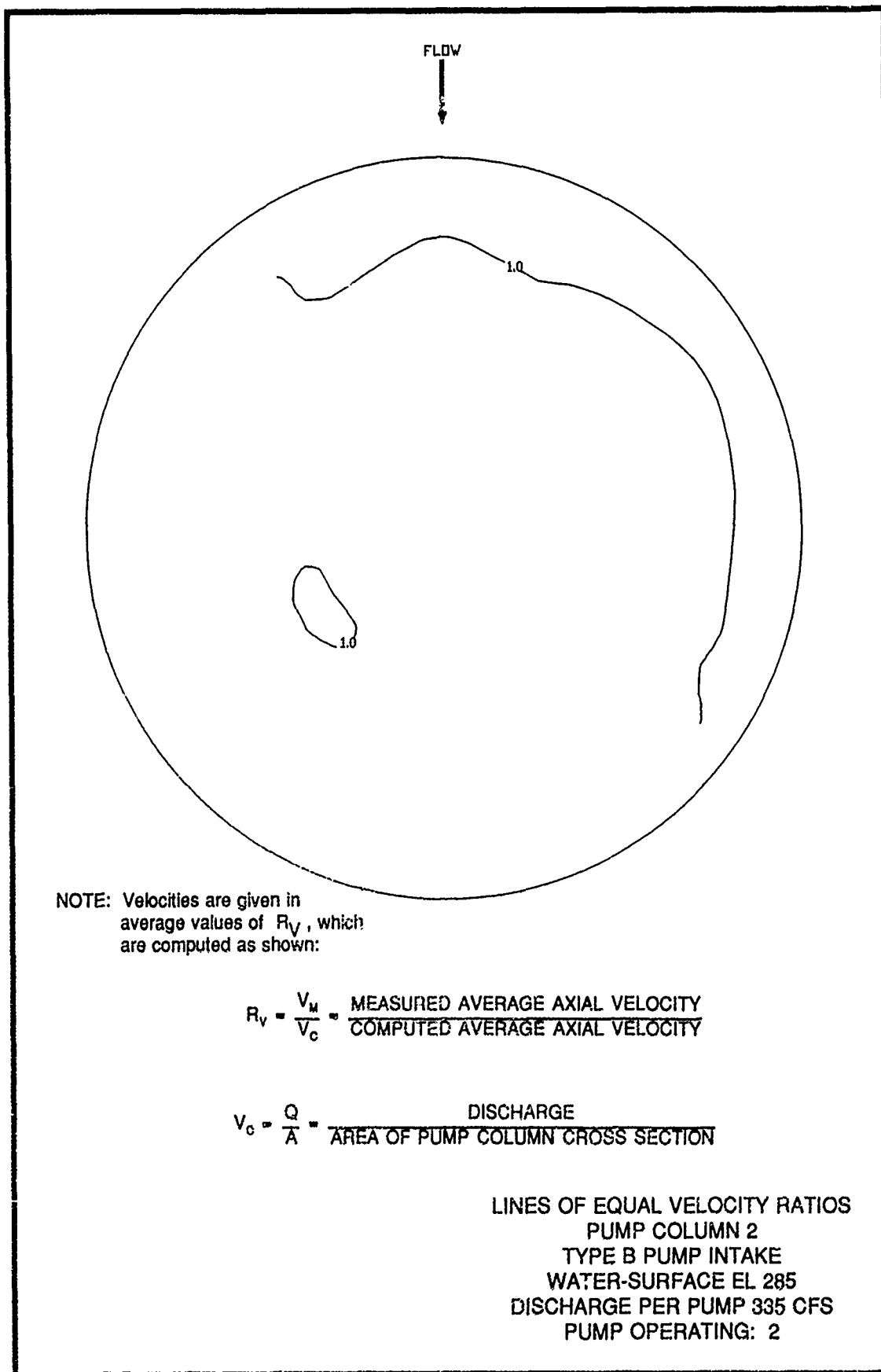


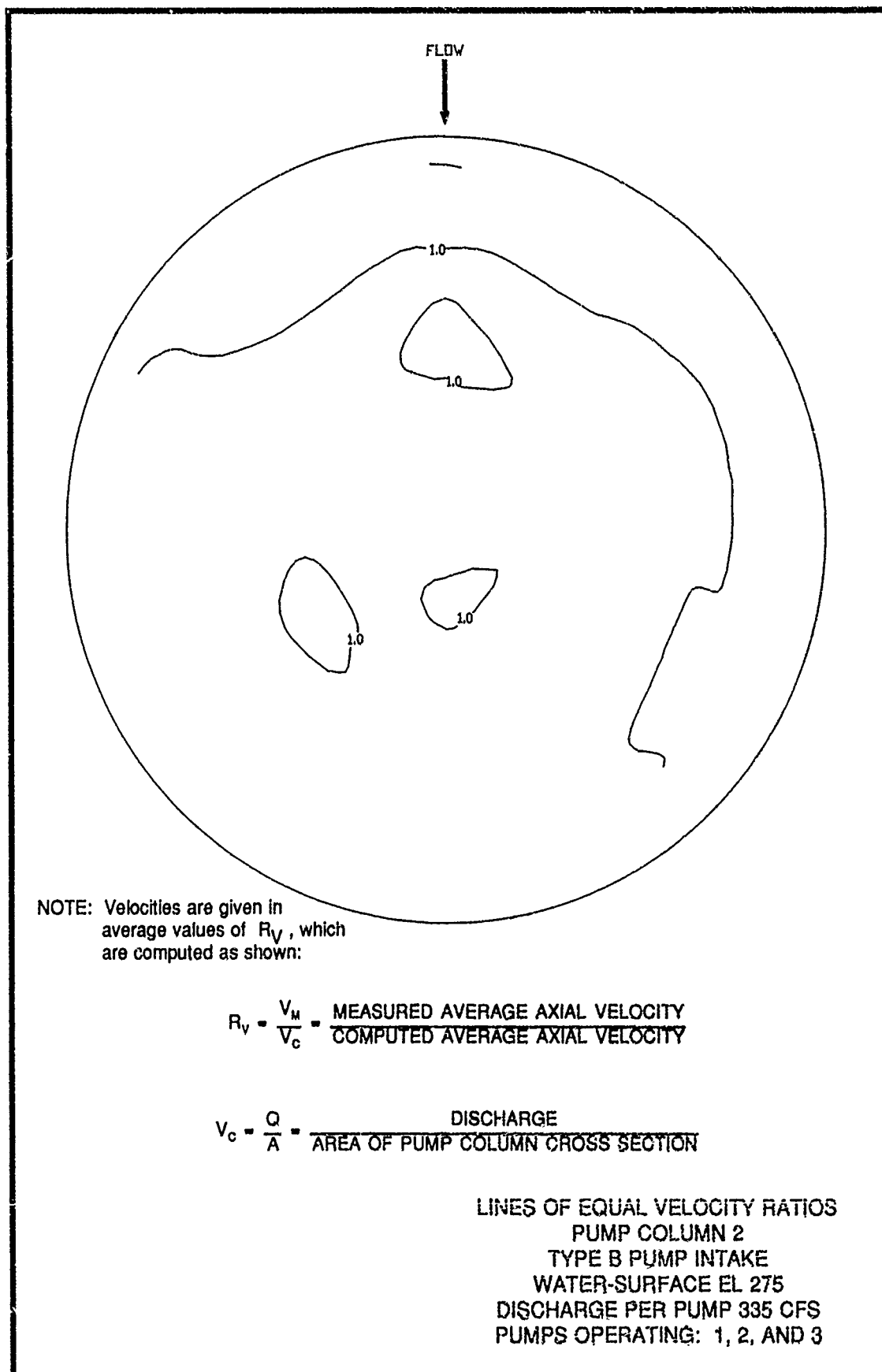
NOTE: Velocities are given in average values of  $R_v$ , which are computed as shown:

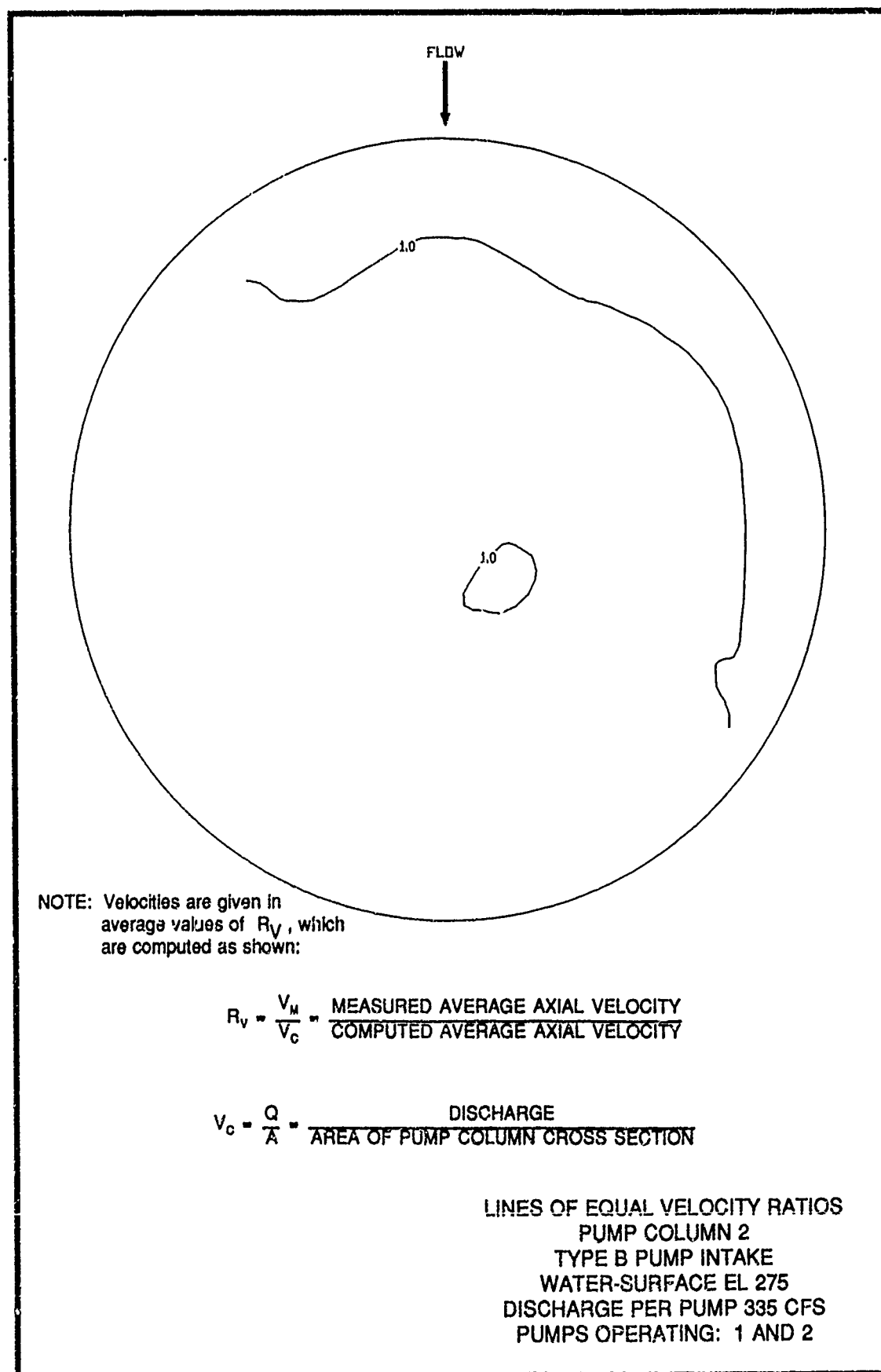
$$R_v = \frac{V_m}{V_c} = \frac{\text{MEASURED AVERAGE AXIAL VELOCITY}}{\text{COMPUTED AVERAGE AXIAL VELOCITY}}$$

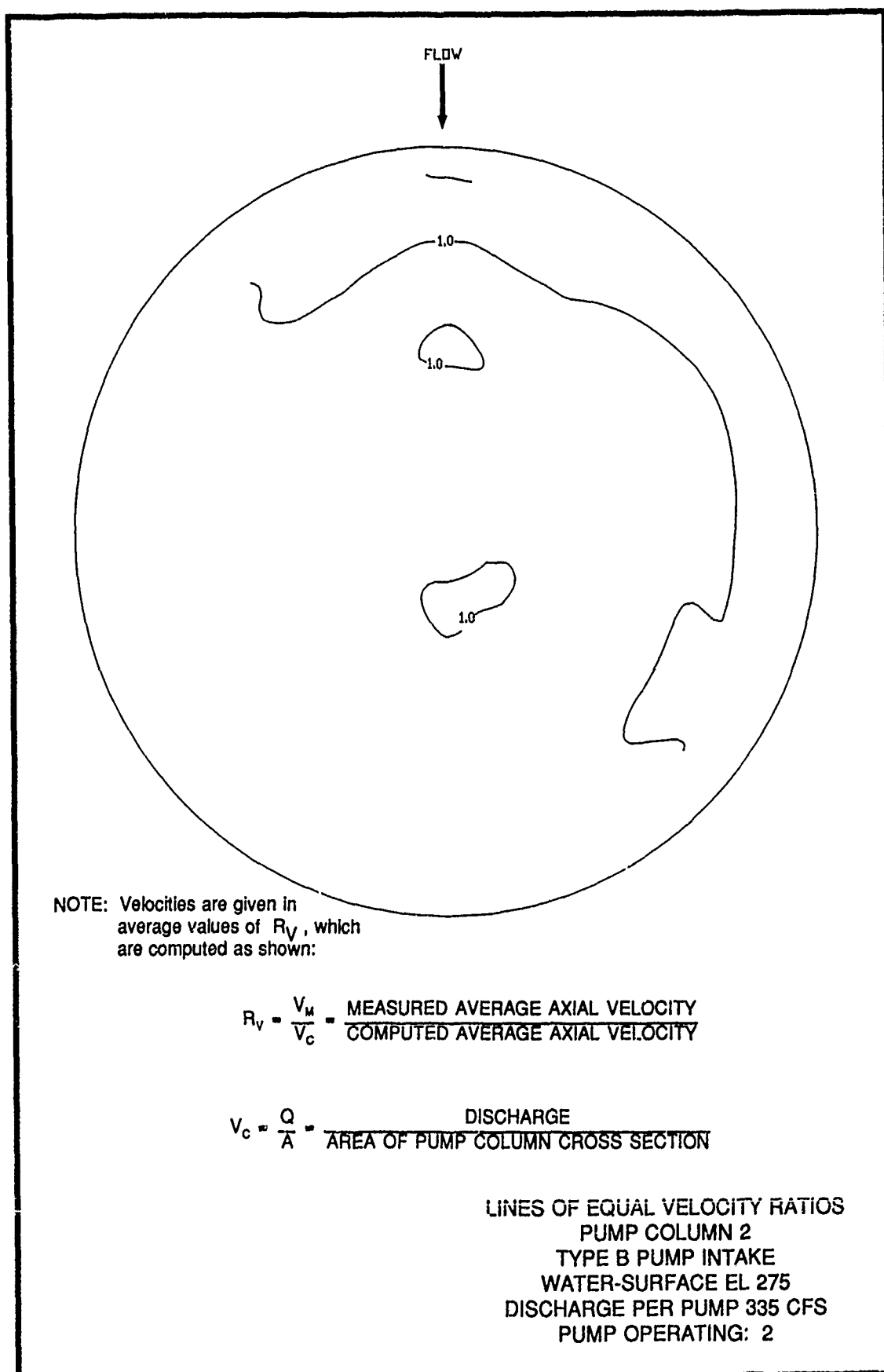
$$V_c = \frac{Q}{A} = \frac{\text{DISCHARGE}}{\text{AREA OF PUMP COLUMN CROSS SECTION}}$$

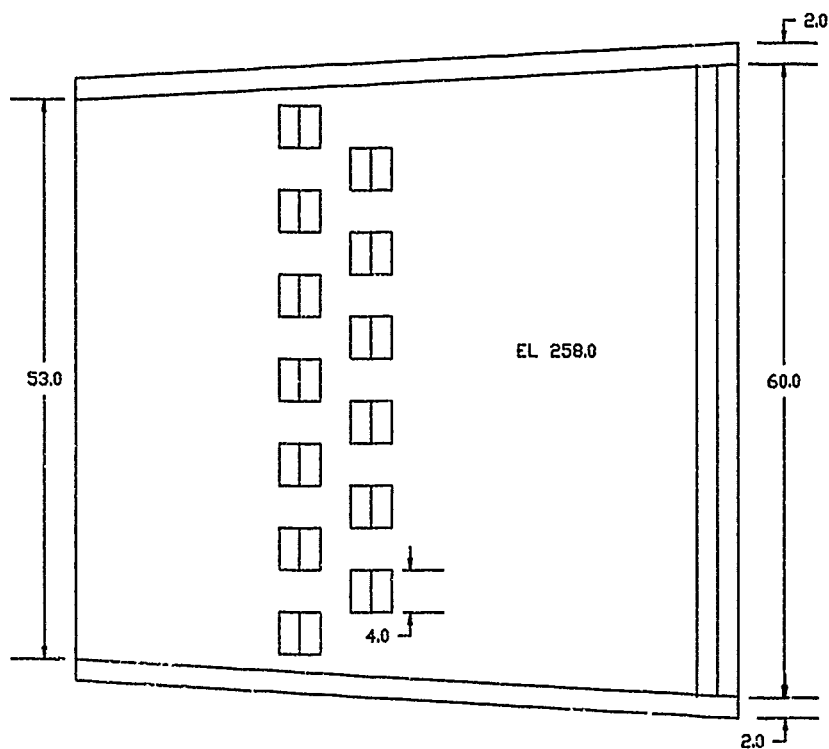
LINES OF EQUAL VELOCITY RATIOS  
 PUMP COLUMN 2  
 TYPE B PUMP INTAKE  
 WATER-SURFACE EL 285  
 DISCHARGE PER PUMP 335 CFS  
 PUMPS OPERATING: 1, 2, AND 3



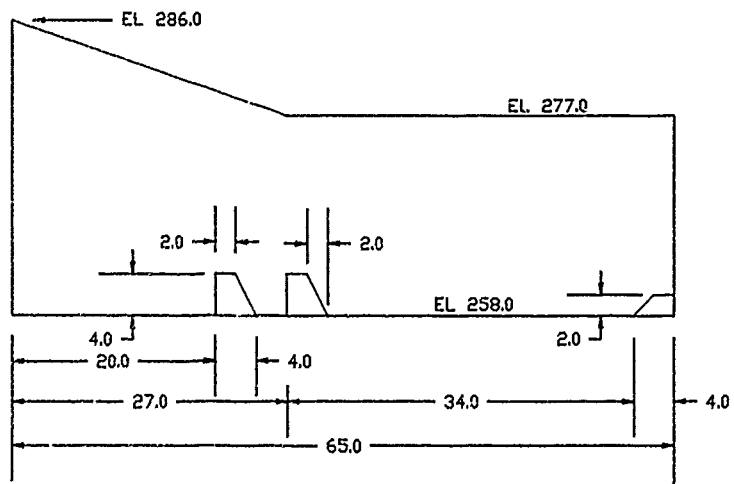








PLAN

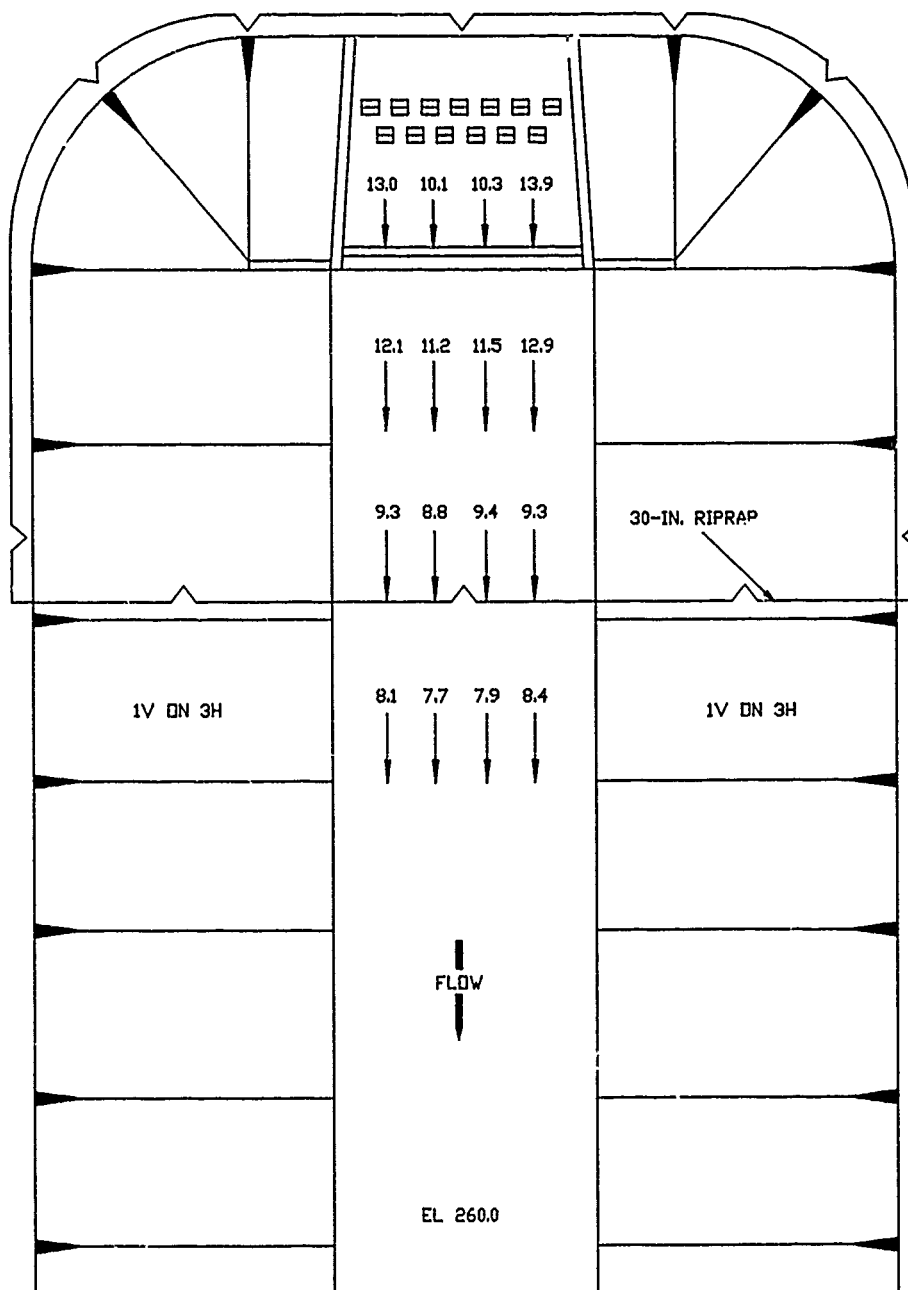


PROFILE

# GRAVITY FLOW STILLING BASIN

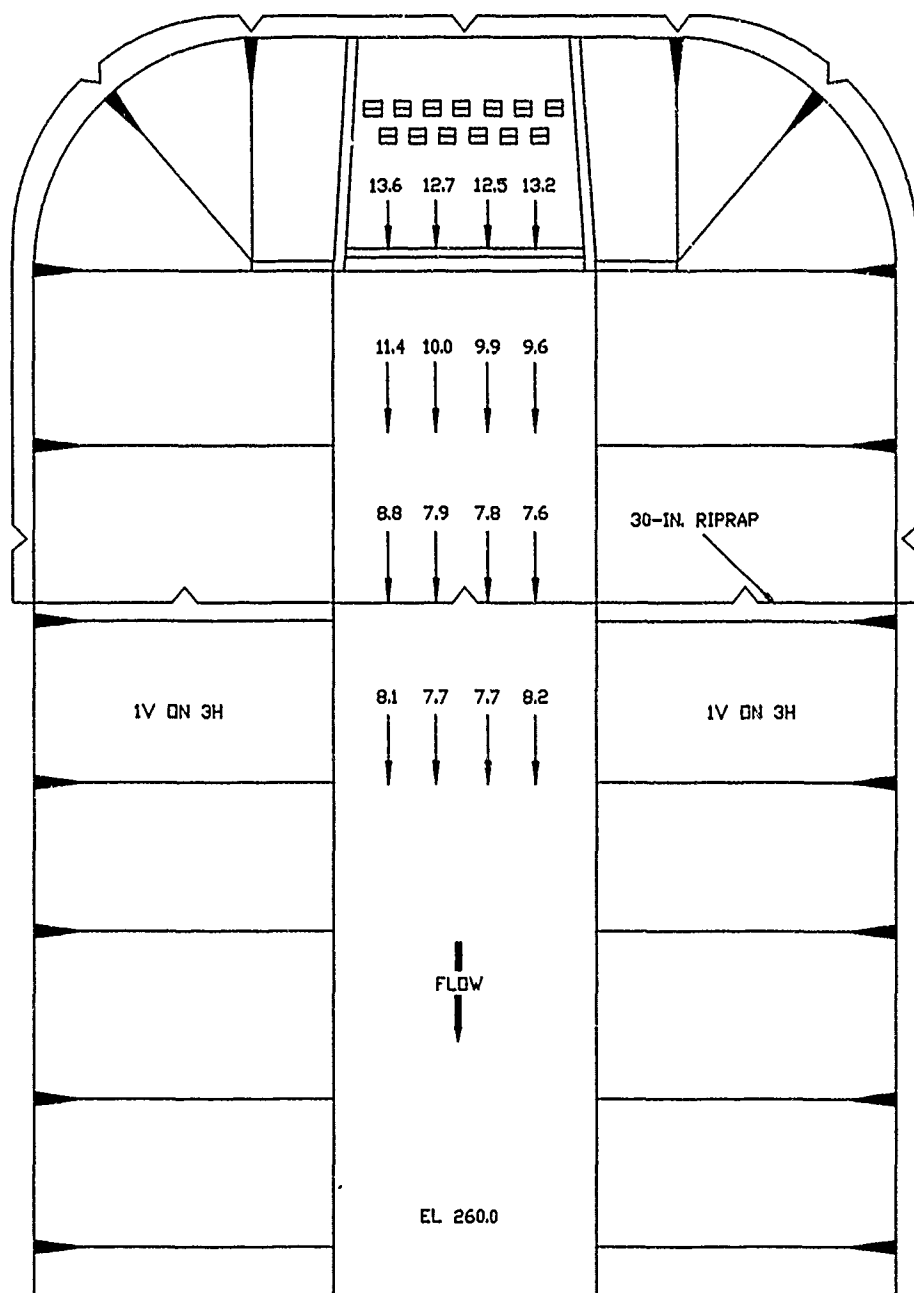
NOTE: ALL DIMENSIONS IN FEET





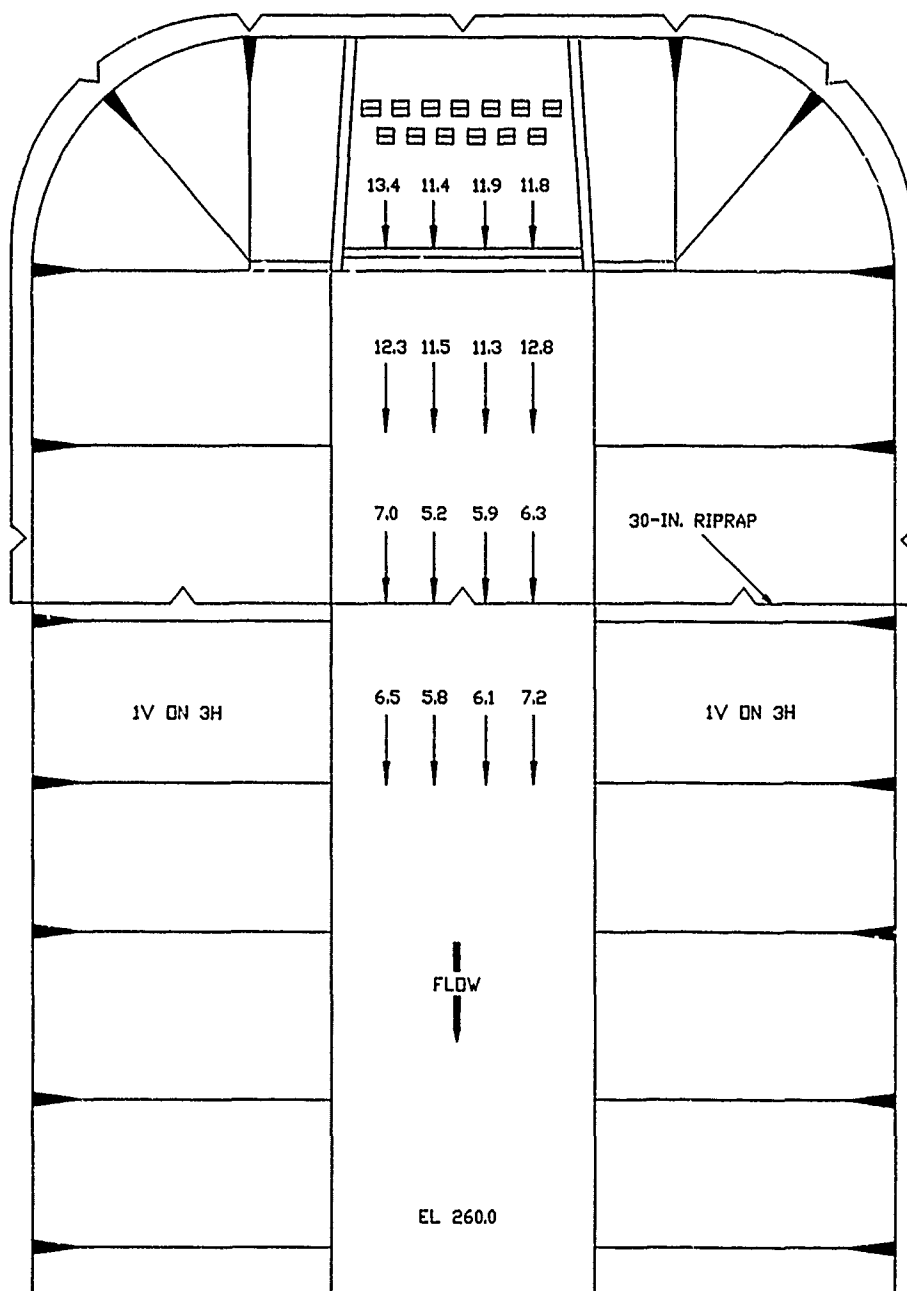
SURFACE VELOCITIES IN VICINITY OF STILLING BASIN  
 DISCHARGE 5,000 CFS  
 HEADWATER EL 274.9  
 TAILWATER EL 267.4

NOTE : VELOCITIES MEASURED IN FEET PER SECOND



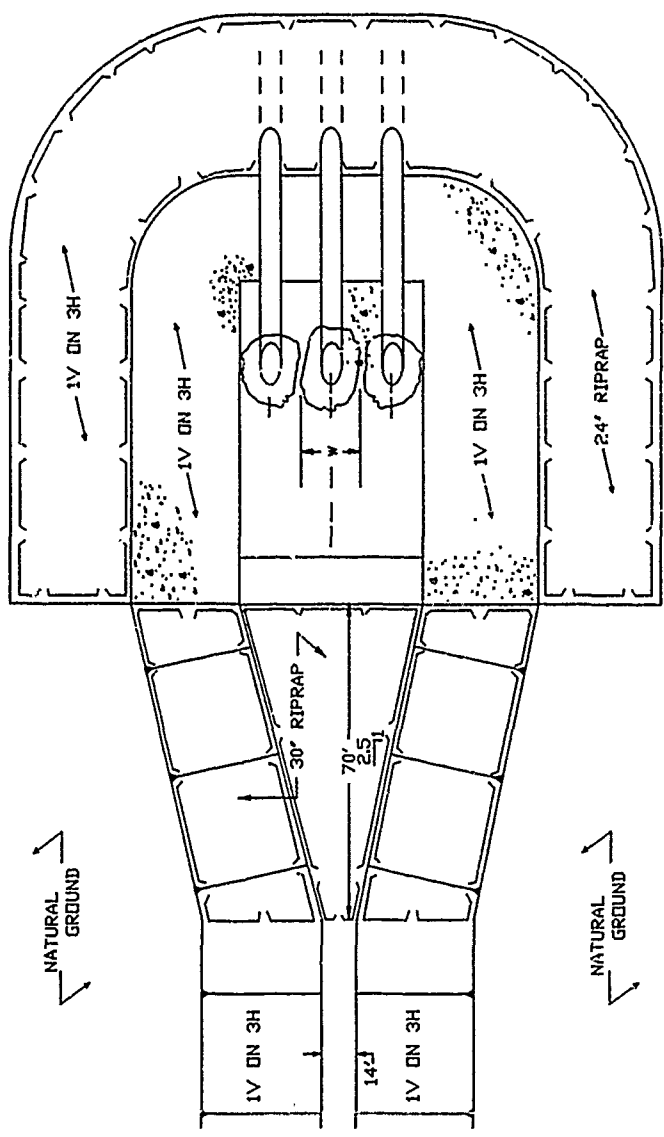
MIDDEPTH VELOCITIES IN VICINITY OF STILLING BASIN  
 DISCHARGE 5,000 CFS  
 HEADWATER EL 274.9  
 TAILWATER EL 267.4

NOTE : VELOCITIES MEASURED IN FEET PER SECOND



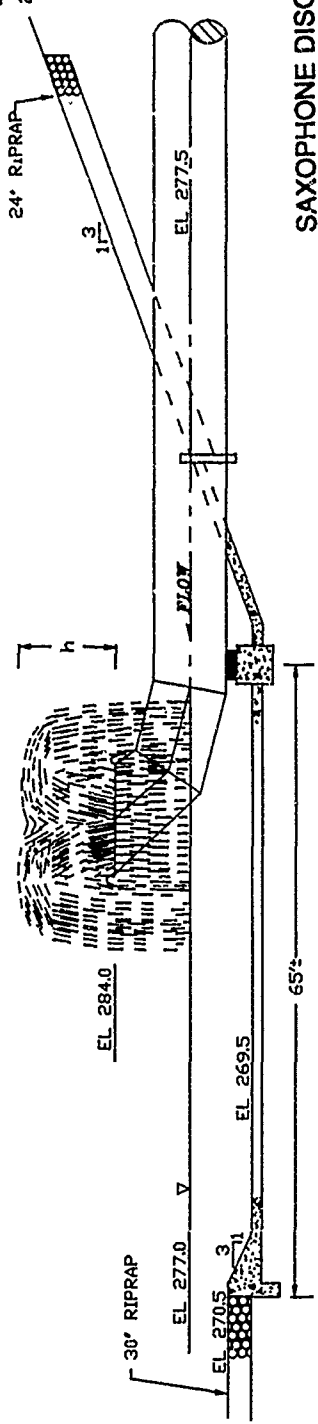
BOTTOM VELOCITIES IN VICINITY OF STILLING BASIN  
 DISCHARGE 5,000 CFS  
 HEADWATER EL 274.9  
 TAILWATER EL 267.4

NOTE : VELOCITIES MEASURED IN FEET PER SECOND



NOTE : NOT DRAWN TO SCALE

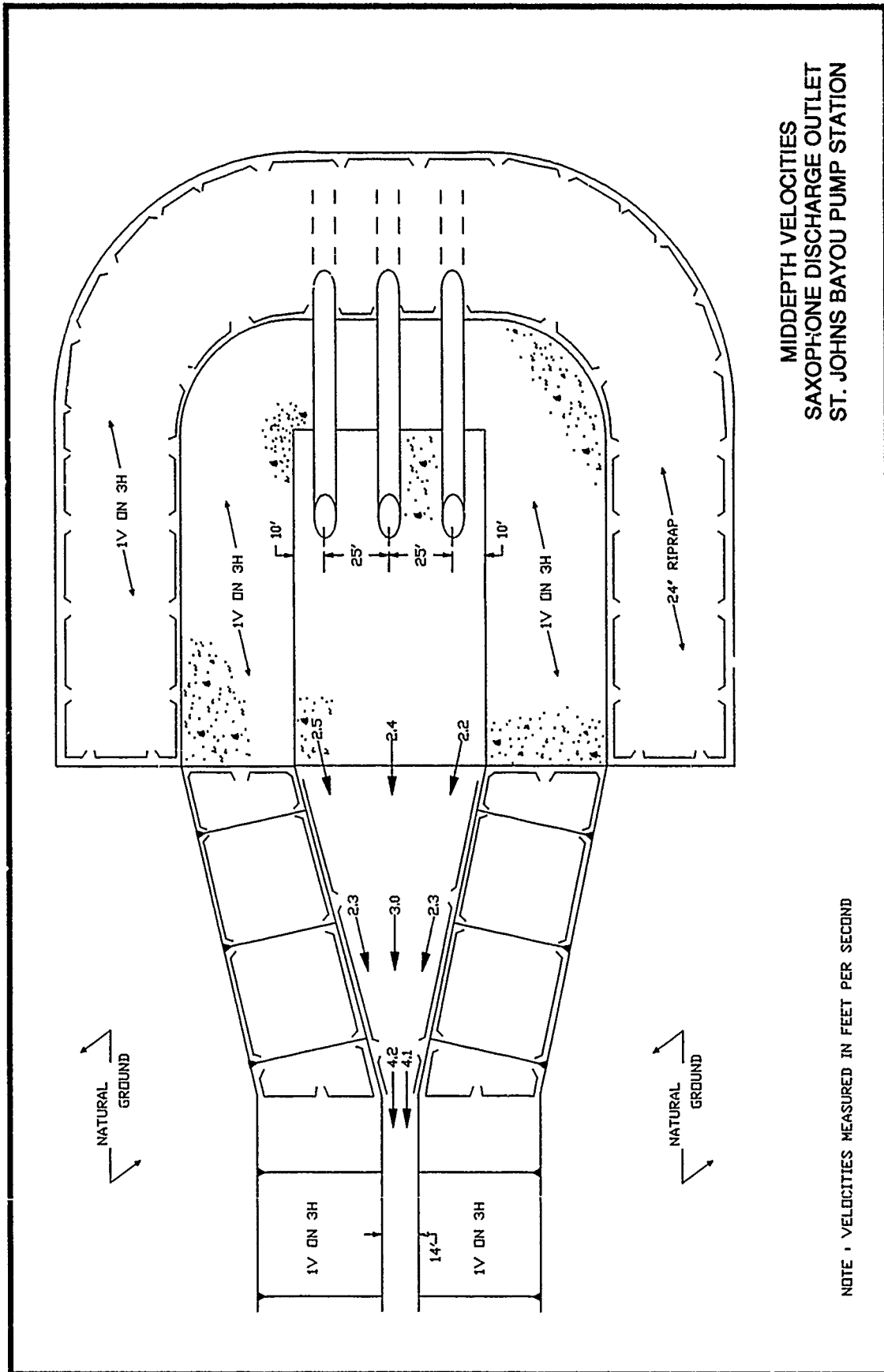
$Q$ cfs	$h$ ft	$\frac{W}{ft}$
333	3.1	18.8
285	2.6	17.7
220	1.9	15.0



SAXOPHONE DISCHARGE OUTLET  
ST. JOHNS SIPHON

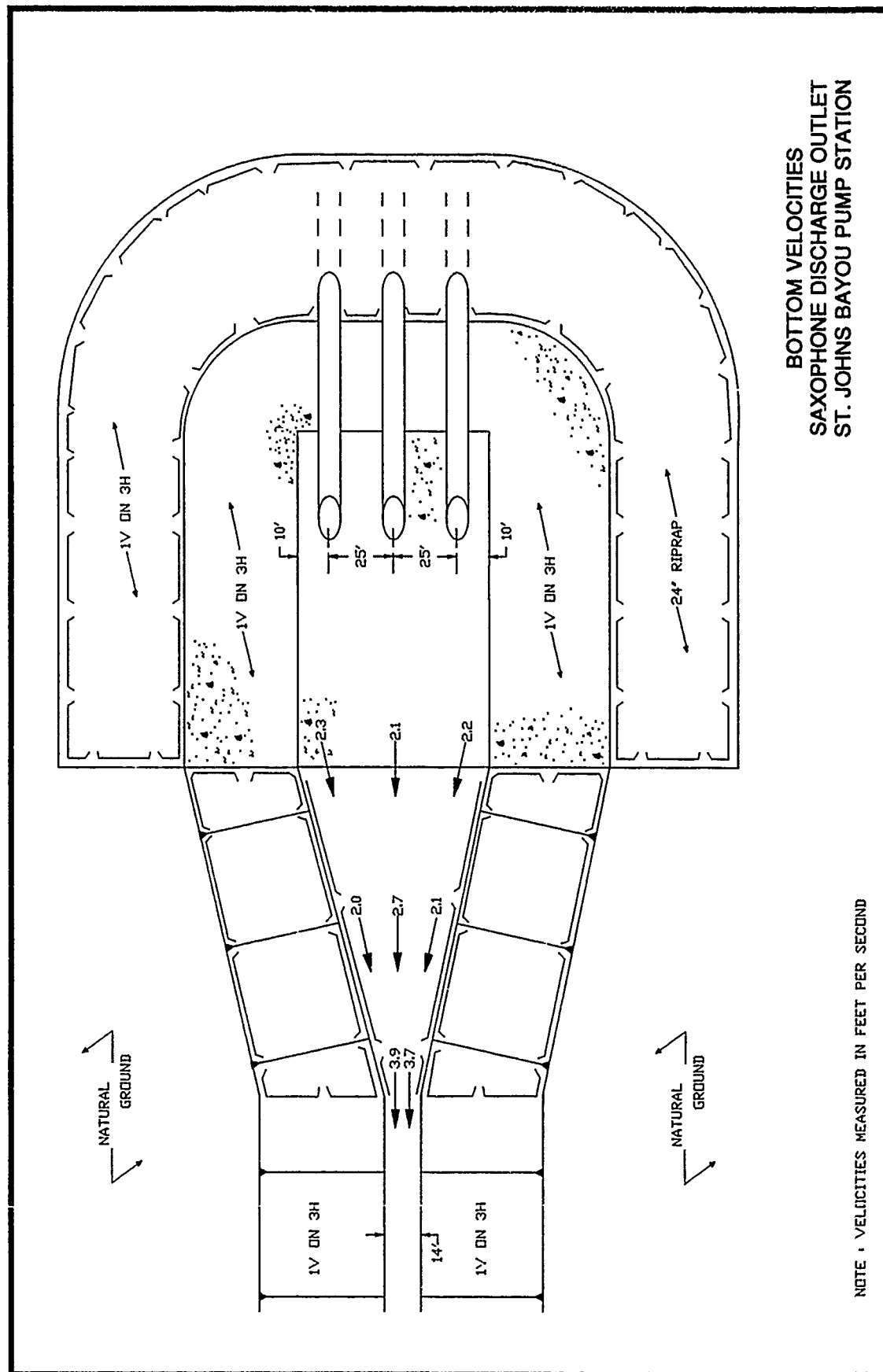


NOTE : VELOCITIES MEASURED IN FEET PER SECOND



MIDDEPTH VELOCITIES  
SAXOPHONE DISCHARGE OUTLET  
ST. JOHNS BAYOU PUMP STATION

NOTE : VELOCITIES MEASURED IN FEET PER SECOND



**BOTTOM VELOCITIES  
SAXOPHONE DISCHARGE OUTLET  
ST. JOHNS BAYOU PUMP STATION**

NOTE : VELOCITIES MEASURED IN FEET PER SECOND